Ciencia y Tecnología
Secretaría de Ciencia, Humanidades, Tecnología e Innovación
CICY

Centro de Investigación Científica de Yucatán, A.C.

Posgrado en Ciencias Biológicas

ANATOMÍA FUNCIONAL Y BALANCE DE ENERGÍA DE MANGLARES CHAPARROS DE *Rhizophora mangle* L. EN LA PENÍNSULA DE YUCATÁN

Tesis que presenta:

Sara Gabriela Cerón Aguilera

En opción al título de
DOCTORA EN CIENCIAS
(Ciencias Biológicas: RECURSOS NATURALES)

Mérida, Yucatán, México

2025

CENTRO DE INVESTIGACIÓN CIENTÍFICA DE YUCATÁN, A. C.
POSGRADO EN CIENCIAS BIOLÓGICAS

RECONOCIMIENTO

Por medio de la presente, hago constar que el trabajo de tesis de Sara Gabriela Cerón Aguilera titulado **Anatomía funcional y balance de energía de manglares chaparros de *Rhizophora mangle* L. en la península de Yucatán, México**, fue realizado en la Unidad de Recursos Naturales, en la línea de investigación Servicios Ambientales de la Biodiversidad, en el Laboratorio de Fisiología Ambiental de Plantas del Centro de Investigación Científica de Yucatán, A.C. bajo la dirección del Dr. José Luis Andrade Torres dentro de la opción de Recursos Naturales, perteneciente al Programa de Posgrado en Ciencias Biológicas de este Centro y la Dra. Laura Yáñez Espinosa del Instituto de Investigación de Zonas Desérticas de la Universidad Autónoma de San Luis Potosí.

Atentamente

Dr. José Luis Hernández Stefanoni
Director de Docencia

Mérida, Yucatán, México, a 04 de junio de 2025

DECLARACIÓN DE PROPIEDAD

Declaro que la información contenida en la sección de Materiales y Métodos, los Resultados y Discusión de este documento proviene de las actividades de investigación realizadas durante el período que se me asignó para desarrollar mi trabajo de tesis, en las Unidades y Laboratorios del Centro de Investigación Científica de Yucatán, A.C., y que a razón de lo anterior y en contraprestación de los servicios educativos o de apoyo que me fueron brindados, dicha información, en términos de la Ley Federal del Derecho de Autor y la Ley de la Propiedad Industrial, le pertenece patrimonialmente a dicho Centro de Investigación. Por otra parte, en virtud de lo ya manifestado, reconozco que de igual manera los productos intelectuales o desarrollos tecnológicos que deriven o pudieran derivar de lo correspondiente a dicha información, le pertenecen patrimonialmente al Centro de Investigación Científica de Yucatán, A.C., y en el mismo tenor, reconozco que si derivaren de este trabajo productos intelectuales o desarrollos tecnológicos, en lo especial, estos se regirán en todo caso por lo dispuesto por la Ley Federal del Derecho de Autor y la Ley de la Propiedad Industrial, en el tenor de lo expuesto en la presente Declaración.

Firma: Gabriela

Nombre: Sara Gabriela Cerón Aguilera

Este trabajo se llevó a cabo en la Unidad de Recursos Naturales del Centro de Investigación Científica de Yucatán A.C. y no formó parte de ningún proyecto específico financiado. Sin embargo, para la realización del trabajo de campo en Yucatán se proporcionó la beca de la International Tropical Timber Organization (ITTO, Japón) con el número de referencia 068/20A.

AGRADECIMIENTOS

Agradezco al Consejo Nacional de Humanidades Ciencias y Tecnología (CONAHCYT) por la beca, que me permitió realizar mis estudios de posgrado. Al Centro de Investigación Científica de Yucatán A.C. (CICY) por permitirme hacer uso de las instalaciones para mi estudio. A la International Tropical Timber Organization (ITTO) por la beca otorgada para realizar el trabajo de campo (068/20A).

Al Instituto de Investigación de Zonas Desérticas (IIZD) de la Universidad Autónoma de San Luis Potosí (UASLP) por permitirme realizar una estancia de investigación en el Laboratorio de Anatomía y Fisiología Vegetal en la cual recibí capacitación en la microtecnia vegetal.

Agradezco a la International Union of Forest Research Organizations (IUFRO) por la beca otorgada a través del Programa Especial de Desarrollo de Capacidades (SPDC), para participar en el Pre-Congress Training Workshops y en el 26th IUFRO World Congress 2024 Estocolmo, Suecia.

A la CONANP por permitir realizar las actividades de muestreo relacionadas al trabajo de investigación.

A mi director de tesis, el Dr. José Luis Andrade, por haberme guiado en el camino de la investigación y de la vida. Estoy profundamente agradecida por tu apoyo y comprensión a lo largo de estos años, los cuales han sido fundamentales para concretar este doctorado. Más allá del conocimiento teórico, me enseñaste la importancia de la empatía para transmitir el saber y formar personas con pensamiento crítico. Gracias por tu dedicación y por dar siempre lo mejor de ti. También por motivar a esta bióloga a entrar en temas de balance y energía; espero poder inspirar a más personas a través de la ciencia, como tú lo has hecho conmigo.

A mi co-directora, la Dra. Laura Yáñez Espinosa, por haberme escuchado y guiado en la conceptualización de este proyecto de doctorado. Gracias por las largas charlas en cada etapa de la microtécnica, por tu paciencia al enseñar y por facilitarme las instalaciones, el equipo y la información necesarios para llevar a cabo mi estancia. Tu dedicación y entrega han sido invaluables, y siempre agradeceré todo lo que has hecho para que este proyecto se hiciera realidad.

Al Dr. Rodrigo Méndez Alonzo, por el entusiasmo e ideas que aportó para mejorar este proyecto. Por sus preguntas que me hicieron mejorar y pensar en más aspectos sobre el balance de energía. Gracias por tus comentarios atinados para mejorarme como científica y por sugerir estrategias de mindfulness. A la Dra. Ileana Echevarría Machado por sus preguntas y comentarios tan certeros que me permitieron mejorar y formar mi pensamiento científico. Nunca olvidaré sobre como pensaba estructurar mi manuscrito para que fuera más sencillo.

A mi comité predoctoral y comité de examen la Dra. Casandra Reyes García, el Dr. Eduardo Cejudo Espinosa, la Dra. Mirna Valdez Hernández y la Dra. María Azucena Canto Aguilar a quienes agradezco por sus comentarios y apoyo para continuar con cada etapa de la obtención del grado. La Dra. Azucena Canto y la técnico Biól. María Rosalina Rodríguez Román por su disposición para hacer uso del microscopio óptico para la toma de micrografías.

Al Ing. Roberth Us Santamaría por su valioso apoyo en campo para la utilización de los sensores de flujo de savia y demás sensores. También por tantas horas en campo donde gritábamos los datos y anotabas velozmente para cumplir con las horas de medición, por ser el martillo de Thor. Se vivieron gratos momentos, gracias por el apoyo académico y tu amistad. A Jesús Garrido Pérez por siempre estar al frente en la batalla del campo, por su actitud de servicio que salvó mi espalda y por su entusiasmo por preguntar y aprender del manglar. Por tu alma de biólogo, gracias por tu apoyo y amistad.

Al Dr. Julio Salas Rabaza por su gran apoyo en la vida académica y de la vida. Agradezco por tu amistad sincera y empática, por apoyarme en todo momento. Por tus comentarios que siempre han sido para impulsar a ser mejor y a pensar en muchas posibilidades para abordar los problemas, tanto de la vida como los científicos. No tengo palabras para decirte lo mucho que te aprecio y que sé que eres y seguirás siendo referencia.

A la Ing. Karina Elizabeth Muñoz por su invaluable apoyo en campo midiendo muchas variables, calcando hojas, por tu paciencia al explicarme sobre R y por permitirme ser parte de tu formación como ingeniera forestal. Por siempre estar dispuesta a ayudar, aunque fuera cansado pasar varias horas bajo el sol y mojada en el manglar. Por darme tu amistad que guardo en mi corazón. Al M. en C. Juan Andrés Mauricio por su invaluable apoyo y horas brindadas para explicar sobre el funcionamiento de R. Siempre estuviste dispuesto a apoyarme y a brindarme tu amistad. Al M. en C. Aarón René Casanova por siempre estar dispuesto para apoyar en campo y cómo ingeniero a explicarme las fórmulas necesarias para desarrollar el balance de energía las veces que fueron necesarias. Ahora no olvido la fórmula de *PaVoRaton.* Por tu amistad sincera dentro y fuera de la academia.

Al grupo de fisiología vegetal, el Dr. Gerardo Carrillo Niquete y la M. en C. Olivia Zapata por sus comentarios para mejorar y seguir adelante, por su amistad sincera.

Al Dr. Frederic Thalasso, la Dra. Brenda Riquelme y la Dra. Sunitha Pangala, quienes, a través de mi estimado amigo y colega Julio Salas, me ofrecieron su apoyo sin conocerme, permitiéndome vivir la experiencia de conocer el fin del mundo, aprender sobre GEI, medir el flujo de savia y enriquecer mi corazón y mente con gratitud y nuevas vivencias. Como mencioné, les estoy eternamente agradecida y, con gusto, pagaré esa deuda.

A la Ing. en Sustentabilidad Berenice Cerón Aguilera, mi hermana y la persona más inteligente que conozco, gracias por tu apoyo invaluable al explicarle a esta bióloga las fórmulas y los conceptos de termodinámica. Soy increíblemente afortunada de poder compartir la vida contigo y de contar siempre con tu confianza en mí. Prometo que cada uno de tus esfuerzos y palabras de aliento valdrá la pena. Te amo inmensamente.

A mi mamá, Lilia Aguilera, quien siempre está para mí, sin importar la distancia, el momento o las dificultades. Con tu amor y sabiduría, me das los mejores consejos, y no solo te preocupas por mí, sino que actúas para asegurar que esté bien. Por todo tu apoyo incondicional y el amor que me brindas, espero algún día poder devolvértelo, porque mereces lo mejor que la vida tiene para ofrecer. No hay palabras suficientes para agradecer todo lo que haces por mí. Prometo siempre esforzarme por dar lo mejor de mí. Te amo más allá de lo imaginable.

A mis tíos y primos, Leticia Aguilera, Jorge Catalá, Enrique Catalá y Jorge Catalá, quienes, ya sea cerca o a la distancia, siempre me han brindado su apoyo y amor incondicional. A mis amados abuelitos, Enrique Aguilera (mi tatai) y María de la Luz (mi mamá Lucha), gracias por rodearme siempre de amor sin condiciones. Ustedes no solo me enseñaron a leer, sino que se sentaron conmigo a hacer dictados y leyeron mis cuentos inventados. Gracias a ustedes nació mi interés por la biología, y han sido una parte fundamental de quien soy, tanto como persona y como profesionista. Sin duda, la vida sin ustedes no es igual, pero sigue valiendo la pena. Y como dice la ley de la conservación de la materia: nada se crea ni se destruye, solo se transforma. De esa misma manera, espero encontrarlos algún día, tal vez como polvo de estrellas o en cualquier otra forma. Siempre vivirán en mí, porque su amor y legado están profundamente arraigados en mi corazón.

A Marco Bravo, mi nuti, quien con su paciencia, sonrisas, empatía y cariño me ha acompañado en los momentos más difíciles y más felices. Gracias por regalarme alegría, ocurrencias, por nuestras largas e inspiradoras conversaciones sobre la vida y los sueños, y por ser ese refugio que hemos construido juntos. Gracias por ser mi espacio seguro. Mit dir ist alles besser. Du bist mein Herz.

A la M.C. Cynthia Carranza, al M.C. Jesús Nieto, la Biól. Arantza Vieyra y la Biól. Alejandra Torres que me abrieron las puertas de su hogar sin conocerme y me trataron como una hermana más, parece que la vida ya nos tenía predestinadas. Gracias en el sentido más amplio de la palabra, por la ayuda en el laboratorio de Anatomía Vegetal de la UASLP, por las risas, por las conversaciones profundas y por su cariño sincero.

Por supuesto a mis compadritos queridos Alejandra Ochoa y Víctor Campuzano que me honraron con la oportunidad de convertirme en madrina de nuestro amado e inteligente Otlahui. A través de ustedes siempre redescubro el mundo y me hacen mejor persona. Gracias por tanto amor. Buscaré ser mi mejor versión para este pequeño cone de amor.

A mis amigos de la vida que están para mi sin importar la distancia, Brandon Licea, Rebeca Arciniega y Jarick Muñóz. Ustedes le dan sabor, risas y aventura a mi vida. Los quiero y extraño montones. A mis amigas cercanas de Mérida, Ale López, Elma e Isa.

A todos los que se han cruzado en mi camino, y a la vida misma, porque este periodo de doctorado no solo representó un crecimiento académico, sino también un desarrollo personal invaluable. Ha sido una aventura desafiante, pero, como todo buen reto, estuvo llena de momentos de diversión, aprendizaje e introspección.

A la sociedad, por permitirme llevar a cabo estos estudios de doctorado gracias al esfuerzo y pago de sus impuestos. Pondré mi conocimiento a su servicio, con la esperanza de aportar un pequeño granito de arena para hacer de nuestro México un lugar donde el sentido crítico, las buenas preguntas, la curiosidad, el respeto por cada ser vivo y por los recursos sean valorados en todos los aspectos.

Cada experiencia, tanto las más felices como las más complicadas, me ha dejado lecciones que llevo conmigo. Este camino ha sido un recordatorio de lo maravilloso y complejo que es crecer, y me siento profundamente agradecida por cada persona y circunstancia que me impulsaron a dar lo mejor de mí. A ustedes que se toman el tiempo de leer esta tesis y a la vida, gracias por ser parte de esta etapa inolvidable.

DEDICATORIAS

A cada día, persona, ser vivo y paisaje que me enseña que la materia y la energía se transforman, agradezco por su enseñanza, porque, al igual que ellos, yo también me he transformado y continuaré haciéndolo a lo largo de mi vida, hasta que, finalmente, me convierta en polvo de estrellas nuevamente. A todos los soñadores y facilitadores que, con su motivación, impulso y esfuerzo, hacen posible que los sueños se vuelvan realidad. Gracias por ser parte fundamental de este viaje, por apoyar a los soñadores.

El cosmos es todo lo que es, lo que fue o lo que será alguna vez.
Llevamos el cosmos dentro, fuimos hechos de estrellas.
Vamos a iniciar un viaje a través del cosmos, de la historia de nuestro planeta, de sus plantas y animales.
Una historia sobre nosotros mismos.
Perseguimos la verdad, sea cual sea; pero para hallarla necesitamos imaginación y escepticismo.
Viajaremos por el cosmos con la nave de la imaginación, perfecta como la nieve, delicada como una pluma.
La nave nos llevará a mundos de sueños, y mundos de hechos.

Cosmos: un viaje personal

LISTA DE LOS PRODUCTOS GENERADOS

ARTÍCULO CIENTÍFICO DEL DOCTORADO

Cerón-Aguilera, G., Laura Yáñez-Espinosa, Ileana Echevarría-Machado, Rodrigo MéndezAlonzo, Jorge Herrera-Silveira, Roberth Us-Santamaría, Julio A. Salas-Rabaza, Karina E. González-Muñoz and José Luis Andrade. (2025). Seasonal dynamics and microenvironmental drivers of transpiration in scrub *Rhizophora mangle*. L. trees from Yucatán. *Forests.*

COLABORACIONES DURANTE EL PERIODO

Salas-Rabaza J.A., Thalasso, F., Yáñez-Espinosa, L., Cejudo-Espinosa, E., **Cerón-Aguilera, S.G**., Us-Santamaría, R. and Andrade, J.L. 2024. Pneumatophore CO2 effluxes decrease with increased salinity in mangrove forests of Yucatan, Mexico. Scientific Reports.

DIVULGACIÓN Y SEMINARIOS

- Tunel de la ciencia. Centro de Investigación Científica de Yucatán. 2024.
- Andrade, J.L., Salas-Rabaza, J.A., Casanova, A.R., **Cerón-Aguilera, G.,** Zapata, O., González Muñóz, K.E., Us-Santamaría, R., Carrillo-Niquete, G.A. Ramas y rap. Teatro. 6° Foro de Arboricultura Tropical. 2024.
- Andrade, J.L., Salas-Rabaza, J.A., Casanova, A.R., **Cerón-Aguilera, G**., Zapata, O., González Muñóz, K.E., Us-Santamaría, R., Carrillo-Niquete, G.A. Ramas y rap. Teatro. Escuela Nacional de Estudios Superiores, Mérida. 2024.
- Participación en programa de radio- Radio Yucatán 92.9 Ciclo del agua. Mérida, Yucatán. 18 de marzo de 2024
- **Cerón-Aguilera**, G. Zapata, O., González-Muñóz, K.E., Us-Santamaría, R., Carrillo-Niquete, G.A., Andrade, J.L., Salas-Rabaza, J.A., Casanova, A.R. Fisiología vegetal. Ponencia. Preparatoria Estatal N.13, Plantel Azteca, Yucatán. 2023.
- **Cerón-Aguilera, G**., Salas-Rabaza, J.A., González-Muñóz, K.E., Yáñez-Espinosa, L., Echeverría-Machado, I., Méndez-Alonzo, R., Us-Santamaría, R., Andrade, J.L. Del suelo al cielo: Aporte de agua a la atmósera por transpiración de manglar chaparro de Rhizophora mangle L. Seminario. Universidad Autónoma de San Luis Potosí. 2023.
- **Cerón-Aguilera, G**. 2022. Manglares: Dioses del agua. Comisión del agua del estado de Veracruz. Unidad de Cultura y Participación ciudadana. Ponencia.

- **Cerón-Aguilera, G**., Alvarado-Barrientos, S., Salas-Rabaza, JA. 2022. Manglares: dioses del agua. En: Crónica y Portal Comunicación Veracruzana, INECOL.

CURSOS IMPARTIDOS

- Fisiología vegetal (25 h). En La Facultad Maya de Estudios Agropecuarios de la Universidad Autónoma de Chiapas en Palenque. Mayo, 2024.
- Las plantas vasculares y su microambiente (6 h). En el Centro de Investigación Científica de Yucatán. Semestre 2023-I. PNCP.
- Comunicación de la ciencia (3 h). En el Centro de Investigación Científica de Yucatán. Semestre 2023-I. PNCP.
- Transporte en el floema de las plantas (2 h). Fisiología de plantas. Escuela Nacional de Estudios Superiores Unidad Mérida. 2022. PNCP.
- Clase magistral: Flujo hídrico en plantas y transpiración (2 h). Hidrología

PARTICIPACIÓN EN CONGRESOS

- IX Congreso Mexicano de Ecología. Modalidad – Ponencia. *Análisis del balance de energía en manglares chaparros de Rhizophora mangle L. con diferente cobertura vegetal*. 2024.
- 26th IUFRO World Congress. Modalidad – Cartel. *From the soil to the Sky: The power of the red mangrove to move up and contribute water to the atmosphere. 2024*
- 5° Congreso Mexicano de Fisiología Vegetal. Yucatán. Modalidad -Ponencia. Colaboradora. *La fisiología de los árboles de bosques de manglar y su relación con los servicios ecosistémicos y el cambio climático.* 2023.
- 5° Congreso Mexicano de Fisiología Vegetal. Yucatán. Modalidad -Ponencia. *Aporte de agua a la atmósfera por transpiración de manglar chaparro de Rhizophora mangle L*. 2023.
- 2° Congreso de Manglares de América. Mérida, Yucatán. Modalidad – Ponencia. Colaboradora. *Bases fisio-ecológicas para la restauración y el entendimiento de la resiliencia de bosques de manglar.* 2022.
- 2° Congreso de Manglares de América. Mérida, Yucatán. Modalidad – Cartel. Colaboradora. *Balance de energía de Avicennia germinans (L.) L*. en Yucatán. 2022
- 2° Congreso de Manglares de América. Mérida, Yucatán. Modalidad – Ponencia. Colaboradora. *Flujos de CH4 y CO2 en árboles de manglar*. 2022
- 2° Congreso de Manglares de América. Mérida, Yucatán. Modalidad - Cartel. *Flujos de agua de bosques de manglar chaparro de Rhizophora mangle L. en Celestún, Yucatán*. 2022

- 4° Congreso Mexicano de Fisiología Vegetal. Chetumal, Quintana Roo. Modalidad – Cartel. *Conexión entre el suelo y el cielo: flujos de agua de bosques de manglar chaparro de Rhizophora mangle L.* 2022.
- 4° Congreso Mexicano de Fisiología Vegetal. Chetumal, Quintana Roo. Modalidad – Cartel. Colaboradora*. Implicaciones fisio-anatómicas en los flujos de gases de efecto invernadero en el mangle rojo.* 2022.
- VIII Congreso Mexicano de Ecología. Oaxaca de Juárez, Oaxaca. Modalidad-Ponencia. *Flujos de agua de bosques de manglar chaparro de Rhizophora mangle L. en Celestún, Yucatán*. 2022

FORMACIÓN DE RECURSOS

- Gisell Celeste Martínez Reyes. Ingeniería Forestal y Restauración*. Influencia de la salinidad en la tolerancia al estrés hídrico de las plántulas de Rhizophora mangle L.* Universidad Autónoma de Chapingo (UACH), división de Ciencias Forestales. Texcoco. 2024. Comité evaluador.
- Karina Elizabeth González Muñóz. Ingeniería Forestal y Restauración. *Influencia de la sal secretada en el balance de energía de Avicennia germinans L. en la península de Yucatán.* Universidad Autónoma de Chapingo (UACH), División de Ciencias Forestales. Texcoco, 2022. Comité evaluador.

ESTANCIA

- Anatomía funcional y balance de energía de manglares chaparros de *Rhizophora mangle* L. en la península de Yucatán, México. Universidad Autónoma de San Luis Potosí (UASPL) – Instituto de Investigación en Zonas Desérticas (IIZD). A cargo de: Dra. Laura Yáñez Espinosa. 9 de enero - 5 de mayo del 2023 y del 3 de junio - 17 de agosto del 2023.

ÍNDICE

LISTADO DE FIGURAS

LISTADO DE TABLAS

ABREVIATURAS

Abreviación	Unidad	Descripción
Microenvironment		
VPD	kPa	Vapor Pressure Deficit
T_{air}	° C	Air temperature
RH	%	Relative humidity
WS	ms^{-1}	Wind speed
PPF	umol m^{-2} s^{1}	Photosynthetic photon flux
S	Wm^{-2}	Solar radiation
$e_{S(T)}$	kPa	Saturated vapor pressure
Sap flow		
F_d	L m^{-2} h^{-1}	Sap flux density
SF	L h^{-1}	Sap flow
ΔV_{max}	K	Temperature difference between the measurement needle at zero flow
ΔV	K	Temperature difference between the measurement needle at a given flux
Ac	cm^2	Conductive tissue
LAI	dimensionless	Leaf area index
LE	MJ m^{-2} h^{-1}	Latent heat
λ	2.43 MJ kg^{-1}	Latent heat of vaporization
Ec	L m^{-2} h^{-1}	Transpiration per area unit
Ec	mm day^{-1}	Transpiration per time unit

RESUMEN

Los bosques de manglar, a nivel mundial tienen distribución tropical y subtropical. Esta localización geográfica los expone a una alta incidencia de radiación solar, la cual se transforma en calor sensible —percibido como el cambio en temperatura de un sistema— y calor latente —asociado a la transpiración y al cambio de estado físico del agua—. Las especies arbóreas que conforman estos ecosistemas han desarrollado estrategias funcionales y anatómicas que les permiten disipar dicha energía sin comprometer sus procesos de crecimiento y reproducción, siendo la transpiración un mecanismo clave para la regulación térmica. Dado que el ascenso de la columna de agua a través del sistema vascular desde el sustrato hasta las hojas se encuentra estrechamente vinculado a las tasas de intercambio gaseoso de dióxido de carbono y vapor de agua. Durante este proceso, la planta pierde agua y contribuye a enriquecer la atmósfera, los árboles mediante la transpiración reducen la temperatura del entorno y contribuyen al ciclo hidrológico.

En este contexto, el presente trabajo analizó el efecto de la variación estacional (temporadas seca y lluviosa) sobre el flujo de savia, la transpiración, el balance de energía y la anatomía funcional de manglares chaparros de *Rhizophora mangle* L., en dos sitios contrastantes del estado de Yucatán: un manglar conservado y uno con perturbación hidrológica. Los resultados indican que, en el manglar conservado de Celestún, el flujo de savia durante la temporada de lluvias fue casi el doble respecto a la temporada seca, a pesar de presentarse una menor demanda evaporativa. Este comportamiento sugiere un fuerte acoplamiento planta-atmósfera. Asimismo, los datos apuntan a que este tipo de manglar podría aportar una mayor cantidad de agua a la atmósfera mediante la transpiración que un bosque seco caducifolio, manteniendo un suministro constante a lo largo del año debido a su condición de especie perennifolia, lo que subraya su relevancia en los procesos ecohidrológicos. En cuanto al balance de energía, se observó que el manglar conservado de Celestún, en comparación con el manglar perturbado de Chuburná, muestra una mayor capacidad de termorregulación, sustentada en procesos fisiológicos y anatómicos que favorecen la disipación de energía principalmente a través del calor latente durante la temporada de lluvias. En contraste, el manglar perturbado disipa mayor cantidad de energía como calor sensible, regulado por el microambiente y una baja resistencia aerodinámica del dosel, lo que evidencia una menor capacidad de regulación térmica y energética. Estas diferencias reflejan distintos mecanismos de termorregulación e intercambio

energético con el ambiente, con implicaciones importantes en la regulación del clima en zonas costeras.

Los resultados indican que la disminución en cobertura de manglares conservados en Yucatán por disturbios antropogénicos, puede afectar directamente su prestación de servicios ecosistémicos particularmente en cuanto a la regulación del clima y la participación en el ciclo hidrológico.

ABSTRACT

Mangrove forests are distributed throughout tropical and subtropical regions worldwide. Their geographic location expose them to high levels of solar radiation, which is transformed into sensible heat—perceived as a temperature change in any system—and latent heat—associated with transpiration, and related to changes in the physical state of water. The species that comprise these ecosystems have developed functional and anatomical strategies that allow them to dissipate energy without compromising their growth or reproduction, with transpiration playing a key role in thermal regulation. Additionally, the ascent of sap from the roots through the vascular system to the leaves is closely linked to the gaseous exchange of carbon dioxide and water vapor. During this process, plant transpiration contributes to reducing ambient temperature and increase their participation in the hydrological cycle.

In this context, the present study aims to analyze the effect of seasonal variation (dry and rainy seasons) on sap flow, transpiration, energy balance, and the functional anatomy of dwarf mangroves of *Rhizophora mangle* L., in two contrasting sites in the state of Yucatán: one conserved and one hydrologically disturbed. The results indicates that, in the conserved mangrove of Celestun, sap flow during the rainy season was twice as high as in the dry season, despite a lower evaporative demand. This suggests a strong plant–atmosphere coupling. Furthermore, these findings indicate that this type of mangrove may contribute more water to the atmosphere through transpiration than a deciduous dry forest, maintaining a constant supply throughout the year due to its evergreen nature. This highlights its importance in ecohydrological processes. Regarding energy balance, the conserved mangrove in Celestún, in contrast to the hydrologically disturbed mangrove in Chuburná, exhibited greater thermoregulatory capacity through physiological and anatomical processes that favored the dissipation of energy primarily as latent heat during the rainy season. In contrast, the disturbed mangrove dissipated more energy as sensible heat, regulated by microenvironmental conditions and the low aerodynamic resistance of the canopy, indicating a reduced ability to regulate temperature and energy. These

differences reveal distinct mechanisms of thermoregulation and energy exchange with the environment, with important implications for coastal climate regulation.

Overall, the results indicate that mangrove forests cover reduction due to anthropogenic disturbances may promote a decline in the provision of ecosystem services, particularly climate and hydrological cycle regulation.

INTRODUCCIÓN

Los bosques de manglar tienen una distribución mundial tropical y subtropical. Debido a ello, se encuentran expuestos a una alta cantidad de radiación solar que es transformada en calor sensible (de conducción y convección) y calor latente (transpiración). Las especies que conforman el bosque de manglar deben contar con estrategias anatómicas y funcionales capaces de disipar la gran cantidad de energía recibida sin comprometer su crecimiento y reproducción; siendo la transpiración uno de los procesos fundamentales que permiten regular la temperatura. Por otra parte, el movimiento de la columna de agua a través del sistema vascular hasta las hojas se encuentra asociado al intercambio gaseoso de dióxido de carbono y vapor de agua. Durante este proceso la planta pierde vapor de agua, disminuye su temperatura y aumenta el aporte al ciclo del agua. Lo anterior es relevante porque los bosques de manglar proporcionan múltiples servicios ambientales que contribuyen a la regulación y mitigación del cambio climático global (Worthington & Spalding, 2018; Rivera-Monroy *et al*., 2017).

A pesar de la importancia de los bosques de manglar, la extensión de estos a nivel mundial, y en México, ha disminuido principalmente por disturbios antropogénicos que ocasionan la disminución de su cobertura, provocando afectaciones a los servicios ecosistémicos de regulación del clima y captura de carbono (Castillo-Elías *et* al., 2019; Giri *et al*, 2010). México ocupa el cuarto lugar a nivel mundial de cobertura de manglar (5.4 %) (Herrera-Silveira & Teutli, 2017). Particularmente, la península de Yucatán alberga más de la mitad de esta cobertura nacional con una superficie 544169 ha (60%) (Velázquez-Salazar *et* al., 2021) y contiene una variedad de ecotipos de manglar, como el manglar de franja, cuenca, petén y chaparro. Estos ecotipos se distinguen principalmente por diferencias en la salinidad, el hidroperiodo y la variabilidad de nutrientes minerales; por lo que cada ecotipo proporciona diferentes servicios ambientales (Zaldívar-Jiménez *et al*., 2010).

En años recientes se han incrementado los proyectos orientados a conocer los servicios ecosistémicos que brindan los distintos tipos ecológicos. Las características del sedimento, la ubicación intermareal y la presencia de hojas perennes promueve la captura y el almacén de bióxido de carbono, denominado carbono azul, tanto aéreo como subterráneo. Estos trabajos han confirmado que el manglar chaparro de *Rhizophora mangle* L. posee una mayor capacidad de almacenamiento subterráneo de carbono orgánico en comparación con otros ecotipos; sin embargo, no se han realizado estudios relacionados al aporte de agua al ambiente (Caamal-Sosa *et al*., 2018; Morales-Ojeda, 2018). Esta especie se caracteriza por presentar estrategias morfo-fisiológicas y reproductivas únicas, entre las que destaca la viviparidad, en donde la semilla germina dentro del fruto unido a la planta madre formando un propágulo (Tomlinson, 2016; Agraz-Hernández et al., 2006).

A causa de las incesantes perturbaciones de los bosques de manglar, se requieren proyectos integrales que contribuyan a generar estrategias de restauración exitosas. Este proyecto plantea explicar el efecto del microambiente en el balance de energía, las relaciones hídricas y la anatomía funcional de manglares chaparros de *Rhizophora mangle* en ambientes con diferentes niveles de cobertura vegetal.

CAPÍTULO I

1.1 ANTECEDENTES

1.1.1 LOS BOSQUES DE MANGLAR

Los bosques de manglar son ecosistemas conformados por árboles y arbustos que habitan en la zona intermareal, por lo que las especies vegetales cuentan con adaptaciones morfológicas, fisiológicas y reproductivas para responder a las diferentes condiciones ambientales como la variabilidad en la salinidad y la inundación (Spalding et al., 2018; Tomlinson, 2016; UNEP, 2016).

Se estima que México posee 905,086 ha de manglar; de las cuales la región de la península de Yucatán presenta la mayor superficie (60 %) (Velázquez-Salazar et al., 2020). Particularmente, en esta última, el gradiente de salinidad dado por el aporte de agua subterránea es un factor determinante para la distribución espacial de las especies, que conforma diferencias microtopográficas, dando como resultado la formación de distintas estructuras ecológicas, denominadas ecotipos (Krauss et al., 2008; Lugo & Snedaker, 1974). En la península de Yucatán destacan los ecotipos de manglar de franja, cuenca, petén y chaparro (Lugo & Snedaker, 1974) (Figura 1.1), estos se diferencian principalmente por la salinidad, el hidroperiodo y los nutrientes minerales (Zaldivar-Jimenez *et al*., 2010):

- Manglar de franja: Se caracteriza por encontrarse en el borde de los cuerpos de agua de costas, ahí las especies se distribuyen debido a los patrones de salinidad, inundación y elevación mediana del sedimento. La exposición a la fuerza del viento y el agua afecta el sistema de raíces, por ello las especies desarrollan un sistema de raíces adventicias concentrado para asegurar su permanencia en el sitio.

- Manglar de cuenca: Este ecotipo se ubica detrás del manglar de franja y usualmente están aislados hidrológicamente, durante fuertes tormentas y huracanes presentan inundación. Debido a la baja conectividad hídrica y la falta de inundación constante la salinidad intersticial es mayor que en el de franja. Las especies dominantes dependiendo de la salinidad son *Avicennia germinans* y *Laguncularia racemosa*.

- Manglar de petén (Hammock): Estos bosques están asociados a cuerpos de agua dulce, como los conocidos “manantiales”, lo que causa una baja salinidad intersticial y alta disponibilidad de nutrientes, por ende, permite que la vegetación adquiera grandes alturas (>25 m) y acumule una gran cantidad de materia orgánica provocando la acreción del sedimento.

- Manglar chaparro: Son bosques monoespecíficos conformados por *R. mangle* o *A. germinans*, estas especies alcanzan alturas máximas de 2.5 metros debido a la baja conectividad hídrica y la dependencia de la precipitación, ocasionando estrés hídrico por la elevada concentración en la salinidad intersticial y baja disponibilidad de nutrientes.

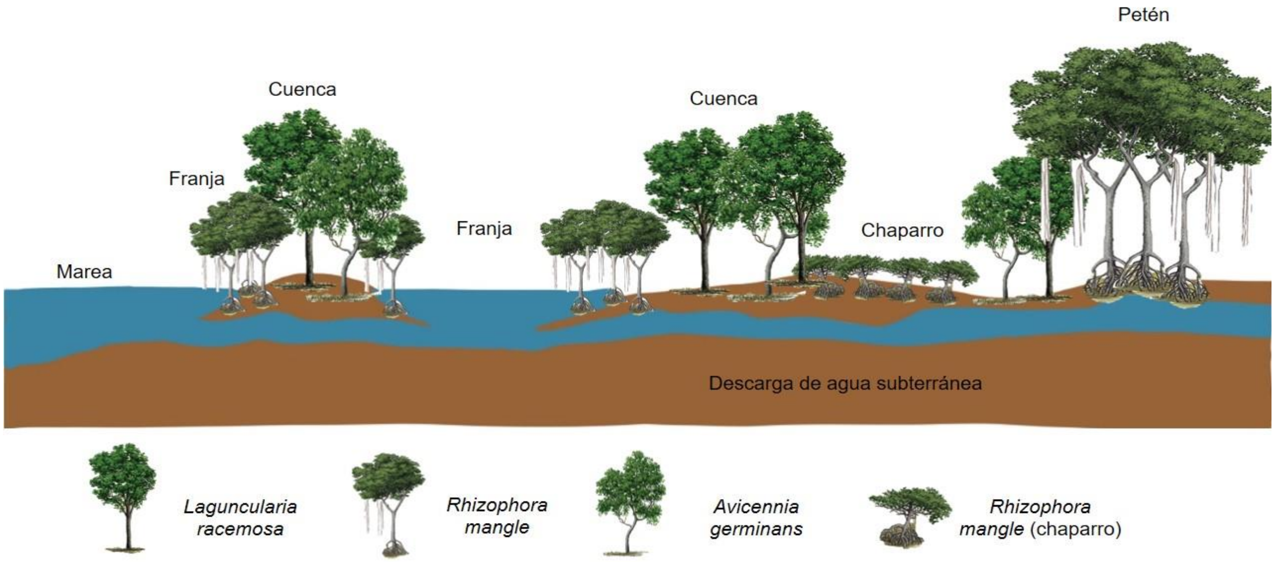

Figura 1.1 Estructura y especies del bosque de manglar en la Reserva de la Biosfera de Celestún. Modificado de (Zaldivar-Jimenez *et al*., 2010)**.**

1.1.2 SERVICIOS ECOSISTÉMICOS DE LOS BOSQUES DE MANGLAR

Los servicios ambientales que brindan los bosques de manglar se han considerado de gran importancia para la humanidad y para las zonas costeras (Figura 1.2), dichos servicios son variables dependiendo del ecotipo de manglares, es decir, no todos los bosques de manglar ofrecen la misma proporción y calidad de servicios ecosistémicos (Ewel *et al*., 1998; Giri *et al.,* 2011). La variación en la calidad y proporción de los servicios depende de las condiciones hidrológicas, sedimento y vegetación presente en cada zona; de manera que cada ecotipo brindará en diferente proporción una serie de servicios ecosistémicos y eso no debe repercutir en la importancia o prioridad de conservar las diferentes zonas de manglar (Batllori-Sampedro & Febles-Patrón, 2007; Teutli & Silveira, 2020). Por lo anterior es importante que se realice una correcta caracterización de los sitios para conocer las variables que tienen mayor peso y de esa forma establecer los servicios ecosistémicos que brinda cada uno de los manglares.

Figura 1.2. Clasificación de los servicios ecosistémicos con base en el beneficio que perciben los humanos y su función ecológica según Marlianingum *et al*. (2019). Modificado de Carvajal-Oses *et al*., 2019.

En la península de Yucatán se han desarrollado investigaciones para conocer los diversos servicios ecosistémicos que brindan los diferentes ecotipos (Silveira *et al*., 2019). Los manglares de tipo franja, cuenca y chaparro presentan una alta productividad, sin embargo, el de ecotipo de franja marino se encuentra mayormente especializado en proveer protección contra tormentas y huracanes. Mientras tanto, el manglar de franja lagunar aporta una gran cantidad de materia orgánica debido a las descargas subterráneas de agua dulce y su conectividad con el mar; también es una zona de refugio para fauna como peces, crustáceos y moluscos (Arceo-Carranza et al., 2016; Batllori-Sampedro & Febles-Patrón, 2007). Con respecto al ecotipo chaparro se ha reportado la depuración de masas de agua como un servicio ecosistémico de importancia. Además, el manglar chaparro conformado por *Rhizophora mangle* L. y *Avicennia germinans* L., captura y almacena una mayor cantidad de carbono en comparación con los demás ecotipos. Lo anterior, se encuentra asociado con altos valores de salinidad intersticial y la baja conectividad hídrica (Caamal-Sosa *et al*., 2018; Morales-Ojeda, 2018; Us-Balam *et al*, 2018).

La gran cantidad de carbono capturado en los bosques de manglar chaparro se encuentra relacionado con el proceso de transpiración, ya que durante el intercambio de gases como el CO_2 y O_2 entre la hoja y el ambiente también ocurre una pérdida de agua en forma de vapor. Sin embargo, a nivel de hoja existe la regulación entre la pérdida de agua y la captura de carbono por lo que son procesos que se encuentran íntimamente ligados (Ball *et al*., 1987). En ese sentido, los bosques de manglar "son más que carbono" porque ofrecen muchos otros servicios ecosistémicos como el aporte de agua a la atmósfera por transpiración. Actualmente el estudio de los bosques de manglar por su contribución al ciclo del agua y su papel ante la regulación del clima en zonas costeras cobra mayor interés (Giri *et al*., 2011; Krauss *et al*., 2007; Leng & Cao, 2020; Mcleod et al., 2011). La cuantificación de los servicios ecosistémicos puede permitir el establecimiento y la aplicación de regulaciones en la gobernanza, además de promover su conservación (Mursyid *et al.*, 2021).

A pesar de lo anterior, la extensión de estos bosques en México ha disminuido debido a perturbaciones naturales (huracanes y tormentas) y en mayor medida por afectaciones antrópicas (cambios hidrológicos, deforestación causada por construcción de infraestructura, actividad agrícola y ganadera, turismo, construcción de carreteras, descargas de desechos urbanos, residuos peligrosos y acuicultura) afectando seriamente la dinámica del manglar y con ello reduciendo la cantidad y calidad de los servicios ecosistémicos que las zonas costeras perciben directamente de los bosques de manglar (Valderrama *et al*., 2014) (Figura 3). Considerando lo anterior y que México se ubica en el cuarto lugar con respecto al porcentaje total global de la cobertura de manglar (5.4 %) (Giri *et al*., 2011) se vuelve de suma importancia comprender el funcionamiento de los bosques de manglar y los servicios ecosistémicos que brindan, con la finalidad de recuperar la cobertura de manglares que se ha perdido durante los últimos años.

Figura 1.3. Servicios ecosistémicos y amenazas (antrópicas y naturales) del manglar. Tomado de Teutli & Silveira, 2020.

1.1.3 LA FISIOECOLOGÍA COMO HERRAMIENTA PARA EVALUAR LA PROVISIÓN DE SERVICIOS ECOSISTÉMICOS

El entendimiento del efecto de las variables ambientales en la fisiología de manglares permite conocer las respuestas de las especies vegetales ante la dinámica de sucesión del ecosistema y las acciones de restauración para con ello evitar la alta mortalidad de plantas adultas y de propágulos por la alta radiación solar global incidente, incremento de temperatura y salinidad, ocasionando altas demandas de evaporación y transpiración, así como la herbivoría, poca disponibilidad de nutrientes y anoxia (Esteban, 2008; Teutli & Herrera Silveira, 2020). Las condiciones fisicoquímicas del sedimento desempeñan un papel importante para las especies vegetales durante la restauración de manglares; sin embargo, también deben considerarse los elementos climáticos que conforman el microambiente, ya que pudieran encontrarse afectando las funciones de las plantas sufriendo un fuerte estrés que generalmente lleva a la muerte. Por lo que considerar todo lo anterior es una parte clave que repercute en el crecimiento, reproducción, producción de tejidos (aerénquima, sistema vascular y parénquima), fotosintética y relaciones hídricas (Barnuevo & Asaeda, 2018; Hoppe-Speer et al., 2011; Salas-Rabaza *et al*., 2024).

Aunque la fisiología es una disciplina que ha incidido en los proyectos de restauración ecológica en diversos ecosistemas (Rindyastuti *et al*., 2018), es evidente la falta de investigación de los parámetros fisiológicos integrados con aspectos ecológicos en el ecosistema de manglar; el entendimiento de lo anterior puede ayudar a explicar los mecanismos de adaptación y estrés de los individuos ante los impactos causados en el ambiente (Cabañas-Mendoza *et al*., 2020; Cisneros-De La Cruz *et al*., 2022; Salas-Rabaza *et al*., 2024) (Figura 4). De esa forma la fisioecología de la restauración puede complementar los estudios para explicar la respuesta de los ecosistemas ante las diferentes técnicas de restauración (pasiva o activa) y alimentar modelos para predecir respuestas de las especies ante el Cambio Climático Global, y que de esta forma los tomadores de decisiones y los restauradores ecológicos tomen decisiones con más información (Cooke & Suski, 2008).

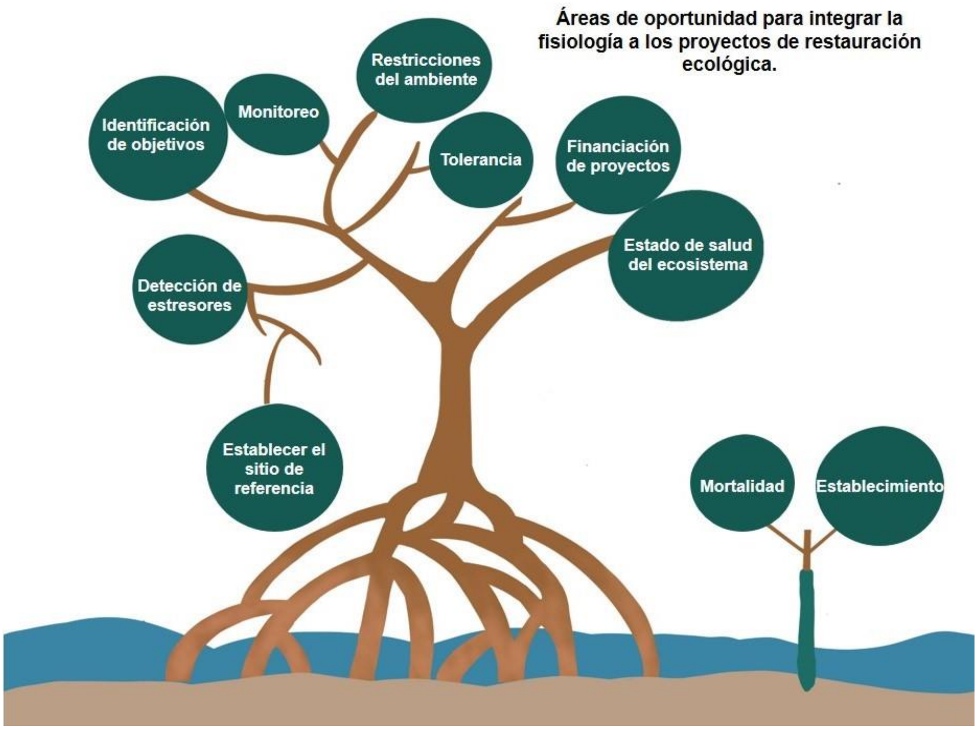

Figura 1.4. Áreas de oportunidad para integrar la fisiología a los proyectos de restauración ecológica según la evaluación de la Sociedad para la Restauración Ecológica Internacional. Información obtenida de Cooke & Suski, 2008.

1.1.4 ECOHIDROLOGÍA

El agua en las plantas es de suma importancia ya que constituye alrededor del 70 – 95 % de los tejidos y tiene repercusiones fisiológicas vitales, tales como la toma y transporte de nutrientes, captura de CO_2, crecimiento, mantenimiento y reproducción (Collazo-ortega, 2013; Nolan *et al.,* 2017).

El estado hídrico del suelo, las plantas y la atmósfera se puede determinar con el potencial hídrico (Ψ) que es una medida representativa de la energía potencial de las moléculas del agua para realizar un trabajo en cualquier sistema, mediante su comparación con el potencial químico del agua pura, que convencionalmente se iguala a 0. Las unidades empleadas para expresar son las de presión (MPa) o tensión (-MPa) donde el potencial químico de la solución menos el potencial químico del agua pura representa un símil de un cambio de energía (Joules, J), implicando movimiento de la zona con valor más cercano a cero al mayor, entre el volumen ($J\ m^{-3}$), resultando en presión (kPa, MPa). En medida que las moléculas de agua reducen su energía libre por la presencia de solutos, el potencial hídrico adquiere valores negativos (Campbell *et al.,* 1998; Lambers *et al*., 2008). Adicionalmente, el potencial hídrico de la planta disminuye por la pérdida de agua y se forma un gradiente que va en disminución desde las raíces hasta las hojas (Lambers *et al*., 2008).

De esta manera, durante la toma de agua se forma un continuo que conecta al *suelo-planta-atmósfera*, en este proceso el agua en forma líquida circula a partir del suelo, ingresa por las raíces y se transporta por el sistema vascular hasta alcanzar las hojas; allí una pequeña porción de agua es almacenada y la mayor parte es liberada por los estomas hacia la atmósfera en forma de vapor. La transferencia de vapor de agua de las hojas a la atmósfera se conoce como transpiración, y esto se ve afectado por la radiación neta y el déficit de presión de vapor (DPV) (Collazo-ortega, 2013; Nobel, 2020; Suárez *et al*., 2021). La transpiración se encuentra íntimamente relacionada con el ciclo del carbono y el balance de energía permitiendo la conexión entre la atmósfera y la vegetación, siendo la ecohidrología un proceso clave en la regulación del clima en la Tierra a diferentes escalas. La comprensión de la transpiración es relevante porque por medio de su estudio se puede estimar el flujo de carbono, más aún, se conoce que la transpiración puede aportar más de la mitad del agua procedente de la evapotranspiración (Jasechko *et al*., 2013; Kool *et al.,* 2014; Nelson *et a*l., 2020; Tarin *et al*., 2020).

Sin embargo, la limitación del agua en el ambiente originada por perturbaciones en los ecosistemas causa estrés hídrico en los individuos durante las diferentes fenofases, esto es de importancia ya que los individuos pudieran tener severas repercusiones principalmente por la baja disponibilidad de agua en el suelo y la poca disponibilidad de nutrientes afectando su anatomía y fisiología (Tyree, 2003). Los ecosistemas perturbados sufren cambios físicos e hidrológicos en el suelo lo que tiene repercusiones en el continuo suelo-planta-atmósfera, el funcionamiento del ecosistema (Lewandrowski *et al*., 2017; Muñoz-Villers *et al*., 2012, 2015).

La disminución en el potencial hídrico se relaciona con una baja tasa de asimilación de CO_2 ocasionada por el control de cierre de estomas. El estrés hídrico también puede estar asociado a la temperatura del ambiente, ocasionando una alta demanda evaporativa e incidiendo en el aumento del calor sensible de la superficie de las hojas y del suelo; por lo que las plantas creciendo en ambientes perturbados con suelos expuestos reciben una alta cantidad de radiación solar e infrarroja, por otro lado, las superficies pueden almacenar una gran cantidad de calor aumentando la temperatura promoviendo un albedo bajo. Esto modifica las condiciones ambientales y afecta la ecohidrología (Asbjornsen *et al*., 2011; Lambers *et al*., 2008; Osmond *et al*., 1987).

1.1.5 BALANCE DE ENERGÍA

Las plantas intercambian materia y energía con el ambiente respondiendo a factores físicos, respondiendo ante las leyes de la termodinámica. La primera ley menciona que la energía no se crea ni se destruye, solo se transforma. Esto se puede apreciar en el balance de energía de una hoja, en el cual la energía entra y sale, mientras que otra pequeña parte es almacenada (Figura 5). Las unidades empleadas para expresar la cantidad de energía por unidad de área y por unidad de tiempo es J $m^{-2}s^{-1}$, que es igual a W m^{-2} (Nobel, 2020).

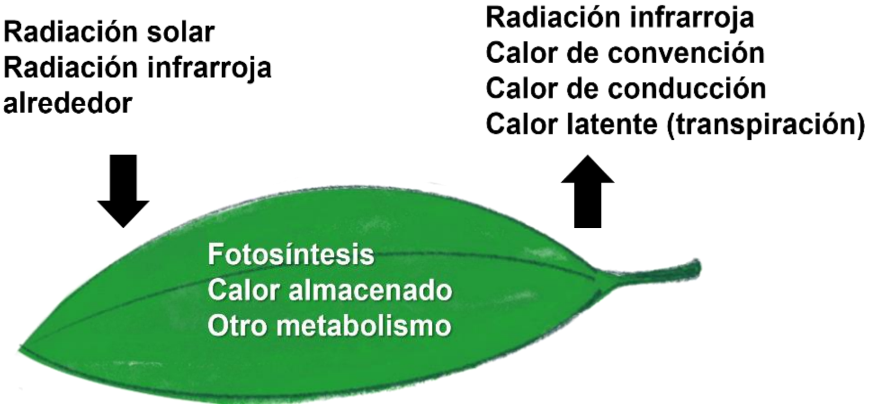

Figura 1.5 Representación de la entrada, salida y acumulación de energía a la hoja. El calor de convección y conducción se considera como calor sensible y la transpiración como calor latente. Información obtenida de Nobel, 2020.

La radiación solar (S) o de onda corta puede clasificarse como directa ($S^{directa}$) e indirecta ($S^{indirecta}$): siendo la primera la radiación que no sufre dispersión o reflexión y la segunda se considera que se dispersa debido a las partículas, gases o nubes presentes en la atmósfera antes de llegar a la hoja (Figura 6). De cualquier forma, es importante considerar la variación en la radiación solar directa e indirecta por el efecto de la temporada del año, latitud y altitud. La radiación solar total para el balance de energía de la hoja se puede considerar de la siguiente manera:

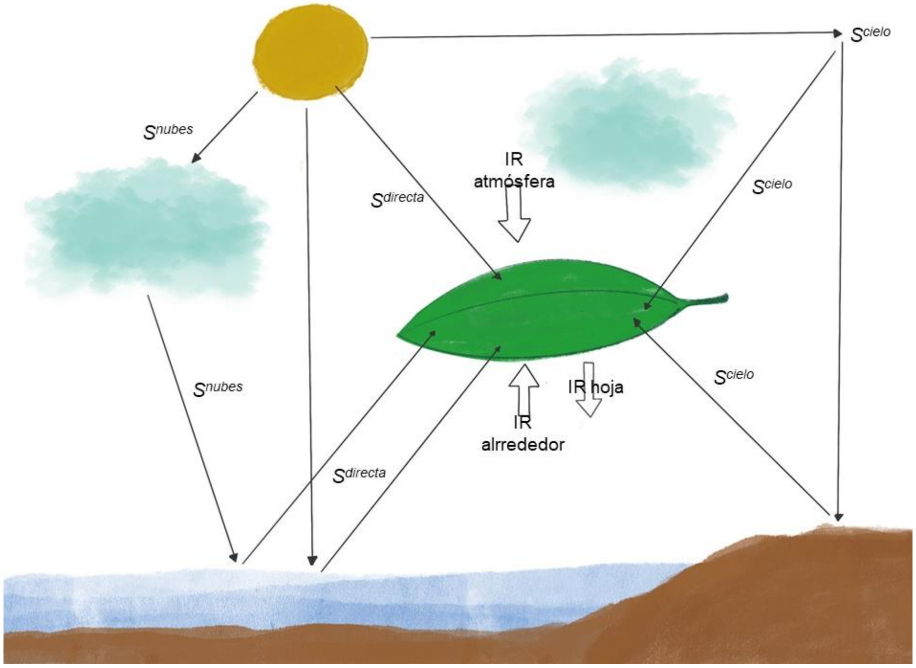

Figura 1.6 Esquema que ilustra la radiación solar incidente en una hoja, incluyendo la radiación de onda corta (s) y de onda larga (ir) que emite y refleja la hoja en un ambiente de bosque de manglar. Modificado de Nobel, 2009.

$$\cong \alpha\left(S^{directa} + S^{nubes} + S^{cielo}\right)\alpha r\left(S^{directa} + S^{nubes} + S^{cielo}\right) = \alpha\,(1+r)S \qquad (1.1)$$

Donde la absorbancia α es la fracción de la densidad del flujo de energía radiante global absorbida por la hoja y la reflectancia *r* es la fracción de la *S* reflejada por los alrededores sobre la hoja.

Además de recibir radiación de onda corta, las plantas también se ven expuestas a la radiación infrarroja (IR) o también conocida como de onda larga y energía térmica. Todos los cuerpos que tienen una temperatura mayor a 0 K emiten IR, por lo que la energía de onda larga es emitida por todos los cuerpos que se encuentren alrededor de la hoja, incluso las hojas aledañas por supuesto que pueden emitir y absorber IR.

La IR o energía térmica (T^{hoja}) emitida por la hoja se expresa empleando la Ley de Stefan-Boltzmann que indica la tasa máxima de radiación emitida por unidad de área:

$$Densidad\ de\ flujo\ de\ energía\ radiante = e\sigma T^4 \tag{1.2}$$

Donde *e* es la emisividad que puede adquirir un valor máximo de 1, que sería un cuerpo negro radiador perfecto; σ es una constante y *T* es la temperatura en unidades kelvin. Esta ley aplicada a la IR emitida por la hoja se considera de la siguiente manera:

$$IR\ emitida\ = 2e_{IR}\sigma(T^{hoja})^4 \tag{1.3}$$

La ecuación considera los mismos componentes, pero añadiendo la energía infrarroja que emiten ambos lados de la hoja.

La cantidad de energía radiante que recibe la planta ocasiona la apertura estomática, debido a esto la planta puede intercambiar agua en forma de vapor con la atmósfera provocando la transpiración. Durante la traspiración las hojas se refrescan perdiendo vapor de agua (calor latente). Sin embargo, la temperatura superficial de las hojas también puede disminuir debido a la convención y conducción (calor sensible) (Nobel, 2020).

Con respecto al calor por conducción y convección, la temperatura de las hojas puede modificarse por dos tipos de convección: forzada y libre. La convección forzada ocurre cuando la velocidad del viento es alta por lo que se da lugar a la transferencia de energía calorífica. La convección libre sucede cuando la primera capa de aire en contacto con la superficie de la hoja se expande, disminuyendo su densidad y posteriormente desplazándose hacia arriba. La capa de aire responsable de transferir la energía entre la hoja y la atmósfera recibe el nombre de capa límite; esta capa puede formar flujos laminares o turbulentos dependiendo de la rugosidad de la superficie de la hoja. El grosor de la capa límite puede presentar variaciones dependiendo del tamaño de la hoja, lo que ofrece una mayor o menor resistencia al intercambio de energía y materia (Collazo-ortega, 2013; Nobel, 2020; Sirvydas et al., 2010). La capa límite puede calcularse a partir de la siguiente ecuación:

$$\delta^{bl}_{(mm)} = 4.0 \sqrt{\frac{l_{(mm)}}{v_{(ms^{-1})}}} \tag{1.4}$$

donde $l_{(m)}$ es la longitud de la hoja con respecto a la dirección del viento predominante en metros, $v_{(ms-1)}$ es la velocidad del viento en m s^{-1} y $\delta^{bl}_{(mm)}$ es el total del grosor de la capa límite en mm y el facto 4.0 considera la temperatura del aire en la capa límite con unidades de mm s^{-1}.

Una vez considerada la capa límite de ambos lados de la hoja, se expresa que la temperatura de la hoja no depende de la apertura estomática sino del viento turbulento que atraviesa la capa límite. Cuando la hoja pierde calor hacia los alrededores el flujo de densidad del calor es positivo.

$$J_H^C = -2K^{aire} \frac{(T^{hoja} - T^{aire})}{\delta^{bl}_{(mm)}} \tag{1.5}$$

Donde:

Transpiración:

$$J_H^T = \frac{H_{vap} D_{wv} (c^{e}_{wv} - c^{ta}_{wv})}{\Delta x^{total}} \tag{1.6}$$

Otro aspecto importante por considerar en el balance de energía es el ángulo de las hojas, ya que las hojas que presentan ángulos cercanos a 90° son capaces de disminuir la cantidad de radiación solar que reciben protegiéndose de la fotoinhibición. Las hojas en posición vertical escapan de altas temperaturas y logran mantener un estado hídrico óptimo, mostrando que aún con una alta cantidad de radiación la fotosíntesis puede continuar (Mc Millen & John H. Mc Clendon, 1979; Lovelock & Clough, 1992).

1.1.6 ANATOMÍA FUNCIONAL DE *Rhizophora mangle*

Rhizophora mangle L. es una especie que se encuentra en primera línea de defensa en los bosques de manglar y se caracteriza por presentar estrategias fisiológicas, anatómicas y reproductivas como las xerófila presente en las hojas (Tomlinson, 2016).

Las hojas de *R. mangle* se caracterizan por tener una capa de cutícula, epidermis uniseriada en ambos lados de la hoja y una hipodermis con seis capas de células que presentan una forma cuadrada a circular. Las hojas también presentan una capa de cutícula que protege las hojas de la radiación solar, así como la presencia de numerosos idioblastos y esclereidas, clasificándose como hojas esclerófilas, esto último es relevante debido a que se sugiere que podría ser una característica diagnosis de especies que invierten en tejidos mecánicamente resistentes debido a la alta radiación y una baja disponibilidad de recursos como agua y nutrientes (Lucena *et al*., 2011; Lima *et al*., 2013). Las hojas esclerófilas podrían mostrar diferentes grados de lignificación y cutinización repercutiendo en su grosor, por ejemplo, se sabe que las hojas de manglar chaparro de *R. mangle* se consideran esclerófilas con un grosor de 1100 um, no obstante, las hojas de la misma especie de otro ecotipo con un grosor de 600 um también fueron consideradas como esclerófilas (Feller *et al*., 2007; Lima *et al*., 2013). El grosor de las hojas relacionada con la esclerofilia podría estar relacionado con el área foliar, así repercutiendo en la resistencia mecánica y el grosor de la capa límite que finalmente actúa como una resistencia para la difusión de gases como vapor de agua y CO_2 (Read *et al*., 2006).

En la cara abaxial se encuentran los estomas de tipo anomocítico y se presume la presencia de glándulas secretoras de sal, sin embargo, no se ha presentado evidencia y tampoco se ha estudiado si la densidad de glándulas se puede ver modificada dependiendo del ambiente Lima *et al*., 2013).

1.1.7 FISIOECOLOGÍA EN ESPECIES DE MANGLAR

La mayoría de los estudios fisioecológicos en especies de mangle se han enfocado en su resistencia a la salinidad, relaciones hídricas, disponibilidad de nutrientes e intercambio de gases (Lugo, 1980; Werner & Stelzer, 1990; Farnsworth *et al*., 1996; Khan *et al*., 2014; Lovelock *et al.,* 2016; Hogan *et al.,* 2021). Estos trabajos han mostrado que la salinidad es un factor clave para el establecimiento y crecimiento de diversas especies de mangle, las cuales presentan adaptaciones fisiológicas y anatómicas que les permiten prosperar en ambientes salinos. En particular, se ha documentado que la salinidad, en niveles moderados, puede favorecer el crecimiento de algunas especies, al mismo tiempo que regula procesos como la absorción de agua y nutrientes (Ball, 1998; Suárez & Medina, 2005).

Sin embargo, el exceso de salinidad también representa un estrés fisiológico que obliga a las plantas a mantener un balance de iones tanto a nivel radicular como foliar para conservar la turgencia celular, evitar el colapso de tejidos y proteger el aparato fotosintético. Para ello, las especies de mangle regulan la acumulación y exclusión de sales mediante diferentes mecanismos como la excreción de sal por glándulas (*Avicennia germinans*), exclusión radicular (*Rhizophora mangle*) y el almacenamiento de sales en vacuolas. Además, estas especies acumulan osmolitos orgánicos e inorgánicos (como prolina, manitol, glicina-betaína, entre otros) que les permiten mantener su potencial hídrico y la actividad enzimática en condiciones adversas (Parida & Jha, 2010).

Las estrategias fisiológicas y anatómicas asociadas a la toma y conservación de agua hacen que los mangles sean altamente eficientes en el uso de este recurso. Esto significa que, a pesar de las condiciones extremas de salinidad e inundación, las especies pueden extraer el agua necesaria para sus funciones vitales y al mismo tiempo minimizar su pérdida durante el proceso de intercambio gaseoso con la atmósfera. Este intercambio está mediado por la apertura estomática, que busca optimizar la captura de CO_2 para la fotosíntesis con la menor pérdida posible de agua por transpiración (Lovelock & Feller, 2003).

En este contexto, algunos estudios recientes se han enfocado en cuantificar el flujo de agua a través del sistema vascular (Cao *et al.*, 2020; Steppe *et al.*, 2015; López-López *et al.*, 2013), ya que este está directamente relacionado con la transpiración y, por tanto, con el aporte de agua a la atmósfera. A pesar de que las especies de mangle son consideradas conservadoras en el uso del agua, se ha planteado la hipótesis de que pueden tener un rol relevante en el ciclo hidrológico costero, contribuyendo al vapor de agua disponible para procesos locales de precipitación y regulación microclimática.

En la Península de Yucatán, los estudios fisioecológicos sobre manglares han avanzado en diversas líneas de investigación, incluyendo, la arquitectura hidráulica en ecotipos de franja y chaparros de *Rhizophora mangle* (Cisneros-De la Cruz *et al.*, 2022); el efecto de la inundación sobre el crecimiento y la tasa fotosintética (Salas-Rabaza *et al.*, 2024); los flujos de CO_2 en neumatóforos de *Avicennia germinans* (Salas-Rabaza *et al.,* 2024); la tolerancia al estrés hídrico en plántulas (Martínez, 2024); las relaciones hídricas entre planta madre y propágulos (Cerón-Aguilera, 2020); la influencia de la excreción de sal sobre el balance energético (González, 2022).

No obstante, a pesar del avance en estas áreas, aún existe una importante laguna en el conocimiento sobre el aporte de agua por transpiración en los bosques de manglar, especialmente bajo condiciones de perturbación antrópica. Además, se requiere mayor entendimiento del balance de energía en manglares conservados en comparación con aquellos afectados por disturbios, ya que estas condiciones pueden alterar significativamente los flujos de energía y materia, y por ende, la capacidad de los manglares para brindar servicios ecosistémicos.

Estudiar la fisiología de los manglares es crucial para entender cómo estas especies responden a cambios ambientales y presiones antropogénicas, lo cual tiene implicaciones directas en su capacidad para proveer servicios ecosistémicos. Entre estos servicios destacan la protección costera frente a tormentas y huracanes, la regulación del clima mediante el almacenamiento de carbono y la transpiración, la conservación de la biodiversidad y la provisión de hábitats para especies clave. Comprender los mecanismos fisioecológicos detrás de estos procesos permite diseñar estrategias de manejo y restauración más eficaces, orientadas a garantizar la resiliencia de los ecosistemas de manglar frente al cambio climático y al desarrollo costero no planificado.

1.1.8 FLUJO DE SAVIA

El transporte de agua en ramas, tallos y raíces se puede medir por medio de trazadores de calor. La aplicación de las técnicas se comenzó a desarrollar hace un poco más de un siglo (James and Baker 1933; Dixon 1914). Las técnicas mayormente empleadas en diferentes estudios son: 1) Pulso de calor (HPM; Marshall, 1958; Huber, 1932); 2) balance de calor en segmentos de tallo (THB; Čermák y Deml 1974); 3) Balance de calor en el tallo (SHB; Sakuratani 1981); 4) Disipación de calor (HD; Granier, 1985) y deformación del campo térmico (HFD) (Nadezhdina *et al.* 1998; Nadezhdina y Čermák 1998).

El método de disipación de calor (HD) es ampliamente usado debido a la sencilles para la construcción de los sensores, bajo costo (comparado con otros métodos), permite medir flujos lentos (0 – 80 cm^3 cm^{-2} h^{-1}) (Steppe, 2010) y la relativa facilidad para procesar los datos. Los sensores de HD se pueden adaptar para contar con mediciones a diferentes profundidades y entonces conocer el flujo de savia radial y considerar los gradientes naturales de temperatura (NTG's). Sin embargo, algunas de las limitantes del método se relacionan con su incapacidad para detectar flujos reversos y muy lentos, otra cuestión es la subjetividad de la estimación del flujo cero (Vandegehuchte & Steepe, 2013; Gutiérrez-López, 2022). Sin embargo, se pueden reducir los errores añadiendo un tercer sensor, realizando pruebas de calibración (gravimetría), manteniendo el provisionamiento de energía constante, establecer una línea base considerando la variación del flujo cero de diferentes días y comparando con datos ambientales, ya que el flujo puede llegar a sufrir fuertes disminuciones de velocidad cuando hay lluvias o condiciones nubladas (Lu *et al.,* 2004).

El principio del método HD se basa en la estimación de la densidad de flujo de savia (F_d; m^3 m^{-2} s^{-1}, g cm^{-2} s^{-1}) calculada a partir de la diferencia de temperatura entre dos sensores colocados de 10 – 15 cm de distancia uno de otro, en el cual el sensor de calentamiento (colocado aguas abajo) se encuentra a una temperatura constante (0.2 watts) y un sensor de referencia (aguas arriba) el cual no debe ser afectado por el calor disipado (Granier, 1985). En el cual:

$$F_d = 118.99\ x\ 10^{-6} \left[\frac{\Delta Tmax - \Delta T}{\Delta T}\right]^{1.231} \tag{1.7}$$

Donde, la diferencia de temperatura máxima está dada por la diferencia de temperatura entre los dos sensores en el cual la savia no tiene desplazamiento. Posteriormente, el F_d puede convertirse a flujo de savia (SF; g s^{-1}, L h^{-1}, m^3 $día^{-1}$) considerando la porción del área conductora (albura) (Fig.1.7).

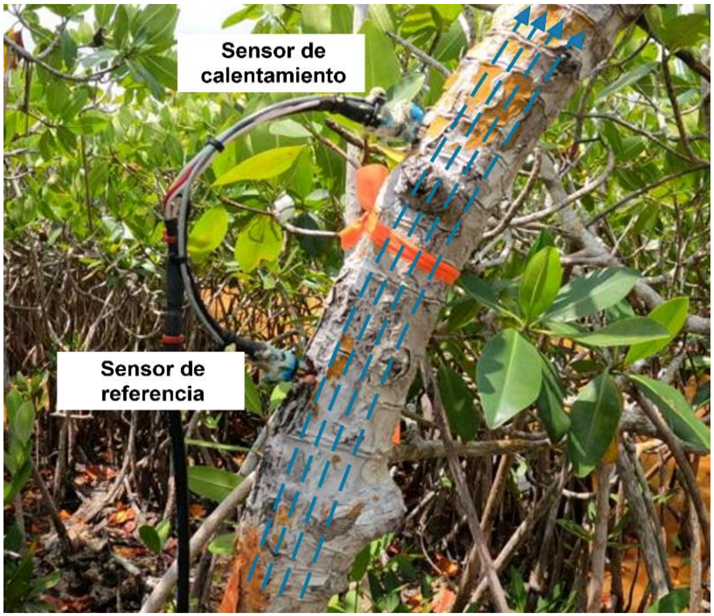

Figura 1.7 Sensor de disipación térmica tipo Granier que mide el flujo de savia instalado en el tronco. Se muestra el sensor de referencia (aguas arriba) y sensor de calentamiento (aguas abajo).

Los sensores contienen un termopar tipo T que consta de una aleación de constantan y cobre (Fig.1.8), en el cual se detecta en el que se considera que por cada diferencia de voltaje éste equivale a una diferencia la diferencia de voltaje (mV) que es convertida en temperatura real, empleando el coeficiente de Seebeck de temperatura (Vandegehuchte & Steppe, 2013; Gutiérrez-López, 2022). Los sensores son conectados a un registrador de datos en el cual se almacenan las mediciones realizadas cada 10 - 60 segundos y promediarse entre 10 – 60 minutos, dependiendo del objetivo de la investigación (Gutiérrez-López, 2022).

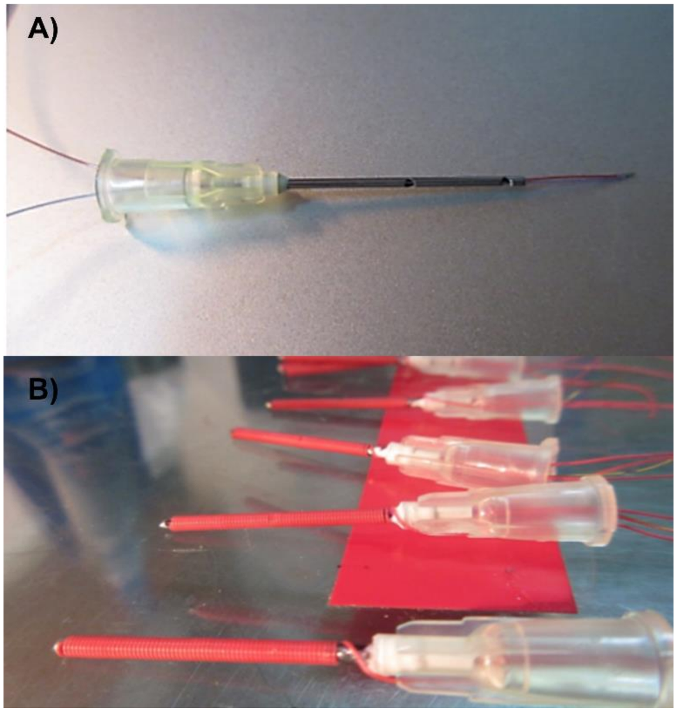

Figura 1.8 Construcción de sensores de disipación térmica tipo Granier. A) Aguja con cables de constantan y cobre y B) sensores de calentamiento terminados. Tomadas y modificadas de Gutiérrez-López, 2022.

1.1.9 MÉTODOS DE BALANCE DE ENERGÍA

Las mediciones del balance energético foliar han cobrado mayor relevancia debido a su influencia sobre la fotosíntesis y las relaciones hídricas, especialmente en ambientes con alta radiación. En estas condiciones, la disipación de calor en forma de calor latente puede verse limitada, ya que las plantas tienden a reducir la pérdida de agua para evitar embolismos. En consecuencia, la regulación de la temperatura foliar ocurre principalmente mediante la disipación de calor sensible (Muller *et al.,* 2023; O'Sullivan *et al*., 2017; Long *et al*., 1994).

La interacción entre el calor sensible, el calor latente y la radiación neta suele medirse en condiciones controladas, mediante hojas artificiales, túneles de viento, fuentes de radiación o cámaras ambientales (Chávez, 2020; Schymanski & Or, 2017). Sin embargo, las mediciones del balance energético a escala foliar en condiciones de campo han sido menos frecuentes debido a la alta variabilidad ambiental y a la influencia de factores como las hojas circundantes, que pueden afectar la transferencia de calor latente y la humedad relativa del entorno (Muller *et al.,* 2023).

A nivel de ecosistema, el balance energético ha sido mayormente estudiado mediante torres de *eddy covariance* (Uuh-Sonda *et al*., 2022; Alvarado-Barrientos *et al*., 2021; Freire *et al*., 2021; Barr *et al.,* 2013; ; Rodda *et al*., 2016), que permiten estimar el flujo de calor latente, calor sensible y radiación neta. No obstante, este enfoque no permite distinguir qué proporción del calor latente proviene de la transpiración frente a la evaporación del suelo (Salas-Acosta *et al*., 2022; Schlesinger *et al*., 2014). Además, al no enfocarse en el nivel foliar, no se pueden comprender con precisión los mecanismos de regulación térmica (termorregulación) que las plantas emplean frente a condiciones ambientales variables.

Varios autores han señalado la urgencia de realizar estudios de balance energético a nivel foliar en campo, con el fin de entender mejor la respuesta de las plantas a los cambios ambientales y sus implicaciones en el contexto del cambio climático (Muller *et al*., 2021, 2023).

Una de las principales dificultades en estos estudios es la estimación del flujo de calor sensible a nivel foliar, ya que, a diferencia del enfoque con torres de *eddy covariance*, este no puede medirse directamente. Por ello, se han propuesto diferentes metodologías para estimar los componentes del balance energético a nivel de hoja, rama o dosel: 1) el modelo de Penman-Monteith, que utiliza mediciones directas y sus variantes (Muller *et al.,* 2023, 2021; Vialet-Chabrand *et al*., 2019; Monteith & Unsworth, 2012), y 2) cálculos basados en principios físicos (Nobel, 2020).

Cada una de estas metodologías presenta limitaciones, especialmente en la estimación de la conductancia estomática y del flujo de calor sensible, ya que ambos están relacionados con la transferencia de materia (vapor de agua) y energía (calor) hacia la atmósfera mediante flujos que no son exclusivamente laminares, sino también turbulentos. Además, es necesario capturar la alta variabilidad de las condiciones microambientales (como la radiación solar y la convección libre o forzada). Sin embargo, esta variabilidad puede reducirse mediante una estrategia de muestreo adecuada — seleccionando grupos de hojas con condiciones similares— y mediante la simplificación de variables, como al considerar la resistencia de la capa límite. Estas aproximaciones permiten obtener estimaciones válidas a nivel foliar.

1.2 JUSTIFICACIÓN

Por todo lo anterior, es fundamental realizar estudios que integren los aspectos ecohidrológicos y la anatomía funcional de los bosques de manglar chaparro de *Rhizophora mangle* en la península de Yucatán. Estos estudios permitirán comprender mejor los mecanismos que rigen los procesos fisiológicos y su relación con los servicios ecosistémicos, como la regulación del ciclo del agua y del clima. Además, el estudio de bosques de manglar con diferentes proporciones de cobertura vegetal contribuye a entender la modificación de estos procesos y los servicios ecosistémicos asociados a la regulación del clima. La información fisioecológica generada puede proporcionar una base científica sólida para los tomadores de decisiones, facilitando la implementación de estrategias de manejo que optimicen la conservación y restauración de los manglares, así como su contribución a la regulación del clima. Asimismo, los resultados obtenidos en esta investigación pueden ser fundamentales para la elaboración de modelos predictivos que guíen acciones efectivas de restauración y conservación de los bosques de manglar, maximizando su capacidad de mitigación de los impactos del cambio climático.

1.3 PREGUNTAS DE INVESTIGACIÓN

- ¿Cuál es la variación del flujo de savia y su relación con las variables microambientales, como la radiación solar, el flujo de fotones fotosintéticamente activos (PPF), el déficit de presión de vapor (VPD), la salinidad intersticial y la velocidad del viento?

- ¿Cuánta agua es transferida a la atmósfera por transpiración a nivel de ecosistema a partir del flujo de savia?

- ¿Cuál es el efecto del microambiente sobre el balance de energía en dos poblaciones de *Rhizophora mangle* en Yucatán, diferenciadas por su grado de conservación y densidad, durante la estación seca y la lluviosa?

- ¿Cómo varían los componentes del balance de energía en hojas de diferentes estratos de plantas adultas en poblaciones con distinta cobertura vegetal?

1.4 HIPÓTESIS

Se espera que el flujo de savia sea mayor durante la temporada de sequía debido a la alta demanda evaporativa generada por el mayor déficit de presión de vapor (DPV), la alta radiación solar y el flujo de fotones fotosintéticos (PPF). En contraste, durante la temporada de lluvia, la disminución del DPV, la radiación solar y el PPF reducirán el flujo de savia. Además, se anticipa que el índice de área foliar (LAI) incrementará en la temporada de lluvia debido a la mayor disponibilidad de agua y a la disminución de la salinidad, lo que promoverá el crecimiento foliar. Estas diferencias entre temporadas también influenciarán la anatomía foliar, esperándose variaciones en el área de la cavidad subestomática entre las estaciones de sequía y lluvia.

Es probable que en los manglares chaparros de *Rhizophora mangle* con menor cobertura vegetal, las hojas presenten adaptaciones anatómicas como mayor esclerofilia, suculencia y cutinización de la epidermis, en comparación con los individuos de manglares con mayor cobertura vegetal. Estas adaptaciones permitirán reducir la pérdida de agua bajo condiciones de mayor exposición solar y menor disponibilidad de recursos hídricos. Además, se anticipa que en los manglares de menor cobertura vegetal el balance de energía se verá modificado, con un incremento en la disipación de calor sensible y una disminución del calor latente, lo que refleja una estrategia de acoplamiento al ambiente para evitar la pérdida excesiva de agua a través de la transpiración.

1.5 OBJETIVO GENERAL

Evaluar el flujo de agua y balance de energía de manglares chaparros de *Rhizophora mangle* L. considerando la variabilidad temporal mediante anatomía funcional en Yucatán, México.

1.6 OBJETIVOS ESPECÍFICOS

Capítulo II

Evaluar la variación diurna y estacional del flujo de savia de *R. mangle*. Analizar la relación del flujo de savia y variables anatómicas foliares y del sistema vascular con variables microambientales, como la radiación solar, el flujo de fotones fotosintéticamente activos (PPF), el déficit de presión de vapor (VPD), la salinidad intersticial y la velocidad del viento, así como estimar la transpiración a nivel de ecosistema.

Capítulo III

Analizar el efecto del microambiente en el balance de energía y anatomía foliar de dos poblaciones de manglar chaparro de *R. mangle* en Yucatán durante las temporadas de lluvia y sequía, así como evaluar los componentes del balance de energía en hojas de diferentes estratos de plantas adultas en poblaciones con variación en la cobertura vegetal.

1.7 ESTRATEGIA EXPERIMENTAL

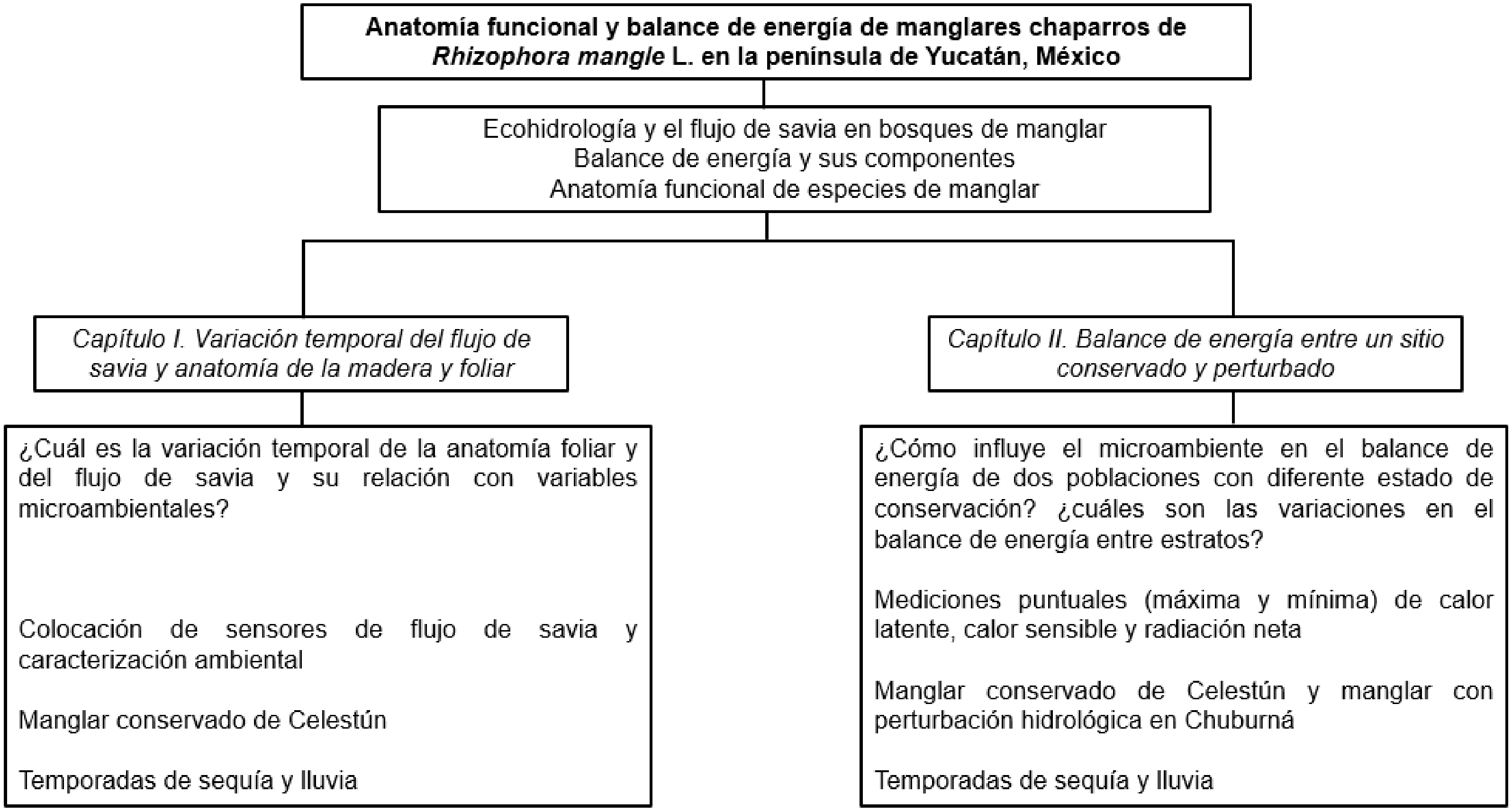

Anatomía funcional y balance de energía de manglares chaparros de *Rhizophora mangle* L. en la península de Yucatán, México

Ecohidrología y el flujo de savia en bosques de manglar
Balance de energía y sus componentes
Anatomía funcional de especies de manglar

Capítulo I. Variación temporal del flujo de savia y anatomía de la madera y foliar

¿Cuál es la variación temporal de la anatomía foliar y del flujo de savia y su relación con variables microambientales?

Colocación de sensores de flujo de savia y caracterización ambiental

Manglar conservado de Celestún

Temporadas de sequía y lluvia

Capítulo II. Balance de energía entre un sitio conservado y perturbado

¿Cómo influye el microambiente en el balance de energía de dos poblaciones con diferente estado de conservación? ¿cuáles son las variaciones en el balance de energía entre estratos?

Mediciones puntuales (máxima y mínima) de calor latente, calor sensible y radiación neta

Manglar conservado de Celestún y manglar con perturbación hidrológica en Chuburná

Temporadas de sequía y lluvia

CAPÍTULO II

SEASONAL DYNAMICS AND MICROENVIRONMENTAL DRIVERS OF TRANSPIRATION IN SCRUB *Rhizophora mangle* L. FROM YUCATÁN

Este capítulo fue aceptado en *Forests* en la sección de *Forest Ecophysiology and Biology* en el número especial de *Water Relations in Tree Physiology* y debe ser citado y referido de la siguiente manera:

Cerón-Aguilera, G.; Yáñez-Espinosa, L.; Echevarría-Machado, I.; Méndez-Alonzo, R.; Herrera-Silveira, J.; Us-Santamaría, R.; Salas-Rabaza, J.A.; González, Muñoz K.E. and Andrade, J.L. (2025). Seasonsal dynamics and microenvironmental drivers of transpiration in scrub *Rhizophora mangle* L. trees from Yucatán. *Forests*. 16(2), 351. https://doi.org/ 10.3390/f16020351

ABSTRACT

Scrub mangrove forests, dominated by *Rhizophora mangle* L., are characterized by high porewater salinity, which might compromise individual sap flow rates (SF) due to seasonal and diurnal microenvironmental variations. We tested the functional, anatomical, and SF responses of 12 individuals to microenvironmental variables such as solar radiation, photosynthetic photon flux, wind speed, evaporative demand, and porewater salinity, measured using an in situ weather station. Measurements were made in the dry and rainy seasons in the Yucatan Peninsula, using Granier heat dissipation sensors, installed on tree branches. During the rainy season, SF was twice as high as that during the dry season (0.22 ± 0.00 L h^{-1} and 0.11 ± 0.00 L h^{-1}, respectively), despite lower evaporative demand. In both seasons, negative relationships between SF with vapor pressure deficit (VPD; dry $\tau = -0.54$; rainy $\tau = -0.56$) and with photosynthetic photon flux (PPF; dry $\tau = -0.97$; rainy $\tau = -0.98$) were found, indicating a strong hydraulic coupling to atmospheric conditions. Sap flow and transpiration rates of this *R. mangle* scrub mangrove forest exceeded those of some tropical dry deciduous forests, suggesting adaptations that support water transport in saline environments. The clustered xylem vessels of *R. mangle* ensure safe sap flow year-round. As an evergreen species, it contributes water to the atmosphere all year-round, underscoring its critical role in the tropical ecohydrological environment.

Keywords: Celestun; sap flow; scrub mangrove; Mexico; red mangrove; vapor pressure deficit; water transport

2.1. INTRODUCTION

Mangrove forests are wetlands found along tropical and subtropical coasts, whose species exhibit distinct morphological and physical traits to cope with factors such as hydroperiod, salinity, and microtopography (Lugo & Snedaker, 1974). Consequently, mangrove species occupy different ecological niches, thus determining the structure, composition, and attributes of mangrove forests. In the Yucatan Peninsula, there are four main ecological types of mangroves, i.e., fringe, basin, petén, and scrub (Tomlinson, 2016; Zaldivar-Jimenez *et al*., 2010). Among these, the scrub mangrove has the widest distribution in the region. Each ecological type provides unique ecosystem benefits depending on its composition and environmental conditions (Velázquez-Salazar *et al*., 2020; Giri *et al*., 2011; Batllori-Sampedro & Febles-Patrón, 2007).

Understanding the ecohydrological processes of scrub mangroves, particularly their contributions to transpiration and water exchange with the atmosphere, provides insights into how these ecosystems function under varying environmental conditions. This knowledge will provide information for conservation and management strategies for mangrove forests worldwide, related to the provision of ecosystem services and climate regulation at different scales, especially in the face of climate change and increasing anthropogenic pressures (Bimrah *et al*., 2022).

The environmental conditions of scrub mangroves are challenging due to high salinity and their dependence on freshwater inputs from precipitation. Indeed, *Rhizophora mangle* L. has unique adaptations to seawater conditions, particularly salinity and flooding levels. As a facultative halophyte, *R. mangle* is capable of coping with varying salinities by storing Cl^- and Na^+ ions to maintain osmotic balance. These adaptations facilitate significant belowground carbon accumulation (Cisneros-De La Cruz *et al.,* 2022; Sánchez *et al*., 2021; Herrera-Silveira *et al*., 2020). High evaporation rates, especially during drought, elevate porewater salinity levels, further impacting the vascular system. These forested wetlands are distinguished by a strong hydraulic connection along the soil–plant–atmosphere continuum that facilitates the continuous exchanges of freshwater and energy through transpiration. However, despite their significance, few studies have explored the contribution of transpiration to atmospheric water in mangrove forests (Krauss *et al*., 2022, 2014, 2007; Liang *et al*., 2019; K. Wang & Dickinson, 2012; Becker et al., 1997; Hirano et al., 1996).

Transpiration is regulated by stomatal conductance, which controls gas exchange, including CO_2 uptake and water release. Stomatal conductance is, in turn, influenced by environmental factors, including vapor pressure deficit (VPD), solar radiation (SR), and wind speed (WS) (Naithani *et al.,* 2012). Exploring the balance between these processes is critical because they reveal how stomatal and canopy conductance are coupled with the atmosphere (Blanken *et al*., 1997; Jackson *et al*., 1997; Jarvis & Mcnaughton, 1986). To document the variability in the rates of transpiration, sap flow measurements are an ideal tool, as they work as a key indicator of this hydraulic connection (Poyatos *et al*., 2020; Steppe *et al*., 2015; Tang *et al*., 2006; Granier, 1987).

A significant amount of water is returned to the atmosphere through transpiration, accounting for up to 40% of the water supplied to land through precipitation and 70% of total evapotranspiration (Oki & Kanae, 2006). This process can be measured at different levels, including leaves, branches, trunks, whole plants, and ecosystems. Measuring transpiration at the individual plant level is particularly practical, as it exhibits less variability compared to leaf-level measurements (Jarvis, 1995).

Transpiration is closely linked to the transport of water from roots to leaves through the sap flow in the plant's vascular system. Thermometric sap flow methods are widely used to measure these dynamics, as they provide insights into daily and interannual variations (Oki & Kanae, 2006) Moreover, sap flow measurements can be upscaled to the whole plant, enabling continuous quantification of the plant's water use (Wilson *et al*., 2008; Oki & Kanae, 2006). This information also allows estimation of the contribution of water to the atmosphere through transpiration.

On the other hand, the anatomical traits of the leaves and vascular system, such as the xylem, reflect the adaptations of *R. mangle* to flooded environments and high salinity in the porewater. Their leaves contain intercellular spaces formed by aerenchyma tissue, a type of parenchyma found in mangrove species, associated with the transport and movement of gases, as well as with the storage water within the parenchyma. This tissue also facilitates the movement of water vapor from the internal plant tissues to the atmosphere (Wang *et al*., 2019). The characteristics of the xylem vessels, such as diameter, vessel density, and vessel grouping, provide valuable information about the plant's hydraulic architecture, revealing its relationship with environmental variables, such as salinity, nutrients, and temperature (Evans & Bromberg, 2010). Given that *R. mangle* plays a crucial role in ecohydrological processes, filtering seawater at the root level, which is subsequently transported to the leaves and released into the atmosphere as water vapor through transpiration (Madrid *et al*., 2014), it is critical to understand the contribution of scrub mangroves, dominated by *R. mangle*, to the ecohydrological processes through transpiration, and to depict the intrinsic (anatomical and functional traits), as well as the extrinsic abiotic environmental factors that control both sap flow and transpiration (Leng & Cao, 2020; Asbjornsen *et al*., 2011; Reef & Lovelock, 2015). Therefore, this research pursues the following aims: (1) to assess the diurnal and seasonal variation of sap flow; (2) to test the relationship of sap flow with microenvironmental variables, such as solar radiation, photosynthetic photon flux (PPF), VPD, porewater salinity, and wind speed; and (3) to estimate ecosystem transpiration based on sap flow. We hypothesize that, during the rainy season, lower VPD will result in decreased sap flow whereas, in the dry season, sap flow will be strongly influenced by solar radiation and VPD. Overall, our results will lead to refined ecohydrological models, taking into account the relevance of this vastly distributed ecosystem within the Yucatan Peninsula, as well as in other equivalent mangrove ecosystems in the tropics.

Mangrove forests play a critical role in mitigating climate change, maintaining biodiversity, and supporting ecosystem services, such as carbon storage and water cycling. Understanding the ecohydrological processes of scrub mangroves, particularly their contributions to transpiration and water exchange with the atmosphere, provides insights into how these ecosystems function under varying environmental conditions. This knowledge can inform conservation and management strategies for mangrove forests worldwide, especially in the face of climate change and increasing anthropogenic pressures.

2.2. MATERIALS AND METHODS

2.2.1. Study area

The Ría Celestun Biosphere Reserve was selected as the study area (Figure1A). The area is characterized by a salinity gradient associated with the lagoon, where many ecosystems, such as deciduous forests, dunes and mangrove ecotypes are present, including fringe, scrub, petén and basin [35, 36]. The Celestun reserve has a seasonal variation related to rainfall, distinguishing dry (March–May), rainy (June–October), and early dry (nortes; November–February) seasons. The porewater salinity during the rainy season in scrub mangrove ranges from 42.7–51.42 ppm, mean sediment water potential is −1.91 MPa, and a maximum vapor pressure deficit (VPD) range from 0.94 to 1.38 kPa (Herrera-Silveira *et al.*, 2020). The climate is predominantly semi-arid, with rain in the summer (767 mm mean precipitation) (Herrera-Silveira, 1994). Most of this preserve is in good conservation condition. It has been designated as a Ramsar site (site no. 133) and is a long-term study site to understand the different ecosystem services that are provided locally and regionally (Cinco-Castro & Herrera-Silveira, 2020).

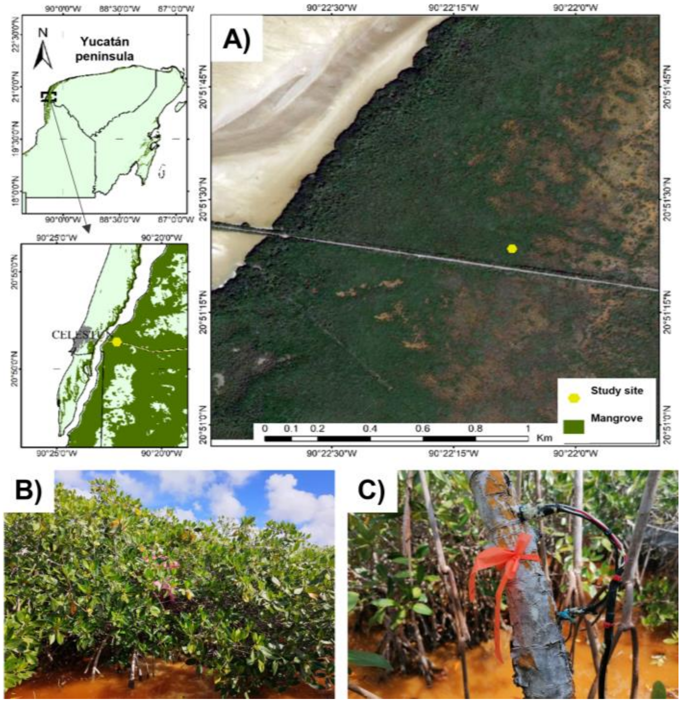

Figure 2.1 Location of the study site in the Celestun Biosphere Reserve. Yellow dots indicate the study site. Created with QGIS (version 3.22.14-Białowieża) (**A**). Scrub *R. mangle* trees (**B**), Granier's sensors probes (heat dissipation method) placed in the tree branches (**C**).

2.2.2. Microenvironment

Microenvironmental data were collected in the study site (20° 51.400′ N, 90° 22.248′ W) during the dry (April) and rainy (October) seasons in 2021. Air temperature and relative humidity were measured with a temperature probe (12 bit temp/rh sensor S-TMB-M003, Onset Computer Corporation, Bourne, MA, USA), wind speed with a cup anemometer, wind direction with a wind vane (S-WCA-M003, Onset Computer Corporation, Bourne, MA, USA), photosynthetic photon flux (PPF) with a quantometer (S-LIA-M003, Onset, Bourne, MA, USA), solar radiation with a pyranometer (S-LIB-M003, Onset, Bourne, MA, USA) and dew deposition with a leaf wetness sensor (S-LWA-M003, Onset, Bourne, MA, USA) (this variable was only measured during the dry season based on the availability of the sensor). The data were recorded using a datalogger (U30-NRC Weather Station, Onset, Bourne, MA, USA) every 10 s and averaged in intervals of 10 min. The VPD was calculated according to Jones (2014)Haz clic o pulse aquí para escribir texto., as follows:

$$VPD = e_S\,(T) - e \tag{2.1}$$

where *e* is the partial pressure of water vapor in air; and $e_S\,(T)$ is the saturation partial pressure of water vapor in function of the temperature. The saturation partial pressure $e_S\,(T)$ can be calculated using the following formula:

$$e_S\,(T) = 6.112\ \cdot exp\left(\frac{18.678-\frac{T}{234.5}}{257.14+T}\right) \tag{2.2}$$

The partial pressure of water vapor (e) is calculated as $e{=}RH$. The relation between air temperature (T) and relative humidity (RH) is known as evaporative demand due to the increase in temperature.

A sample of porewater was drawn using an acrylic tube at a depth of 30 cm and salinity was measured with a multiparameter probe (Model Pro2030, YSI, Yellow Springs, OH, USA) at every sampled tree.

2.2.3. Microenvironment

Sap flux density (F_d) was continuously recorded for eight days during the dry and rainy seasons in branches of twelve individual trees, with mean diameter of 4.5 cm, using custom-made Granier (Granier, 1987) (Granier, 1987) type sensors (Figure 1C). The selection of branches with these diameters was based on previous observations during a related study, where we noted that the conductive sapwood in *R. mangle* branches was sufficiently large to accommodate the temperature probes without exceeding the conductive portion. Pairs of 30-mm-long, 2-mm temperature probes were inserted into the sapwood of the branches. The upper probe was heated continuously with a constant power supply (0.2 W), supplied by a 12-V deep cycle marine battery connected to a solar panel, while the bottom unheated probe (10 cm below) recorded the sapwood temperature. This steady temperature approach allows for the identification of dynamic changes and low sap flow rates, reducing biases. The protruding portions of both probes were insulated with a layer of foam surrounded by an outer shield of reflective material and transparent plastic. Probe temperatures were recorded continuously at 10-s intervals with a datalogger (CR3000, Campbell Scientific, Logan, UT, USA), and 10-min averages were downloaded. Temperature differences between both sensor probes were used to calculate F_d (L m^{-2} h^{-1}), using the following equation:

$$F_d = 118.99\ x\ 10^{-6} \left[\frac{\Delta Tmax - \Delta T}{\Delta T}\right]^{1.231} \tag{2.3}$$

where, ΔT_{max} is the maximum temperature difference between sensor probes at zero flux and ΔT is the temperature difference at a given F_d.

To calculate sap flow (SF), the sapwood cross-sectional area (Asw) was determined by injecting vegetable dye into cores from branches, at the same height at which the sap flow sensors were installed, after the dry and rainy measurements were completed. The dye was allowed to move through the vascular system for one hour before extracting the cores using an increment borer (5.5 mm diameter, Haglöf, Längsele, Sweden). Then, the length of the sapwood was measured using a caliper (Scherr-Tumico, Syracuse, NY, USA), and the area (AswAsw; cm^2) was obtained using the following equation:

$$A_{sw} = \frac{\pi}{4}\left(D^2 - d^2\right) \tag{2.4}$$

where, π= pi value, D= larger diameter (cm), d= shorter diameter (cm). Sap flow (SF; L h^{-1}) was calculated as follows:

$$SF = Fd * A_{sw} \tag{2.5}$$

2.2.4. Transpiration

Transpiration per branch was estimated from sap flow (SF) scaled by the total leaf area (TLA) of the branch. The TLA was calculated by multiplying the branch’s canopy cover area by the leaf area index (LAI). The branch canopy cover area was mapped at ground level, and the LAI was measured using a Plant Canopy Analyzer (LAI-2200C, LI-COR Biosciences, Lincoln, NE, USA) by taking four measurements in the cardinal direction at 90°, with one additional measurement outside the canopy under full light conditions for reference.

Additionally, TLA was independently estimated by counting the total number of leaves on the branch and multiplying by the average leaf area measured with an area meter (LI-3100, LI-COR, Lincoln, NE, USA) (Jackson et al., 1997) (Jackson et al., 1997).

Finally, transpiration per branch was multiplied by the branch density per hectare to upscale (E_L) the stand transpiration (mm day^{-1}). This approach allowed the integration of sap flow (SF) measurements to estimate transpiration at the stand level.

2.2.5. Vascular system and leaf anatomy

The wood samples of the 12 stems were collected at the end of the sap flow measurements. The wood segments were cut at a height of 1.3 m and 20 cm in length, then fixed in FAA (formaldehyde–ethanol-glacial acetic acid, distilled water 10:50:5:35) for 48 h. Afterward, they were washed with tap water and stored in glycerin–ethanol-distilled water (1:1:1) until sectioning. Each stem sample was sectioned into subsamples of 5 × 7 × 3 cm. Xylem transverse, radial and tangential sections were obtained using a sliding microtome (GSL-1, Swiss Federal Research Institute WLS, Birmensdorf, Switzerland) at a thickness of 50 μm. The sections were rinsed, bleached with commercial chlorine (50%), then washed with tap water. The sections were dehydrated in a degraded ethanol series through 50%, 70% and 95% and stored until sectioning. The sections were stained with safranin-fast green and mounted in synthetic resin.

The slides were observed with an Olympus optical microscope (U-CMAD3, Tokyo, Japan) with an integrated camera (Infinity 1, Teledyne Lumenera, Ottawa, ON, Canada). Six images were taken for each individual slide. The radial and tangential vessel diameter, lumen area, and the vessel density were measured. The obtained images were analyzed using ImageJ (U.S. National Institutes of Health, Bethesda, MD, USA).

During both the rainy and dry season measurements, three mature leaves per stem branch of the third order (considering the main axis as the first order) were collected, from which sap flow (SF) was measured. Immediately after cutting the leaves, they were fixed in FAA (formalin–ethanol-glacial acetic acid, distilled water 10:50:5:35) for 24 h. Afterwards, they were washed with tap water and stored in glycerin–ethanol-distilled water (1:1:1) until sectioning. Subsequently, leaves were infiltrated in a graded glycol–methacrylate (GMA) (7100, Techno-vit. Kulzer & Co., Hanau, Germany) [41] series from ethanol through 10%, 20%, 50%, 70%, 100%, embedded in glycol–methacrylate to obtain 3-μm-thick transverse sections with a rotatory microtone and stained with 0.6% brilliant cresyl blue. Next, the leaf samples were polymerized and mounted on wooden blocks to make cuts using the manual rotary microtome RM2125RT, Leica Biosystems, Richmond, IL, USA). The sections were stained on slides for observation under an optical microscope (Olympus, U-CMAD3, Tokyo, Japan) and photographed with an integrated camera (Infinity 1). The sub-stomatal cavity area was measured from eight slices of each individual. The obtained images were analyzed using ImageJ (U.S. National Institutes of Health, Bethesda, MD, USA).

2.2.6. Statistical analysis

All collected data were subjected to normality and homoscedasticity using the Shapiro–Wilk and Levene tests, respectively. Data on SF and microenvironmental variables, such as VPD, SR, PPF, and dew, as well as F_d, SF, and transpiration, were separated into two groups based on the observed onset of SF movement: daytime (7:30–19:20 h) and nighttime (19:30–7:20 h). Microenvironmental variables, such as VPD, PPF, SR, and porewater salinity were compared between seasons for daily maximum values using the nonparametric Mann–Whitney U test. To evaluate daily and seasonal variability in sap flow, the interquartile range test (IQR) was applied. Linear and polynomial regressions were performed between SF and microenvironmental variables. The Generalized Additive Model (GAM) was used to test the hypothesis regarding the effect of microenvironmental variables on sap flow (SF) within seasons, as no linear relationship was observed between the predictor and response variables. The model was evaluated using the Generalized Cross-Validation (GCV) criterion, and the smooth functions helped prevent overfitting through penalization. Additionally, the model's intercept represents the expected value of the response variable when the explanatory variables are zero, serving as a reference point to adjust the model and calculate the effects of the predictors. To assess the relationship between functional, anatomical and microenvironmental variables, mean values per season were analyzed using a Kendall correlation. Microenvironmental, SF and anatomical data were averaged over the same seasonal period to ensure temporal alignment for the correlation analysis. The substomatal cavity area was compared between seasons using the Mann–Whitney U test. All analyses were conducted using R language (4.3.2) (Posit Team, 2023).

2.3. RESULTS

2.3.1 Microenvironmental conditions

Significant differences were observed between seasons in the daily maximum values of the microenvironmental variables, including PPF, wind speed, solar radiation, and VPD ($p < 0.001$). Additionally, significant differences were detected in the daytime average values of these variables ($p < 0.05$). Porewater salinity also differed between seasons ($p < 0.001$; Table 2.1).

Table 2.1. Microenvironmental variables, plant physiological variables divided by day and night, and upscaled sap flow per season. PPF: Photosynthetic Photon Flux; VPD: Vapor Pressure Deficit; Fd: Sap flux density. Data are presented as means ± standard error. Significant differences between seasons, revealed by Mann-Whitney U tests ($p < 0.05$), are indicated by an asterisk

Variable	Season	
	Dry	Rainy
Microenvironment		
PPF (µmol m^{-2} s^{-1})	1989.4 ± 7.02*	1123.54 ± 8.83
Solar radiation (W m^{-2})	1050.45 ± 6.04*	526.33 ± 4.63
Air temperature (°C)	35.14 ± 0.96*	31.19 ± 0.02
Relative humidity (%)	50.97 ± 4.20*	65.5 ± 0.07
VPD (kPa)	2.88 ± 0.35*	1.40 ± 0.05
Porewater salinity (ppm)	39.9 ± 3.00*	28.66 ± 0.84
Plant physiology		
Cumulative sap flow (L d^{-1})	8.14 ± 0.59*	19.9 ± 1.9
Total leaf area	1.16 ± 0.24*	3.97 ± 1.21
Leaf area index (m^{2} m^{-2})	1.39 ± 0.64*	2.19 ± 0.33
Daytime		
Fd (g m^{-2} s^{-1})	26.36 ± 0.24*	49.34 ± 0.52
Sap flow (L h^{-1})	0.11 ± 0.00*	0.22 ± 00
Transpiration (mmol m^{-2} s^{-1})	1.80 ± 0.958*	17 ± 0.691
Nighttime		
Fd (g m^{-2} s^{-1})	1.93 ± 0.04*	11.25 ± 0.19
Transpiration (mmol m^{-2} s^{-1})	0.162 ± 0.0236*	5.89 ± 0.184
Upscaled		
Sap Flow (L h^{-1} ha^{-1})	3041.21	5767.82
Transpiration (mm day^{-1})	7.29	13.8

2.3.2 Sap flow density, sap flow and transpiration

Sap flux density (F_d) provided valuable insights into the intrinsic water transport capacity of the xylem. Seasonal differences in F_d were evident both during the daytime ($p < 0.001$) and nighttime ($p = 0$). During the rainy season, higher variability was observed during the day (IQR = 44.40) and night (IQR = 11.88) compared to the dry season (daytime IQR = 21.3; nighttime IQR = 1.68).

Sap flow (SF) values revealed significant differences in average daytime values between seasons ($p = 0.001$). When comparing nighttime SF values, sap movement was detected exclusively during the rainy season, which was highly significant ($p < 0.001$) (Figure 2A). The SF distribution displayed a bimodal pattern in both seasons, indicating distinct temporal dynamics (Figure 2B).

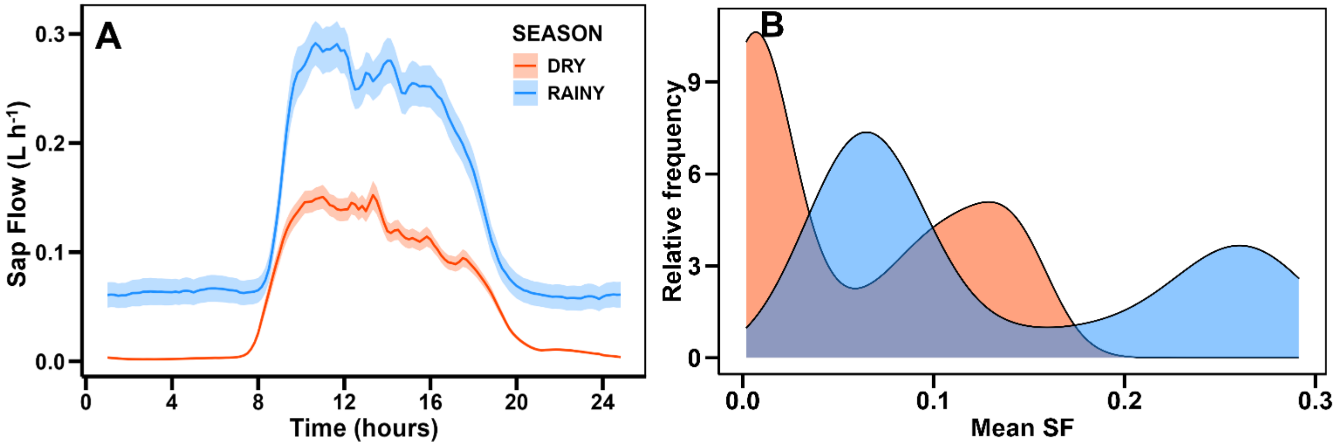

Figure 2.2. Diurnal mean patterns of sap flow (SF) measured over a continuous 8-day period during the dry and rainy seasons for *Rhizophora mangle* scrub mangroves. (**A)** Mean sap flow throughout a 24-hour cycle. (**B)** Relative frequency of mean sap flow with a bimodal pattern in both seasons.

Differences in transpiration were primarily linked to increased leaf area index (LAI) during the rainy season. Transpiration varied significantly between seasons and between daytime and nighttime ($p < 0.001$).

2.3.3 Sap flow and microenvironment

Correlation analysis revealed distinct patterns in the relationships between variables across the dry and rainy seasons (Figure 3). During the dry season, a strong positive correlation was observed between SR and PPF ($\tau = 0.97$), indicating a strong dependence of photosynthetic activity on light availability. Additionally, a significant negative correlation was found between xylem vessel density and xylem radial diameter ($\tau = -0.5$), suggesting a potential hydraulic adjustment strategy in response to water stress (Figure 3A). During the rainy season, while the relationship between SR and PPF persisted (τ = 0.98), the correlation between xylem vessel density and xylem radial diameter (τ = 0.59) attenuated, and SF and VPD showed a strong correlation (τ = 0.56) which could indicate a shift in water conduction efficiency (Figure 3B).

A

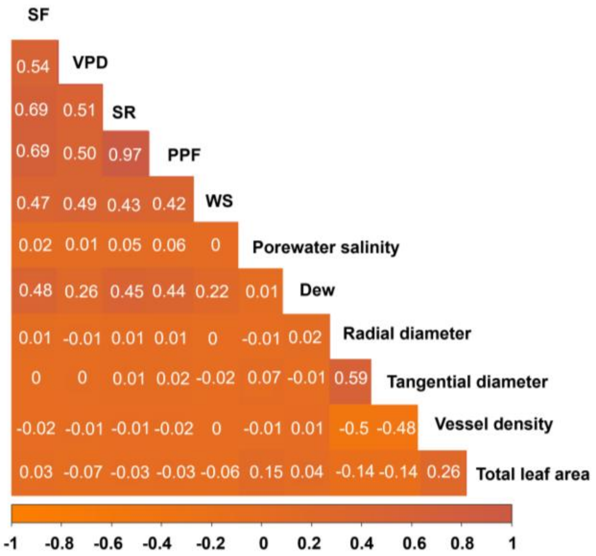

	SF	VPD	SR	PPF	WS	Porewater salinity	Dew	Radial diameter	Tangential diameter	Vessel density
VPD	0.54									
SR	0.69	0.51								
PPF	0.69	0.50	0.97							
WS	0.47	0.49	0.43	0.42						
Porewater salinity	0.02	0.01	0.05	0.06	0					
Dew	0.48	0.26	0.45	0.44	0.22	0.01				
Radial diameter	0.01	-0.01	0.01	0.01	0	-0.01	0.02			
Tangential diameter	0	0	0.01	0.02	-0.02	0.07	-0.01	0.59		
Vessel density	-0.02	-0.01	-0.01	-0.02	0	-0.01	0.01	-0.5	-0.48	
Total leaf area	0.03	-0.07	-0.03	-0.03	-0.06	0.15	0.04	-0.14	-0.14	0.26

B

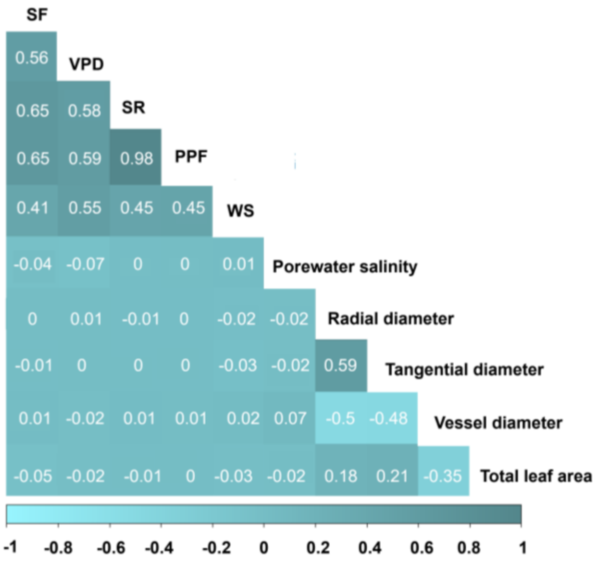

	SF	VPD	SR	PPF	WS	Porewater salinity	Radial diameter	Tangential diameter	Vessel diameter
VPD	0.56								
SR	0.65	0.58							
PPF	0.65	0.59	0.98						
WS	0.41	0.55	0.45	0.45					
Porewater salinity	-0.04	-0.07	0	0	0.01				
Radial diameter	0	0.01	-0.01	0	-0.02	-0.02			
Tangential diameter	-0.01	0	0	0	-0.03	-0.02	0.59		
Vessel diameter	0.01	-0.02	0.01	0.01	0.02	0.07	-0.5	-0.48	
Total leaf area	-0.05	-0.02	-0.01	0	-0.03	-0.02	0.18	0.21	-0.35

Figure 2.3. Kendall correlation matrix for environmental and anatomical variables, and Sap Flow (SF) during both seasons. (**A**) Dry season; (**B**) Rainy season. Variables include Sap Flow (SF), Vapor Pressure Deficit (VPD), Photosynthetic Photon Flux (PPF).

Although the Kendall correlation showed a strong relationship between SF and PPF, the GAM analysis evaluated the effect of all the microenvironmental variables and detected that VPD was the main driver of sap flow in both seasons, as it allowed the modeling of nonlinear relationships. During the dry season, VPD showed a significant third-degree polynomial relationship with SF ($p < 0.001$), explaining 49% of its variability (adjusted R-squared = 0.47, intercept value = 0.05 ± 0.001, deviance explained of 48.9%) (Figure 4A). Dew also had a significant impact on SF ($p < 0.001$), with a second-degree polynomial relationship, suggesting the importance of water availability in modulating xylem transport (Figure 4E). Secondary effects were observed for SR, PPF, wind speed, and salinity, but their influence was weak (Figure 4B,C).

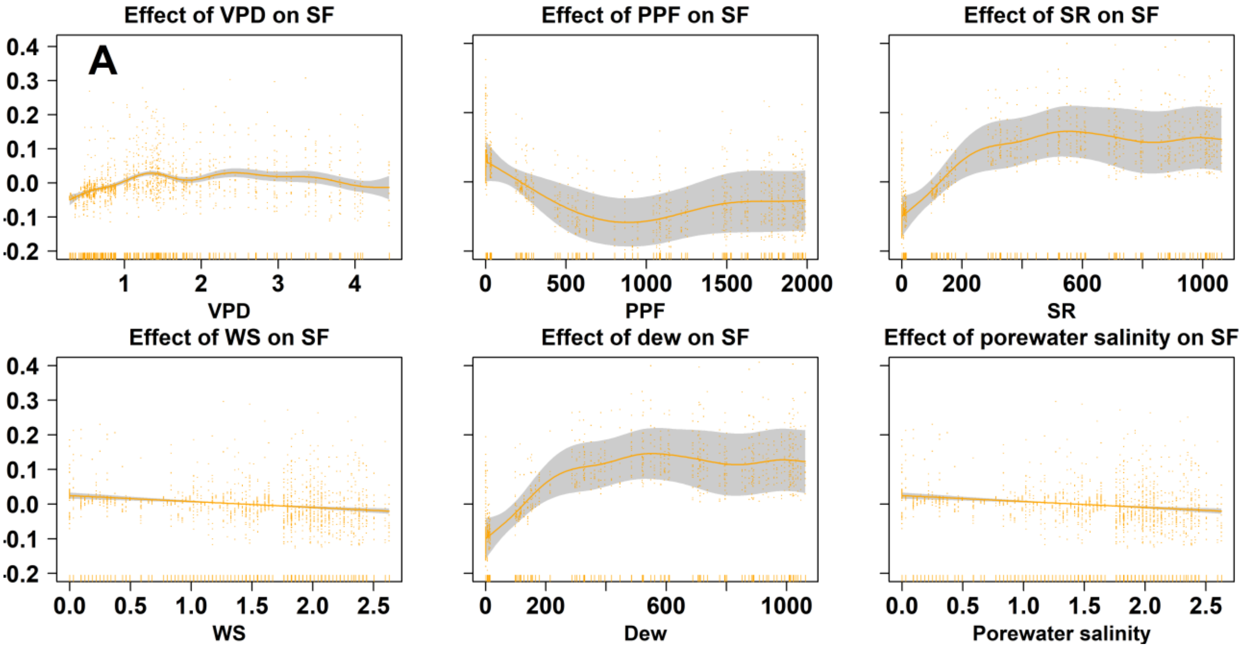

Figure 2.4. Smooth effects of environmental variables on sap flow (SF) during dry seasons analyzed using Generalized Additive Models (GAM). (A) Effects of Vapor Pressure Deficit (VPD); (B) Photosynthetic Photon Flux (PPF); (C) solar radiation (SR); (D) wind speed (WS); (E) dew; and (F) porewater salinity.

During the rainy season, VPD remained the only significant variable affecting SF ($p < 0.001$), with a nonlinear relationship that stabilized at higher values (Figure 5A). Other variables, including

PPF, solar radiation, wind speed, and salinity, had no significant effect (p > 0.2) (Figure 5B–E). SF doubled during the rainy season compared to the dry season, highlighting the importance of atmospheric variables over porewater salinity in driving sap flow.

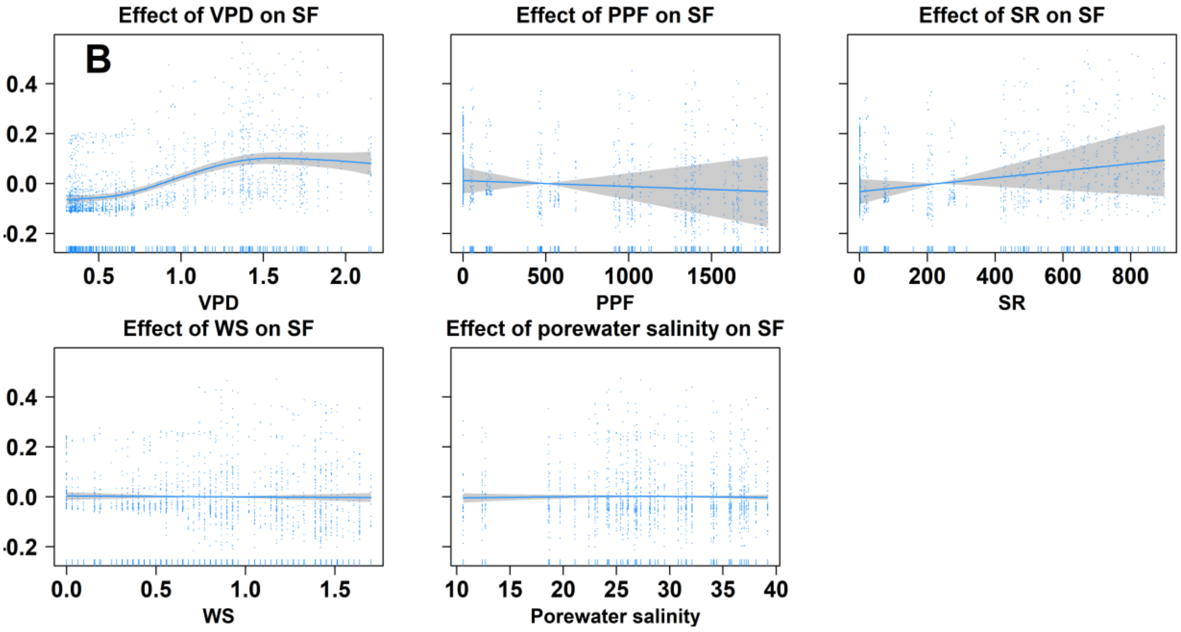

Figure 2.5. Smooth effects of environmental variables on sap flow (SF) during rainy season analyzed using Generalized Additive Models (GAM). (**A**) Effects of Vapor Pressure Deficit (VPD); (**B**) Photosynthetic Photon Flux (PPF); (**C**) solar radiation (SR); (**D**) wind speed (WS); and (**E**) porewater salinity.

Additionally, SF exhibited a twofold increase during the rainy season when VPD, PPF and salinity were low. Despite the significance of salinity in mangroves, there is no strong enough relationship between porewater salinity and SF in the dry and rainy seasons, emphasizing the importance of atmospheric variables in regulating SF depending on the seasonality.

2.3.4 Vascular system, and leaf anatomy

Xylem vessel elements are principally grouped, rather than solitary (Table 2). During the dry season, SF was strongly and positively correlated with solar radiation, PPF and VPD; however, there was not a significant relationship between SF and the number of vessels during the dry season. In the rainy season, a negative correlation was observed between the number of vessels and tangential diameter (TD), whereas its correlation with porewater salinity was weak (Figure 6).

In addition, the substomatal cavity area (µm^2) was not affected by seasonality (dry season 5035 ± 351 µm^2; rainy season 5077 ± 438 µm^2) (p = 0.93) (Figure 6D).

Table 2.2. Mean ± (standard error) of *R. mangle* stem xylem vessel traits.

Variables	
Vessel radial diameter (RD)	59.55 µm ± 12.2
Vessel tangential diameter (TD)	59.45 µm ± 38.64
Lumen area (LA)	2582.95 µm^2 ± 869.8
Vessel density	50.66 (no. of vessels mm^2) ± 20.85

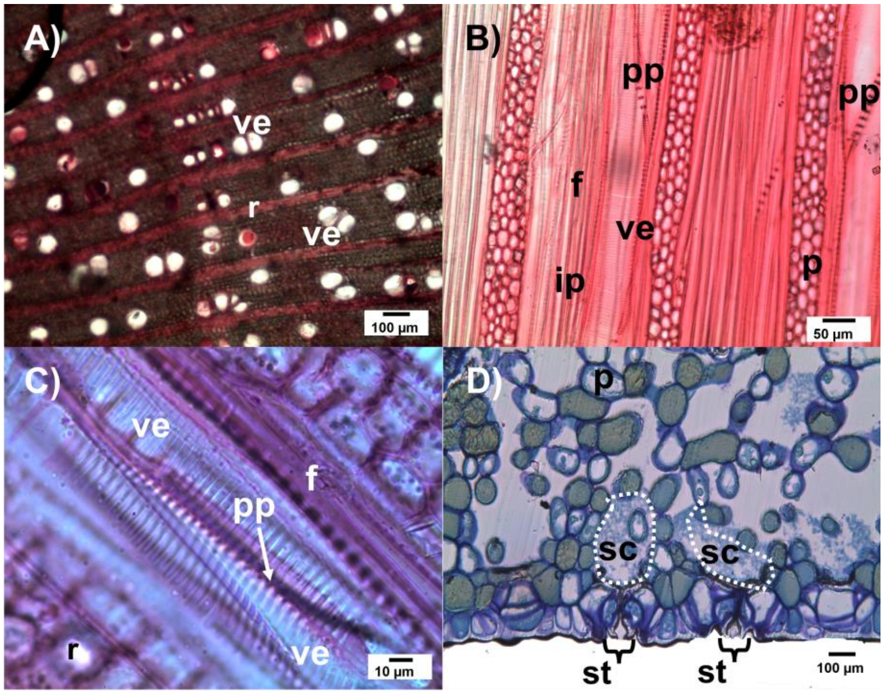

Figure 2.6. Stem secondary xylem: (**A**) transverse section showing diffuse porosity and vessel density, with a scale bar of 100 µm; (**B**) tangential section showing the scalariform perforation plate, scalariform intervascular pits of xylem vessels and wide xylem rays, with a scale bar of 50 µm; (**C**) radial sections showing detail of scalariform perforation plates overlapping at the tips of two vessel elements, with a scale bar of 10 µm; (**D**) dry season leaf transverse section showing epidermis, stomata, sub-stomatal chamber area (delimited by dotted line) and mesophyll parenchyma, with a scale bar of 100 µm. pp: perforation plates; f: fibers; ip: intervascular pits; ve: vessel elements; r: parenchymatous ray; sc: substomatal cavity; st: stomata; p: parenchyma.

2.4. DISCUSSION

The sap flow (SF) of *Rhizophora mangle* L. was strongly correlated with microenvironmental variables, such as VPD, PPF, and SR, which exhibited daily and seasonal variations, with lower values during the dry season compared to the rainy season. Additionally, total leaf area was 3.5 times greater during the rainy season than in the dry season, influencing transpiration at both the individual and stand levels. Notably, SF remained high during the rainy season, even at night, indicating continuous water uptake.

2.4.1 Sap flow and transpiration

Scrub mangroves exhibit a sympodial growth pattern (Aubréville's model) instead of a monopodial pattern (Attim's model), forming branches that grow to a certain extent before subdividing. This creates multiple pathways for water flow within the tree, influencing how sap flow is distributed and determining the hydraulic functions within the tree (Tomlinson, 2016; Hallé *et al*., 1978). This architectural adaptation may play a significant role in the ability of scrub mangroves to transport water effectively, even under challenging environmental conditions.

Sap flux density (Fd) in scrub mangroves reached mean values of up to 49.34 g m^{-2} s^{-1} during the rainy season, which is notably higher than the 20 g m^{-2} s^{-1} reported for *Byrsonima crassa* (L.) Kunth in savanna ecosystems (Scholz *et al*., 2002). Species such as *R. mangle and Laguncularia racemosa* (L.) Gaertn have been reported to exhibit Fd values of 19.0 g m^{-2} s^{-1} and 26.1 g m^{-2} s^{-1}, respectively, in mangrove ecosystems (Krauss *et al*., 2007). In contrast, our study found mean Fd values of up to 26.36 g m^{-2} s^{-1} for scrub mangroves during the dry season, aligning closely with these previously reported values. Furthermore, our study adjusted the Fd values to express transpiration as mmol m^{-2} s^{-1}, considering the conductive area of the xylem, providing a more direct comparison with other reports.

Fringe or riverine mangroves with waterlogged soils and species like *L. racemosa* and *R. mangle*, of similar sizes to those in this study, exhibit comparable sap flow density (Fd) values. In contrast*, Avicennia germinans* L., which thrives under higher salinity conditions, shows lower Fd in both waterlogged and drained soils. This suggests that short-statured mangroves, with a high leaf area index, can efficiently mobilize water, even in saline environments, while more conservative ecotypes, like *A. germinans*, maintain lower water transport rates (Krauss *et al.*, 2007).

Scrub mangrove forests in the Sundarbans, averaging 5 m in height, have shown maximum evapotranspiration rates of 5.5 mmol m^{-2} s^{-1}, which account for both transpiration and evaporation (Rodda *et al.*, 2016). In our study, considering only transpiration, we recorded maximum values of 5.89 mmol m^{-2} s^{-1}, indicating notably high transpiration rates. Upscaled sap flow in mangrove forests has been reported to reach values as high as 4 mm day^{-1}, while species such as *Picea*, *Fagus*, and *Quercus* in mature forests show average values of 2.5 mm day^{-1} in some terrestrial ecosystems (Ko Èstner, 2001). This comparison highlights the significant role that scrub mangroves of the Yucatan Peninsula play in filtering seawater and transporting it through their vascular system as sap flow, emphasizing their unique ecological importance.

It is essential to note that the magnitude of sap flow can vary depending on seasonal factors. Previous studies have shown that sap flow distribution in mangrove forests does not follow a normal distribution but is instead bimodal and highly influenced by seasonality (Leng & Cao, 2020). This finding is consistent with our results, suggesting that seasonal variability must be considered when evaluating sap flow rates in these ecosystems.

Sap flow and transpiration in forests are regulated by plant diversity and physiology (Bucci et al., 2004). Previous studies have utilized various scales and techniques, including sap flow measurements and evapotranspiration estimates derived from eddy covariance methods, to quantify transpiration and evapotranspiration rates in mangroves and tropical forests (Uuh-Sonda *et al.*, 2022; Orozco Medina *et al.*, 2019; Barr *et al.*, 2014; McJannet *et al.*, 2007). Consistent with these studies, the stand transpiration values reported in our study are higher in both seasons (dry season: 1.8 mmol m^{-2} s^{-1}; rainy season: 17 mmol m^{-2} s^{-1}) compared to those observed in a tropical dry deciduous forest on the Yucatan Peninsula (Salas-Acosta *et al.*, 2022) (late dry season: 0.36 mmol m^{-2} s^{-1}; late rainy season: 0.44 mmol m^{-2} s^{-1}).

Burman *et al.* (2022) reported that scrub *Rhizophora* spp. and *Avicennia marina* (Forssk.) Vierh. exhibited similar LAI values to those observed in this study. Additionally, using the eddy covariance method, they found that transpiration rates were higher than evaporation, even during the dry season. At least, despite the limitations of the Granier method, such as zero and reverse flows, it can detect high, medium, and low sap flow densities (Lu *et al*., 2004). Furthermore, the steady-temperature approach in Granier probes minimizes the influence of heat storage in the trunk, thereby reducing bias in sap flow measurements (Hölttäa *et al*., 2015). Nighttime sap flow has also been reported using this methodology (Fang *et al*., 2024; Snyder *et al*., 2008).

These findings contribute to a better understanding of the significance of transpiration in scrub mangrove ecosystems. Similarly, our results indicate that, during the rainy season, not only was higher sap flow recorded, but an increase in total leaf area was observed. This may be linked to enhanced carbon capture and storage in scrub mangroves of the Yucatan Peninsula.

2.4.2 Nocturnal transpiration

Nocturnal transpiration is influenced by several factors, including nighttime stomatal opening, water recharge to restore embolisms, nutrient uptake, and carbohydrate transport (Forster, 2014; J. Wu *et al*., 2020; Zeppel *et al*., 2019). This phenomenon has been documented in tropical ecosystems characterized by warmer or drier climates and nutrient-poor soils. Mangroves have been observed to sustain some water movement during the night. In scrub mangrove species, such as *Kandelia obovata* (S., L.) Yong and *Aegiceras corniculatum* (L.) Blanco, nocturnal sap flow plays a critical role in water recharge, embolism repair, and water storage in parenchymal tissue (Wu *et al*., 2023). Furthermore, Avicennia marina has been shown to absorb water through its leaves to repair embolisms.

Additionally, nocturnal transpiration in mangroves can vary by species and has been associated with increases in vapor pressure deficit (VPD) (Li *et al*., 2023). Nocturnal transpiration is crucial for several ecosystem processes, such as early morning carbon fixation, stomatal opening, oxygenation, and nutrient uptake. However, information on nocturnal transpiration in scrub mangrove species remains limited. Generally, sap flow at night remains unaffected unless extreme stress occurs, making nocturnal transpiration relatively stable under normal conditions. Neglecting nocturnal transpiration could result in underestimations of its contributions to ecosystem functioning (Hayat *et al*., 2021; Dawson *et al*., 2007).

Nighttime water movement also promotes hydrological connectivity within the ecosystem through hydraulic redistribution, facilitating water transfer between different soil layers or even neighboring plants (Forster, 2014).

2.4.3 Sap flow and microenvironment

Increases in VPD promote the column water maintaining stomatal closure; otherwise, transpiration rises, leading to reduced water potential and potential embolism formation (Bachofen *et al.,* 2023; Manzoni *et al*., 2014). This process may be more complex in environments such as mangrove forests, as suggested by our results, where seasonal variations in VPD, followed by changes in radiation and porewater salinity, influenced sap flow depending on seasonality (Deb Burman *et al*., 2022; Benyon *et al*., 2001). Our findings indicate a coupling with the atmosphere, as suggested by the decreased sap flow and transpiration during the dry season.

Studies have explored the relationship between whole-tree canopy conductance, derived from sap flow, and VPD, identifying VPD as a main driver of water flow in trees (Deb Burman *et al*., 2022; Flo *et al*., 2022). However, in Indian mangroves, porewater salinity was strongly related to transpiration, with seasonal variations: during the pre-monsoon, the greatest amount of transpiration is released to the atmosphere, reducing the dry sensible heat from the soil to the atmosphere (Grossiord *et al*., 2020). Globally, VPD is often the main driver of water flow in tree canopies, although this relationship varies across biomes. In tropical mangrove forests, VPD, PPF, and soil water content (SWC) primarily influence sap flow (Broughton *et al*., 2021; Novick *et al*., 2019; Ball, 2002; De Boeck *et al*., 2010; Rodriguez-Pérez, 2006; Stout & Simpson, 1978). Our study supports VPD as the main driver of sap flow in mangroves, accounting for seasonal variability.

The anatomical traits of the *R. mangle* xylem in the scrub mangrove ecotype showed a high vessel density and larger tangential and radial diameters compared to previous reports (Cisneros-De La Cruz *et al*., 2022). High vessel density is associated with efficient water transport, essential for coping with high porewater salinity and minimizing embolisms (Cruziat *et al*., 2020). This adaptation, along with increased hydrostatic pressure and osmotic potential, facilitates water movement and distribution to leaves (Méndez-Alonzo *et al*., 2016; Tyree & Zimmermann, 2002). Scrub *R. mangle* exhibited a lower tangential and radial vessel diameter compared to the values reported by Cisneros-de la Cruz *et al*. (2022) in adult individuals of the same species. The vessel density in this study was also higher than that of the previous study (Cisneros-De La Cruz *et al*., 2022) (50.66 vessels/mm^2, compared to 32 vessels/mm^2). Furthermore, compared with fringe mangroves of *R. mangle*, scrub *R. mangle* has higher vessel density and shorter tangential and radial diameters because of the lower salinity in the former mangrove ecotype. High vessel density, narrow vessel diameter, warm climate, and high salinity allow for a secure water transport capacity (Cisneros-De La Cruz *et al*., 2022). On the other hand, high vessel density is negatively correlated with the average vessel diameter (Figure 6), a trait closely associated with resistance to hydraulic dysfunction, which is reflected in the length of the conductive aboveground hydraulic pathways (Santini & Lovelock, 2015). Given that the average tree height of the scrub mangroves is 2 m, it can be expected that individuals withstanding this environment should have more resistance to drought than taller trees in other geo-forms; however, to our knowledge, such a test has not been performed.

Drought resistance may involve strategies such as accelerated leaf senescence and cellular osmoregulation, which help limit transpiration (Stout & Simpson, 1978). Leaf senescence during drought conditions reduces water loss through transpiration (Coopman et al., 2021). In some species, leaves may exhibit differences in tissue responses to seasonal variations. The substomatal cavity influences transpiration and CO_2 assimilation. Reduced water availability can expand the cavity area, allowing for greater CO_2 storage (Oliveira *et al*., 2023, 2022; Haworth *et al*., 2021). Nevertheless, in this study, no differences were found in the substomatal cavity area between seasons, despite variations in the main driver, the VPD.

This finding is particularly relevant for scrub mangroves, as the lack of seasonal differences in substomatal cavity area suggests that they can continue capturing and storing carbon without limiting productivity. In fact, their carbon storage has been reported to be quite high, and greater than that of other mangrove ecotypes, due to their distribution (Herrera-Silveira *et al*., 2020). This could be attributed to contrasting microclimatic conditions among ecotypes.

In this context, it can be observed that anatomical traits influence not only transpiration but also the carbon cycle. Moreover, the consistently large substomatal cavity in *R. mangle* across seasons suggests a stomatal coupling with the atmosphere that limits water loss, particularly during the dry season. Larger substomatal cavities and intercellular spaces can enhance internal CO_2 concentration, boosting photosynthesis while reducing water loss through transpiration, especially in drought-tolerant species (Lavinsky *et al*., 2015; Ni *et al*., 2014; Evans & Bromber, 2012; Lin & Stenberg, 1992).

It would be important to explore the relationship between substomatal cavity size and water exchange to better understand drought tolerance strategies (Evans & Bromberg, 2010; Lin & Stenberg, 1992). Mangroves are known to be highly efficient in water use, a mechanism to cope with the high salinity of their habitats. Scrub mangroves are specialized for survival in high-salinity environments, playing a critical role in mitigating climate change by storing large amounts of belowground carbon (Augusto da Silva *et al*., 2016). Additionally, we highlight their significant role in the water cycle through transpiration.

The relationship between leaf area index (LAI) and the influence of VPD and SWC indicates that higher LAI weakens the relationship with VPD and SWC (Terashima et al., 2006). Nevertheless, in our research, during the rainy season, we observed an increase in LAI and a strong relationship with VPD, despite lower VPD values compared to the dry season. This suggests that increased LAI combined with low VPD might promote consistently higher levels of SF.

Other variables, such as salinity, wind speed, and dew, which did not show strong correlations with SF, might be more associated with other biogeochemical or physiological processes (Ni *et al.*, 2014). The study of sap flow and transpiration is critical due to its ecohydrological implications at both local and global levels in the water cycle, especially considering drastic seasonal changes driven by climate change (Mencuccini *et al*., 2019, Gutiérrez-Mendoza & Herrera-Silveira, 2015; Ogle *et al*., 2015; Krauss *et al*., 2014). Moreover, the humidity generated by plant transpiration can benefit the biodiversity of other plants, such as epiphytes, and various animal groups in mangrove forests (e.g., insects, vertebrates) (Williams *et al.*, 2003). Furthermore, transpiration and salinity are closely related to photosynthesis, impacting the carbon cycle (Mencuccini *et al.*, 2019; Chiew & McMahon, 2002). The low availability of porewater during the dry season can affect the maintenance of the water column, especially when atmospheric evaporative demand is high. This promotes strict stomatal control to prevent excessive water loss (Sippo *et al.*, 2018; Robert *et al*., 2011; Pounds et al., 2006; Chiew & McMahon, 2002; Stout & Simpson, 1978). However, because our research in scrub mangroves of *R. mangle* suggests that correlation of salinity with transpiration is not stronger enough, more research is needed.

Our results highlight the importance of scrub mangroves, which can show seasonal transitions, modulating their response based on soil water availability and the evaporative demand of the atmosphere. Although transpiration is low during the dry season, it remains continuous, while in the rainy season, it is compensated by higher transpiration, making it a key system for energy and ecohydrological balance, particularly in tropical areas, and in the context of climate change scenarios.

Considering that, in Celestún, the mean precipitation during the dry season is around 30 mm and increases to approximately 140 mm during the rainy season (CONAGUA, 2025), this suggests that a significant amount of water is returned to the environment not only during the day but also at night. This underscores the ecological importance of scrub mangroves in water cycling. It is crucial to understand these aspects in other types of mangroves to ensure their conservation, as each provides unique ecosystem services. In this regard, protecting mangroves that regulate the local climate through transpiration not only helps to regulate climatic conditions but also benefits human communities and the biodiversity on which they depend for sustainable use.

2.5 CONCLUSIONS

Even when salinity is often regarded as a critical factor influencing sap flow in mangroves, our findings emphasize the importance of atmospheric variables, such as vapor pressure deficit (VPD), solar radiation, and photosynthetic photon flux (PPF), as significant determinants of sap flow variations. These atmospheric factors can have a substantial impact on sap flow, underscoring the need to account for multiple environmental variables when studying sap flow dynamics in mangrove ecosystems.

Seasonality plays a crucial role in sap flow variations, with the rainy season showing higher sap flow rates, increased transpiration (both day and night), and an expansion in total leaf area. These changes can have important implications for ecohydrological processes and energy balance. However, further studies are needed to fully understand these dynamics in mangroves, especially in ecosystems as widespread as those in the Yucatan Peninsula. Interestingly, the observed increase in nocturnal sap flow during the rainy season suggests hydraulic recovery and canopy leaf area growth strategies in scrub *R. mangle*, further suggesting adaptations not only to diurnal changes but also to seasonal variability.

The anatomy of the vascular system plays a crucial role in ensuring the safe transport of sap flow in scrub *R. mangle*, as it increases vessel density and decreases vessel diameter to prevent embolisms, regardless of seasonal changes. On the other hand, although there is no seasonal variation in substomatal cavity area, their large area promotes gas exchange, including water vapor, particularly during the rainy season.

This study underscores the significance of scrub *R. mangle* mangroves in Yucatán, not only due to their extensive distribution and substantial carbon storage but also for their contribution to atmospheric water flux through year-round transpiration, supported by their evergreen strategy. Understanding the role of transpiration in mangroves is crucial not only for regulating local climate but also for recognizing their potential in water filtration, particularly in coping with and mitigating salinity impacts. This knowledge could lead to increased efforts to harness mangroves for nature-based solutions (NbS), such as improving water quality in coastal zones.

Moreover, the carbon storage potential of mangroves, combined with their role in water filtration, opens the door for innovative market opportunities. For instance, mangrove forests could be integrated into emerging markets that connect global carbon markets with water-related services, creating a dual benefit for conservation and sustainable resource management. Understanding water-related processes in mangroves provides a baseline for expanding knowledge on the importance of these ecosystems, particularly concerning carbon storage, and can serve as a foundation for forecasting the future of these ecosystems under climate change scenarios. It will be crucial to integrate these findings into mangrove management strategies, focusing on enhancing their role in climate change mitigation and the potential development of markets around both carbon and water provisioning through effective conservation and restoration efforts.

2.6 AUTHOR CONTRIBUTIONS

Conceptualization, methodology and supervision, G.C.-A., J.L.A., L.Y.-E. and J.A.S.-R.; field sampling, G.C.-A., R.U.-S., K.E.G.-M. and J.H.-S.; formal analysis, G.C.-A., K.E.G.-M. and J.A.S.-R.; writing–original draft, G.C.-A., J.L.A.; funding acquisition, G.C.-A., J.A.S.-R. and J.L.A.; and review and editing I.E.-M., R.M.-A. and J.H.-S. All authors have read and agreed to the published version of the manuscript.

2.7 FUNDING

This research was partially supported by the International Tropical Timber Organization (ITTO) (068/20A). G.C.A. (838830) and J.A.S.R (760092) received a fellowship from Consejo Nacional de Humanidades, Ciencias y Tecnologías (CONAHCYT). K.E.M. recieved a fellowship from Centro de Investigación Científica de Yucatán (CICY) (1210021).

2.8 DATA AVAILABILITY STATEMENT

The original contributions presented in the study are included in the article; further inquiries can be made to the corresponding author.

2.9 ACKNOWLEDGMENTS

We thank CONANP for the facilities provided to carry out the research. We also thank Jesús Garrido and Aarón Casanova for their great support with fieldwork. Our gratitude goes to Azucena Canto and Rosalina Rodríguez for their assistance with the use of the microscope.

2.10 CONFLICTS OF INTEREST

The authors declare no conflicts of interest.

CAPÍTULO III

MANGROVE ANTROPOGENIC DISTURBANCE MODIFIES THE ENERGY BALANCES WITHIN AND ACROSS SEASONS IN YUCATÁN, MÉXICO.

ABSTRACT

Mangrove forests are key ecosystems in tropical and subtropical regions, where high solar radiation must be dissipated as latent and sensible heat to maintain ecosystem functioning. Mangrove species use physiological and anatomical mechanisms to regulate leaf temperature according to absorbed energy. However, increasing anthropogenic disturbances not only alter hydrodynamics and vegetation distribution but may also impact their thermoregulatory strategies.

This study evaluated the seasonal effect on leaf energy balance across two canopy strata (upper and lower) in *Rhizophora mangle* L. scrub mangroves, in both conserved and disturbed sites in Yucatán. The conserved mangrove dissipated more energy as latent heat, indicating greater thermal efficiency, while the disturbed site dissipated more as sensible heat, revealing lower physiological regulation and greater environmental dependence. In the conserved site, temperature differences between strata were evident. During the dry season, the boundary layer and evaporative demand were the main drivers of energy balance, whereas in the rainy season, temperature and evaporative demand were more influential. In contrast, energy dissipation in the disturbed mangrove depended mostly on environmental conditions, with wind speed and boundary layer being key variables in both seasons.

These findings show that disturbance affects not only mangrove structure and functioning but also their ecological roles, emphasizing the urgent need for protection and restoration due to their critical role in coastal climate regulation.

3.1. INTRODUCTION

Anthropogenic climate change has triggered unprecedented warming, with global mean temperatures rising by 1.2°C since the pre-industrial era (IPCC, 2021), driving cascading impacts across ecosystems. These alterations disrupt forest ecosystem functioning (Breshears *et al.*, 2021; McDowell *et al.,* 2020). Rising temperatures impair carbon sequestration and storage, alter the hydrological cycle, by altering evaporation and transpiration rates and soil water retention

(Bonan, 2016). Such impacts are acutely manifested in mangrove forests-among the most productive ecosystems globally (Alongi, 2014; Donato *et al*., 2011)- where transpiration driven water flux regulates regional hydrology (Cerón-Aguilera *et al*., 2025; Deb Burman *et al*., 2022; Rodda *et al*., 2016). Temperature also governs plant survival and ecosystem function through its regulation of physiological processes (Jones & Rotenberg, 2001). Thermoregulation in leaves and canopies arises from the interplay of plant functional traits and environmental variables. Key plant physiological mechanisms related to heat tolerance include transpiration, boundary layer reduction, leaf area adjustments, water-use efficiency optimization, canopy architecture, leaf angle, and aerodynamic resistance (Blonder & Michaletz, 2018; Dong *et al*., 2017; Michaletz et al., 2016; Kumagai *et al*., 2004). Energy dissipation occurs primarily at the leaf level, where stomatal transpiration cools tissues by overcoming resistances to vapor flow (e.g., stomatal conductance, boundary layer) and releasing latent heat via the vaporization of water within the stomatal chambers (Guo *et al*., 2022; Medlyn *et al*., 2011). Wind enhances this process by displacing the warm air layer around leaves (Jones, 2014), breaking or reducing the width of the boundary layer, where the diffusion of gases operates and promoting mass exchange.

Identifying thermal thresholds (optimal/min/max) is therefore vital for assessing ecological niche sensitivity (Diamond, 2018), particularly as climate-change related disturbances disrupt energy balances. At leaf and canopy scales, temperature drives transpiration-mediated heat dissipation, interacting with vapor pressure deficit (VPD) and stomatal conductance to shape carbon/water cycling (Farella *et al*., 2022; Lin *et al*., 2020), but there is wide variation across spatiotemporal scales and across ecosystem types that reveals the influence of evapotranspiration on biogeochemical cycles and species distribution (niche to global levels) (Farella *et al*., 2022; Taillardat *et al*., 2018). To estimate the energy budget across forest canopies, is critical to determine first the variation in leaf temperatures, which in turn depends on the radiative energy inputs and exchange (shortwave and longwave radiation) and the convective energy outputs (sensible and latent heat fluxes) (Fernandes de Oliveira *et al*., 2024; Nobel, 2020; Jones, 2014; Lambers *et al*., 2008). While plants utilize a fraction of incident solar radiation (400–700 nm) for photochemistry, most radiant accumulated energy is dissipated as latent heat (transpiration) or sensible heat (convection/conduction). Crucially, longwave radiation (infrared) dominates the energy budget of leaves and their microenvironment (Fernandes de Oliveira *et al*., 2024; Nobel, 2020).

Temperature is also a pivotal determinant of global mangrove forest distribution and physiology (Tomlinson, 2016). Physioecological studies have previously elucidated mangrove responses to environmental stressors, including temperature effects on stomatal conductance, photosynthetic efficiency, and water-use efficiency (Kimball *et al*., 2016; Schymanski *et al*., 2013; Araujo *et al*., 2013; Cooke & Suski, 2008). Such knowledge is critical as climate change exacerbates exposure to solar radiation, wind, and hydrological shifts (Friess *et al*., 2022; Gilman *et al*., 2008; Naidoo, 2016; Ward *et al*., 2016), even informing conservation and restoration strategies (Friess *et al*., 2022; Farella *et al*., 2022; Valliere *et al*., 2022; Taillardat *et al*., 2018; Kimball *et al*., 2016; Naidoo, 2016; Ward *et al*., 2016; Araujo *et al*., 2013; Schymanski *et al*., 2013; Cooke & Suski, 2008; Gilman *et al*., 2008; Veneklaas & Poot, 2003). For example, degradated mangroves exhibit poorer thermal regulation than conserved stands, with tropical forests showing greater resilience to fluctuations (Li *et al*., 2015).

Understanding these thermoregulatory strategies is essential for mangrove ecosystems, where forest density—whether conserved or disturbed—shapes interactions with net radiation and heat dissipation at leaf and canopy levels. Accessible methodologies like point-based heat exchange measurements (Mahmood *et al*., 2013) can elucidate these dynamics.

Despite thriving under extreme conditions (elevated temperatures, intense solar radiation, high evaporation rates), mangroves maintain critical ecosystem services, including biodiversity support, hydrological regulation, and carbon sequestration (Sievers *et al*., 2019; Adame *et al*., 2018; Krause *et al*., 2017; Krauss *et al*., 2015). However, anthropogenic disturbances—such as infrastructure development and urban wastewater discharges disrupt microenvironmental temperatures via hydrological changes, often precipitating vegetation loss and ecosystem service degradation (Valderrama *et al*., 2014). Given the strong linkage between hydrological dynamics and mangrove species distribution, physiognomy, and salinity zonation at local scales (Tomlinson, 2016; Spalding *et al*., 2010), any modification of the mangrove energy balance due to anthopogenic disturbance may precipitate changes in the whole-ecosystem functionality. These impacts should be particularly worrisome in the areas of the world where socioeconomics have more dependence to the mangrove ecosystem. For example, in the Yucatán Peninsula, South México, the mangroves are widely distributed across the coasts and the few rivers, promoting coastal protection, nursery sites for economically relevant fish species, tourism and cultural and aesthetic values. Within the Yucatán Peninsula, four distinct ecological types fringe, basin, petén, and scrub (Tomlinson, 2016; Zaldívar-Jiménez *et al*., 2010) can be observed on the basis of the hydrological availability, the latter being most widely distributed in that area (Morales-Ojeda *et al.*, 2019).

Owing to the ongoing disruption of mangrove energetic balances due to climate change. Forest degradation, and land cover changes, in this study, we aim to 1) analyze the effect of the microenviromental on the energy balance of two *Rhizophora mangle* scrub mangrove populations in Yucatán differing in conservation status during the rainy and dry seasons; 2) to quantify the components of the leaf energy balance across different strata of adult’s plants; 3) to determine the differences between conserved and disturbed mangrove regarding their thermoregulatory strategies. We hypothesize that during the dry season, the conserved mangrove will maintain lower leaf temperatures than ambient air temperature, with higher aerodynamic resistance due to greater individual density. In the conserved mangrove, upper canopy strata will exhibit elevated temperatures, offset by cooler lower strata where reduced radiation exposure enhances heat dissipation. In conjunct, our results will allow to establish baseline measurements of the possible impact of mangrove anthropogenic disturbance on the heat balance of this region.

3.2. MATERIAL AND METHODS

3.2.1. Study area

The conserved mangrove area was located within the Ría Celestún Biosphere Reserve (Fig. 3.1), a coastal lagoon system supporting diverse ecosystems along a salinity gradient, including deciduous forests, dunes, and distinct mangrove ecotypes (fringe, scrub, petén, and basin) (Herrera-Silveira, 1994). The study focused on a monospecific scrub mangrove stand dominated by *Rhizophora mangle* L., with a high population density (26,217 ind ha^{-2}) and low average canopy height (1.8 m). Environmental conditions during the rainy season recorded interstitial salinity levels of 42.7–51.42 ppm, sediment water potential of −1.91 MPa, and maximum vapor pressure deficit (VPD) values of 1.38 kPa (Cisneros-De La Cruz *et al.*, 2022), reflecting the hypersaline conditions typical of Yucatán's carbonate coastal mangroves.

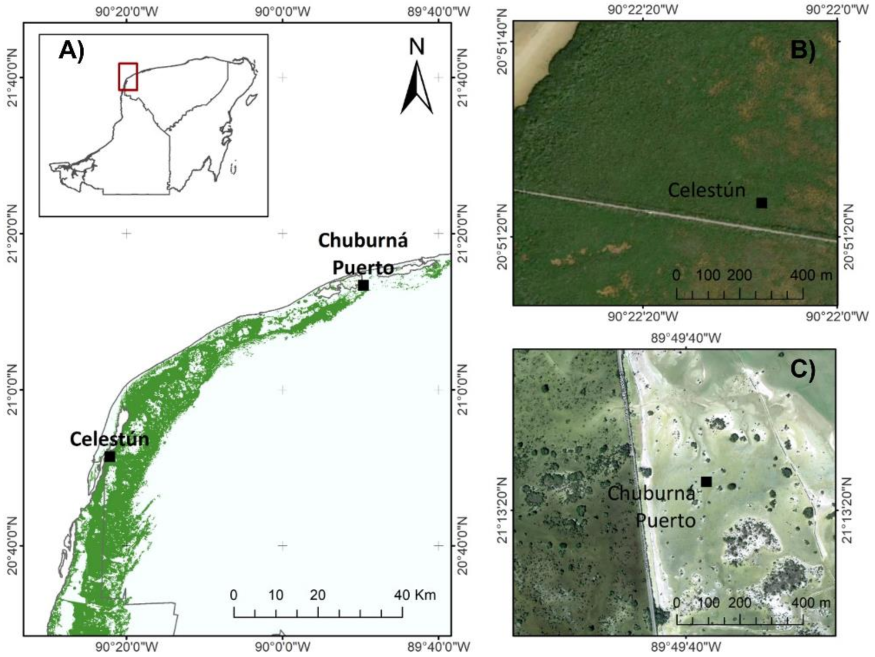

Figure 3.1 A) Location of the study sites in the Celestun Biosphere Reserve and Chuburna. Black dots indicate the study sites. Created with QGIS (version 3.22.14-Białowieża). B) Location of conserved *R. mangle* chaparro mangrove. C) Location of hydrologically disturbed *R. mangle* chaparro mangrove.

The perturbed mangrove site was located within the state reserve Cienagas y Manglares de la Costa Norte de Yucatán (referred throughout the text as Chuburna), a complex wetland system divided into three zones (western, central, and eastern) supporting fringe, scrub, and petén mangrove ecotypes. Hydrological fragmentation caused by road construction in 1940 (Zizumbo, 1986) has altered species distribution and ecotype zonation. Despite limited studies in the area, available data indicate hypersaline conditions in the central zone (>60 ppt) with elevated dry-season evaporation (Batllori-Samperio *et al*., 1999). The studied *R. mangle* scrub mangrove exhibited lower stand density (8,400 ind m^{-2}) but slightly greater average height (2.1 m) compared to the conserved site, reflecting disturbance-mediated structural changes.

Both study areas experience marked seasonal variation, with defined dry (March-May), rainy (June-October), and early dry (nortes; November-February) periods (Zaldívar et al., 2004). However, they contrast in hydrology: Celestun has remain relatively undisturbed in hydrology, acting as a long-term reference site, whereas Chuburna has been chronically impaired by the road infrastructure (>50 years). Partial restoration efforts have yet to achieve ecosystem recovery in affected sectors.

3.2.2 Microenvironment

In dry (April) and rainy (October) 2021, leaves and data were collected in scrub mangrove near the road Kinchil-Celestún Celestún (20° 51.400' N, 90° 22.248' O). Air temperature (T, °C) and relative humidity (RH, %) were measured with a temperature probe (S-TMB-M003, Onset Computer Corporation, Bourne, MA), wind speed (m s^{-1}) with a cup anemometer, and wind direction with a wind vane (S-WCF-M003, Onset Computer Corporation, Bourne, MA), photosynthetic photon flux (PPF, µmol m^{-2} s^{-1}) with a quantometer (S-LIA-M003, Onset, Bourne, MA), and solar radiation with a pyranometer (SR, W m^{-2}) (S-LIB-M003, Onset, Bourne, MA). The data were recorded using a data logger (U30-NRC Weather Station Starter Kit, Onset, Bourne, MA) every 10 seconds and 10 minutes on average. Maximum Vapor Pressure Deficit (VPD, kPa) was calculated with the temperature and relative humidity using the formulas, according to Jones (2014):

$$DPV = \pi e_{S\,(T)} - e \tag{3.1}$$

Where, *e* is the partial pressure of water vapor in air; and $e_{S(T)}$ is the saturation partial pressure of water vapor in function of the temperature $e = HR\ x\ e_{S(T)}\pi r^2$. The relation between air temperature and relative humidity is known as evaporative demand by the increased of the temperature.

A sample of porewater was drawn using an acrylic tube at a depth of 30 cm and it was measured with a multiparameter probe (Model 30, YSI, Yellow Springs, OH) at every sampled tree.

3.2.3. Energy balance

Leaf temperature was monitored using Type-T thermocouples distributed across three vertical strata (lower, middle, upper canopy) per tree, with four replicate sensors per stratum (n = 12). Simultaneously, sediment and water temperatures were recorded using identical sensors (n=8). Continuous measurements were conducted over seven consecutive days, with data logged at 10 second intervals and subsequently averaging 10 minutes resolution using CR1000 dataloggers (Campbell Scientific, USA).

The leaf energy balance was estimated through direct measurements of net radiation (NR-01 net radiometer, Campbell Scientific), latent heat (LI-6800 portable photosynthesis system, LI-COR), and sensible heat flux (HC2S3 anemometer, Campbell Scientific), following the modified energy balance equation from Nobel (2020):

$$\text{EB} = \text{Net radiation} + (\text{- sensible heat}) + (\text{- latent heat}) \qquad (3.2)$$

Net radiation:

Net radiation considers absorbed solar irradiation, absorbed IR from surroundings, and emitted IR radiation. It can be expressed as:

$$R_n = a\,(1 + r)S * \cos angle + aIR\sigma\,[(T^{surr})^4 + \,(T^{sky})^4] - 2eIR\sigma(T^{leaf})^4 \qquad (3.3)$$

Where, R_n is the net radiation, *a* is the leaf shortwave absorption coefficient, *r* is the value of reflected radiation relative to the incident radiation, and the leaf inclination angle was measured using the Ahmes app (Escribano-Rocafort et al., 2014).*S* is the direct solar radiation, a_{IR} is the leaf's absorption coefficient, set at 0.96, σ is the Stefan-Boltzmann constant, and e_{IR} is the leaf emissivity coefficient, which, according to Kirchoff's Law, is equal to the absorption coefficient, being 0.96. The temperature in *K* was measured around the leaf, the sky, and the leaf itself.

Sensible heat (J_H^C):

Sensible heat considers heat conduction from the leaf surface through the boundary layer on both sides of the leaf, meaning that heat conduction does not depend on stomatal aperture.

$$J_H^C = \frac{2K_{air}(T^{leaf} - T^{air})}{\delta_{bl}} \qquad (3.4)$$

Where K^{air} is the thermal conductivity coefficient of air, temperature in *K* and δ_{bl} is the boundary layer of the leaf.

Boundary layer is the portion of air next to the leaf. Wind speed affects the thickness; also, it influences heat exchange and diffusion of gases such as CO_2, H_2O and O_2. The movement of heat and gases is assisted by *eddy*; that is, the air moves in vortices and behaves as if it were moving in small units or packets. Instead of describing the local transfer processes in the laminar and turbulent regions, whose thicknesses vary across the leaf surface, an effective or equivalent boundary layer thickness, referred to as δ_{bl} is used as an average over the entire leaf surface.

$$\delta^{bl}_{(mm)} = 4\sqrt{\frac{l_{(m)}}{v_{(m\,s^{-1})}}} \tag{3.5}$$

Where, *l* is the mean length of the leaf and *v* is the wind speed. Factor 4 is specifically related to wind speed on leaves at a given temperature.

Latent heat:

We represent the flux density of water vapor diffusing out of a leaf as J_{wv} , which corresponds to the transpiration rate. By multiplying J_{wv} the amount of water lost per unit time and per unit leaf area by H_{vap}, the energy required to evaporate a unit amount of water at the leaf's temperature, we obtain the heat flux density associated with transpiration, denoted as J_H^T.

$$J_H^T = J_{wv}\,H_{vap} = \frac{H_{vap}\,D_{wv}\,(c_{wv}^{e} - c_{wv}^{ta})}{\delta_{bl}} \tag{3.6}$$

Where, J_{wv} represents the diffusion coefficient of water vapor according to Fick's law, H_{vap} is the energy required to convert one mole of water at a given temperature (T°C of the leaf), D_{wv} is the diffusion coefficient of water vapor, c_{wv}^{ta} is the concentration of water vapor in the air, c_{wv}^{e} is the concentration of water inside the leaf and δ_{bl} is the boundary layer.

Aerodynamic resistance:

Aerodynamic resistance (ra, s m^{-1}) was calculated based on three equations described by Monteith and Unsworth (1990), which provide estimations at different levels of the system. The first approach considers the characteristics of the boundary layer and the diffusion coefficient of water vapor in air. The second is based on latent heat flux ($J_H^T = LE$) and the vapor pressure deficit (VPD). The third estimation incorporates the momentum transfer approach, which accounts for the physical exchange of mass and energy between the canopy surface and the surrounding atmosphere.

$$r_a = \frac{\delta_{bl}}{D_{wv}} \tag{3.7}$$

Where, D_{wv} is the diffusion coefficient of water vapor in air (2.4 x 10^{-5} m2 s^{-1}).

$$r_a = \frac{\rho \, c_p \, VPD}{LE} \tag{3.8}$$

Where, ρ is the air density (1.1 kg m^{-3}) considering temperature, c_p is the specific heat of air (1005 J kg^{-1} K^{-1}), VPD is the vapor pressure (kPa) and LE is the latent heat flux (W m^{-2}).

$$r_a = \frac{In\left(\frac{z_d - d}{z_0}\right)}{k^2 \, U} \tag{3.9}$$

Where z_d = 1.8 m (wind measurement height), d = 0.67 *hc* (canopy displacement height), z_0 = 0.1 *hc* (aerodynamic roughness length), *k* = 0.41 (von Kármán constant), and *U* = wind speed (m s^{-1}) for each site and season.

3.2.4. Leaf anatomy

The anatomical analysis was conducted only for the scrub mangrove of *R. mangle* located in Celestun. The leaves were collected during the rainy and dry seasons. Three leaves per stem branch of the third order (considering the main axis as the first order) was measured, and oriented towards the north. Immediately after cutting the leaves, they were fixed in FAA (formalin-ethanol-glacial acetic acid) for 24 hours. Afterward, they were washed with water and stored in GAA (glycerine-ethanol-water). Subsequently, the leaves were infiltrated and embedded in glycol-methacrylate (GMA) (7100, Techno-vit. Kulzer & Co., Hanau, Germany) (Brandizzi & Ruzin, 1999). The embedded samples were then polymerized and mounted onto wooden blocks. Transverse sections of 3-μm-thick were obtained using a manual rotatory microtome (RM2125RT, Leica Biosystems, Richmond, IL, USA). The sections were stained with 0.6% brilliant cresyl blue, a panchromatic stain suitable for embedded tissue sections, and then observed under an optical microscope (Olympus, U-CMAD3, Tokyo, Japan) and photographed with an integrated camera (Infinity 1). The area of the substomatal chamber was measure by delimiting the space directly beneath the stomatal pore down to the underlying mesophyll tissue. The area of each mucilage idioblast was measured individually. Leaf thickness, cuticle thickness, and the thickness of the parenchyma and hypodermis were also measured. The analyzed sections were obtained from the middle portion of the leaf blade. Several transverse sections were obtained from the middle portion of each leaf. A total of eight leaves were analyzed, and three slides were prepared from each leaf as technical replicates. On each slide, multiple measurements were taken by scanning the entire section. The images were analyzed using ImageJ (U.S. National Institutes of Health, Bethesda, MD, USA).

3.2.5. Statistical Analysis

All data were subjected to the Shapiro-Wilk normality test. Microenvironmental variables were grouped within the 11:00–13:00 h period, considering this as the peak time, and these hours were compared to assess statistical differences within sites and between seasons, as well as between sites with similar seasons, using the non-parametric Kruskal-Wallis test. Leaf temperatures in the upper (A) and lower (B) canopy strata, along with water temperature, were categorized into two groups: daytime (07:30–19:20 h) and nighttime (19:30–07:20 h) to evaluate differences using Kruskal-Wallis analysis. Principal component analysis (PCA) was conducted for environmental variables and leaf temperatures in the upper and lower strata. Subsequently, linear regressions were applied to the leaf temperatures in strata A and B and the microenvironmental variables, including vapor pressure deficit (VPD), solar radiation (SR), photosynthetic photon flux (PPF), wind speed, and dew point. These variables were averaged hourly over the seven-day measurement period for both study sites (Chuburna and Celestun) and seasons (dry and rainy).

Anatomical leaf traits were only measured in Celestun. The evaluated variables included substomatal cavity area, cuticle thickness, parenchyma thickness, idioblast cell area, and total leaf thickness. Statistical comparisons were conducted between seasons within each stratum, and between strata within each season. These comparisons involved only two groups at the time and the Wilcoxon rank-sum test with p values were adjusted using the Bonferroni method. All analyses were conducted using R language (version 4.3.2) (Posit Team, 2023).

3.3. RESULTS

3.3.1 Microenvironment

The microenvironmental variables at both sites and in each season exhibited similar diurnal and nocturnal patterns across days. In general, most environmental variables, such as VPD, solar radiation, wind speed, PPF, and dew point, did not follow a normal distribution. The comparison of microenvironmental variables between seasons in Chuburna and Celestun revealed significant differences ($p < 0.001$). Regarding the comparison between the rainy season in Celestun and Chuburna, significant differences were found only for PPF and solar radiation ($p < 0.001$). In contrast, the comparison between the dry season in Celestun and Chuburna showed significant differences across all variables ($p < 0.001$) (Table 3.1). Porewater salinity was nor different in both sites; during the dry season was 37.14 ± 0.39 ‰ in Celestun and 37.0 ± 1.72 ‰ in Chuburna, whereas during the rainy season it was 28.6 ± 0.83 ‰ in Celestun and 30.37 ± 1.01 ‰ in Chuburna. However, the differences between seasons at each site were highly significant ($p < 0.0001$).

Table 3.1. Maximum microenvironmental variables (11:00 – 13:00 h) per site and season. PPF: Photosynthetic Photon Flux; VPD: Vapor Pressure Deficit. Data are presented as means ± standard error. Significant differences between seasons are indicated by lower case and differences between sites are indicated by capital letter. Differences are revealed by Kruskal-Wallis tests.

Season	Site	Solar radiation (W m^{-2})	Wind speed (m s^{-1})	PPF (µmol m^{-2} s^{-1})	VPD (kPa)	Dew (°C)
Dry	Celestun	973.23 ± 14.34^{aA}	1.97 ± 0.07^{aA}	1889.24 ± 20.52^{aA}	2.71 ± 0.18^{aA}	23.17 ± 0.23^{A}
	Chuburna	926.17 ± 21.53^{aB}	2.72 ± 0.26^{aB}	1730.19 ± 46.20^{aB}	1.88 ± 0.12^{aB}	10.04 ± 0.36^{B}
Rainy	Celestun	701.10 ± 28.76^{bA}	1.01 ± 0.05^{bA}	1477.90 ± 51.17^{bA}	1.66 ± 0.06^{bA}	NA
	Chuburna	862.97 ± 28.74^{bB}	1.13 ± 0.09^{bA}	1788.93 ± 48.61^{bB}	1.72 ± 0.04^{bA}	9.92 ± 0.08

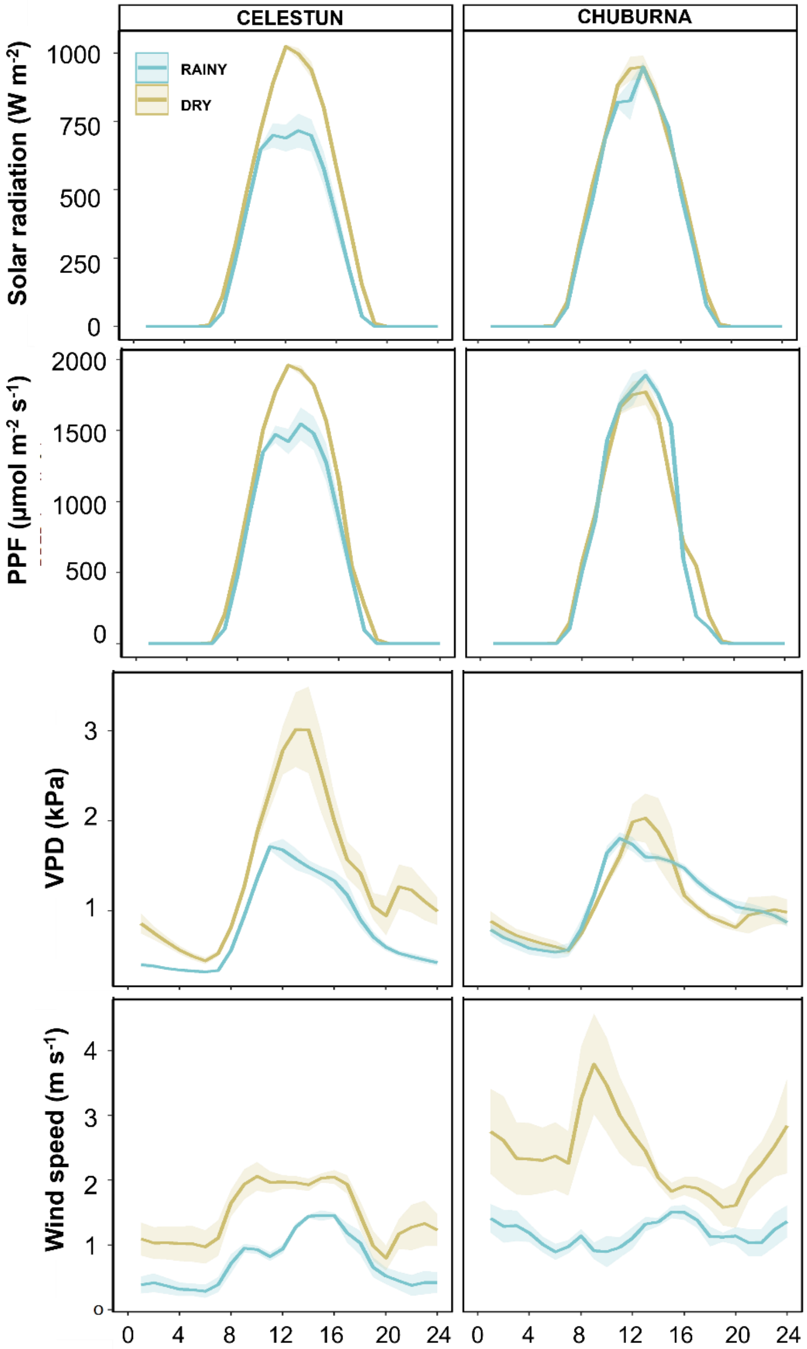

Figure 3.2 Mean microenvironmental variables measured in Celestun and Chuburna during the dry (brown) and rainy (blue) seasons. PPF: Photosynthetic Photon Flux (µmol m^{-2} s^{-1}), VPD: Vapor Pressure Deficit (kPa). Shaded areas represent the standard error.

3.3.2 Energy balance

3.3.2.1 Temperatures during the daytime

In the Celestun scrub mangrove, significant seasonal differences were observed for the foliar temperature of the upper stratum ($\chi^2=9.0362$, $p=0.0026$) (Figure 3.3A), lower stratum ($\chi^2=9.8$, $p=0.0017$) (Figure 3.3B), and water temperature ($\chi^2=9.8216$, $p=0.0017$) (Figure 3.3C). In contrast, in the Chuburna scrub mangrove, only the lower stratum ($\chi^2=9.0$, $p=0.0027$) and water temperature ($\chi^2=7.3673$, $p=0.0066$) (Figure 3.3B, C) showed significant seasonal variations. The upper foliar stratum of the mangrove in Chuburna did not exhibit significant seasonal differences ($\chi^2=0.1837$, $p=0.6682$) (Figure 3.3A).

In Celestun, leaf angle measurements for both the upper and lower strata showed significant differences between the dry and rainy seasons ($p < 0.05$). These differences were particularly notable int the upper stratum, where significantly higher leaf angle values were recorded during the dry season (73.4 ± 1.41) compared to the rainy season (54.4 ± 3.29). The lower stratum in Celestun also exhibited significant seasonal variation, with leaf angles averaging 40.4 ± 2.50 in dry season and 37.9 ± 3.18 in rainy season, indicating differences in foliar angles in response to seasonal changes in temperature.

In Chuburna, significant seasonal differences were observed in the lower stratum, with leaf angles increasing from 16.5 ± 0.31° in the dry season to 29.8 ± 0.77° in the rainy season. However, no significant seasonal differences were found in the upper stratum, where leaf angles were 47.3 ± 1.03° in the dry season and 62.9 ± 0.94° in the rainy season.

When comparing sites within the same season, significant differences were detected in the upper foliar stratum during the dry season ($\chi^2 = 7.3673$, $p = 0.0066$). The conserved scrub mangrove of Celestun showed higher leaf angles (73.4 ± 1.41°) than Chuburna (47.3 ± 1.03°), as well as higher temperatures (Figure 3.3A). In contrast, water temperature was significantly higher in the disturbed scrub mangrove of Chuburna than in Celestun ($\chi^2 = 9.0248$, $p = 0.0027$; Figure 3.3C). During the rainy season, leaf angle values in the lower stratum were also significantly higher in Celestun (37.9 ± 3.18°) compared to Chuburna (29.8 ± 0.77°).

During the rainy season, Celestun exhibited significantly higher leaf temperatures in the upper foliar stratum compared to the lower stratum ($\chi^2 = 9.8$, $p = 0.0017$). In contrast, Chuburna did not show significant temperature differences between the upper and lower foliar strata during the same period.

During the dry season, Chuburna recorded significantly higher water temperatures than Celestun ($\chi^2 = 9.8$, $p = 0.0017$). Leaf angle values in the lower stratum also followed this pattern: Chuburna showed higher angles during the rainy season (29.8 ± 0.77°) compared to Celestun (37.9 ± 3.18°).

No significant differences were found in the upper foliar stratum between sites ($\chi^2 = 0.3313$, $p = 0.5649$). Similarly, no significant differences in leaf angle were observed within sites for the upper stratum between the dry and rainy seasons (47.3 ± 1.03° in the dry vs. 62.9 ± 0.94° in the rainy season).

3.3.2.1 Temperatures during the nighttime

In the Celestun scrub mangrove, significant seasonal differences were observed for the upper foliar stratum ($\chi^2=3.9224$, $p=0.0476$) (Figure 3.3A) and water temperature ($\chi^2=6.8612$, $p=0.0088$) (Figure 3.3C), while the lower leaf temperature remained stable across seasons ($\chi^2=0.1020$, $p=0.7494$). In the Chuburna scrub mangrove, only nocturnal water temperature showed significant seasonal variations ($\chi^2=3.9224$, $p=0.0476$; $Z=-1.9805$, $p=0.0238$), with no significant changes in the foliar temperatures for the upper nor lower stratum ($p>0.05$).

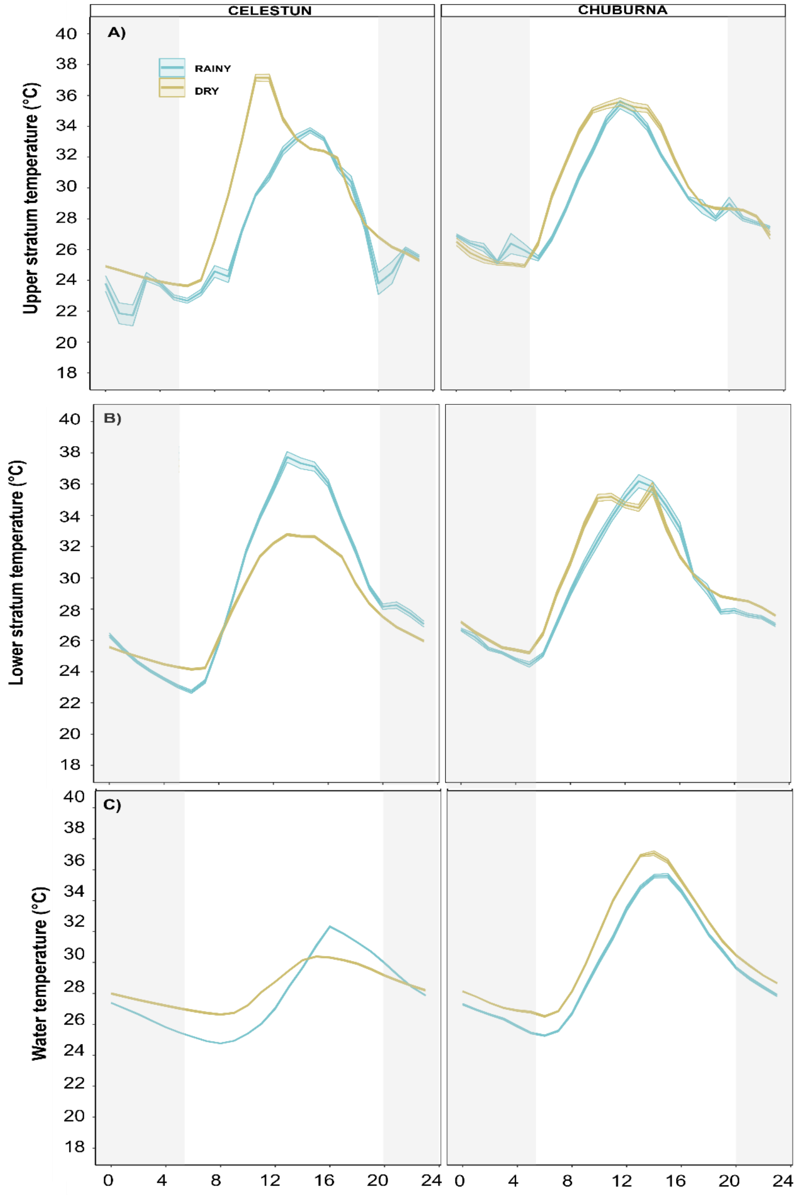

Figure 3.3 Diurnal means patterns of canopy and water temperatures (°C) measured over a continuous 7 day period during the dry and rainy seasons in Celestun and Chuburna *Rhizophora mangle* scrub mangrove. **A)** Mean upper strata temperature. **B)** Mean lower stratum temperature. **C)** Water temperature. Shaded lines represent nighttime.

During the dry season, no significant differences were detected between Celestun and Chuburna for any variable ($p > 0.05$), indicating similar nighttime conditions. However, in the rainy season, all variables exhibited significant differences between sites: upper stratum ($\chi^2 = 9.8$, $p<0.001$) (Figure 3.3A), lower stratum ($\chi^2 = 5.0$, $p = 0.0253$) (Figure 3.3B), and water temperature ($\chi^2 = 9.8$,

$p<0.001$) (Figure 3.3C). These results suggest that nighttime temperatures are more influenced by site location during the rainy season, while remaining stable across sites in the dry season.

3.3.2.3 Leaf temperatures and microenvironmental variables

Celestun exhibited pronounced seasonal and stratified physiological responses. In the upper stratum during the dry season, 56.4% of leaf temperature variability was explained by a model where VPD showed a significant negative effect ($\beta = -1.94$, $p = 0.01$), indicating transpiration limitation under high evaporative demand. Conversely, in the lower stratum ($R^2 = 0.97$), solar radiation increased leaf temperature ($\beta = 0.0069$, $p < 0.001$) while PPF decreased it ($\beta = -0.0033$, $p < 0.001$), revealing light-dependent stomatal regulation. During the rainy season, wind emerged as the primary cooling factor in the upper stratum ($\beta = -1.55$, $p < 0.001$), though its effect was counteracted by VPD ($\beta = 3.10$, $p < 0.001$), suggesting trade-offs between convective dissipation and water stress.

Chuburna showed markedly different patterns. In the dry season, dew formation increased leaf temperature in both upper ($p = 0.007$) and lower strata ($p = 0.0028$), potentially by reducing transpiration efficiency. While solar radiation heated lower leaves ($p < 0.001$), PPF had a cooling effect ($p < 0.001$), similar to Celestun. During rainy season, wind was the dominant modulator of leaf temperature ($p = 0.0006$ upper stratum; $p = 0.0002$ lower stratum), but unlike Celestun, VPD showed only marginal influence ($p = 0.014$) and radiation maintained its warming effect ($p = 0.0097$) in the lower stratum.

Both sites shared air temperature as the most consistent leaf temperature predictor ($\beta = 0.97$-1.28, $p < 0.001$ in all models), highlighting its central role in leaf warming. However, divergent sensitivities to VPD, wind, and PPF underscore contrasting thermal regulation strategies between conserved and disturbed mangroves.

3.3.2.4 Leaf anatomy

The leaves of *Rhizophora mangle* from Celestun exhibit a uniseriate epidermis composed of quadrangular and rectangular cells covered by a thick cuticle (Table 3.2), particularly prominent on the adaxial surface (Figure 3.5C). Below the epidermis a multilayered hypodermis (five layers) (Figure 3.5A). The mesophyll is differentiated into two types of parenchyma: a well-developed palisade parenchyma with elongated, densely packed, chlorenchyma cells; and a spongy parenchyma located toward the interior, composed of irregularly shaped cells and large intercellular spaces (Figure 3.5D, E). Numerous mucilaginous idioblasts and astrosclereids are scattered throughout the mesophyll (Figure 3.5 D, F). The stomata are hypostomatic, with noticeable cuticular extensions and large substomatal cavities (Figure 3.5A, B, E). Additional structures such as cork warts and terminal tracheids are also present (Figure 3.5A).

Distinct anatomical patterns were observed between the upper and lower strata, as well as between seasons. During the dry season, the upper stratum showed significantly greater cuticle thickness (12.75 ± 1.14 µm; W= 53, p.adj= 1), palisade parenchyma thickness (186 ± 16.07 µm; W= 120, p.adj= 1), idioblast cell area (7496.11 ± 1676 µm^2; W= 18, p.adj= 0.05), and leaf thickness compared (718.42 ± 62.83 µm; W= 120, p.adj= 1) to the lower stratum. Leaf width also differed between strata, being wider in the upper stratum during the dry season (W= 120, p.adj= 1). In the rainy season, only cuticle thickness (12.64 ± 0.72 µm; W= 45, p.adj= 0.9) and idioblast cell area (5884.59 ± 336.77 µm^2; W= 45.5, p.adj= 0.7) remained significantly higher in the upper stratum than in the lower (Table 3.2).

When comparing seasons, most anatomical variables remained consistent across both canopy strata. No statistically significant seasonal variation was observed in either stratum, except for idioblast cell area in the lower stratum (W = 38, p.adj = 1; Table 3.2). These findings indicate that anatomical plasticity is more pronounced across leaf strata than across seasons, with only a few traits showing significant responses to seasonal changes.

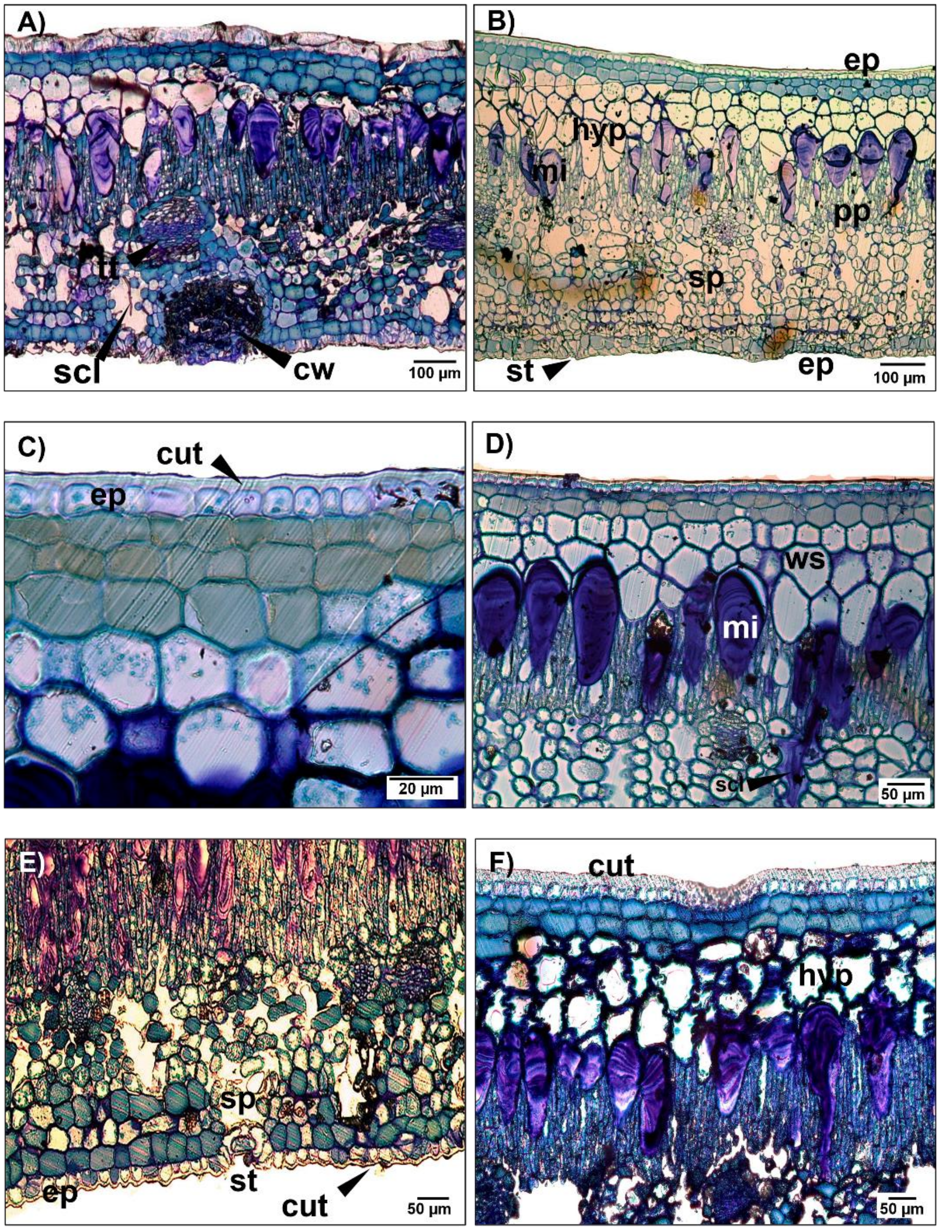

Figure 3.5 Cross section of *Rhizophora mangle* scrub leaves from Celestun. A–D) Leaves collected during the dry season. E–F) Leaves collected during the rainy season. A) Dorsiventral mesophyll with cork wart, scattered sclereids, and vascular tissue. B) Dorsiventral mesophyll, showing a single layer of epidermal cells, multiple layers forming the hypodermis, palisade parenchyma, idioblasts embedded within the palisade parenchyma, and spongy parenchyma with well-defined intercellular spaces (aerenchyma). The abaxial epidermis presents stomata, characterizing the leaf as hypostomatic. C) Adaxial cuticle, a single row of epidermal cells, and detail of the hypodermis with thickened cell walls. D) Details of mucilaginous idioblasts, sclereids, and aerenchyma. E) Abaxial side of the leaf in cross-section showing spongy parenchyma (aerenchyma), abaxial epidermis, sunken stomata with guard cell showing

a cuticular ledge, and a large substomatal cavity. F) Thick adaxial cuticle with hypodermal cells having irregular cell walls, presence of idioblasts, and palisade parenchyma. Scale bars: (A, B) = 100 µm, (C) = 20 µm, (D, E, F) = 50 µm. Abbreviations: **Scl**: sclereid, **cw**: cork wart, **st**: stomata, **eo**: epidermis, **pp**: palisade parenchyma, **sp**: spongy parenchyma, **hyp**: hypodermis, **cut**: cuticle; **mi**: mucilage idioblast. Note that each micrograph displays a different toolbar. A, B= 100 µm, C= 20 µm, D, E, F= 50 µm.

Table 3.2 Anatomical variables evaluated in the leaves of scrub Rhizophora mangle from Celestun are presented. Data are expressed as means ± standard error. Significant differences between seasons are indicated by uppercase letters, while differences between strata are indicated by lowercase letters. Differences were determined using Wilcoxon rank-sum test and p-values were adjusted using the Bonferroni for multiple testing.

Season	Stratum	Cuticule thickness (µm)	Hypodermis thickness (µm)	palisade parenchyma (µm)	Mucilage idioblast area (µm^2)	Substomatal cavity area (µm^2)	Leaf thickness (µm)
Dry	Upper	12.75 ± 1.14^{Aa}	173.43 ± 18.59^{Aa}	186.26 ± 16.07^{Aa}	7496.11 ± 1676.16^{Aa}	5533.96 ± 503.68^{Aa}	718.42 ± 62.83^{Aa}
	Lower	8.06 ± 0.66^{Ab}	139.35 ± 9.59^{Aa}	131.81 ± 5.97^{Ab}	4233.94 ± 280.15^{Ab}	7425.75 ± 1305.84^{Aa}	553.97 ± 14.09^{Ab}
Rainy	Upper	12.64 ± 0.72^{Aa}	178.39 ± 10.49^{Aa}	148.82 ± 5.61^{Ba}	5884.59 ± 336.77^{Aa}	6397.51 ± 1166.04^{Aa}	700.3 ± 33.1^{Aa}
	Lower	8.95 ± 1^{Ab}	131.52 ± 10.09^{Aa}	132.54 ± 8.96^{Aa}	4244.7 ± 469.38^{Bb}	4233.18 ± 560.34^{Aa}	555.06 ± 35.06^{Aa}

3.3.2.5 Overall leaf energy balance

For the leaves of the Celestun scrub mangrove, significant differences were observed between the dry and rainy seasons for most of the analyzed variables showed statistically significant differences: energy balance ($p < 0.001$), sensible heat ($p < 0.05$), latent heat ($p < 0.001$), net radiation ($p < 0.001$), solar radiation ($p < 0.05$), wind speed ($p < 0.001$), leaf temperature ($p < 0.01$), leaf length ($p < 0.001$), and boundary layer ($p < 0.001$). No significant differences were detected for air temperature ($p > 0.05$) and leaf angle ($p > 0.05$) (Fig. 3.4A).

For the leaves of the Chuburna scrub mangrove, significant differences were also found between the dry and rainy seasons for most variables: energy balance ($p < 0.001$), sensible heat ($p < 0.001$), latent heat ($p < 0.001$), solar radiation ($p < 0.001$), wind speed ($p < 0.01$), boundary layer ($p < 0.001$), and angle ($p < 0.05$) showed significant differences. No significant differences were observed for leaf temperature ($p > 0.05$), net radiation ($p > 0.05$), and leaf length ($p > 0.05$) (Fig. 3.4B).

Whem comparing between Celestun and Chuburna during the dry season, differences were detected for energy balance ($p < 0.001$), sensible heat ($p < 0.05$), latent heat ($p < 0.01$), net radiation ($p < 0.001$), wind speed ($p < 0.05$), leaf length ($p < 0.001$), air temperature ($p < 0.01$), and angle ($p < 0.001$). No significant differences were found for solar radiation ($p > 0.05$), net radiation ($p > 0.05$), leaf temperature ($p > 0.05$), and boundary layer ($p > 0.05$).

The comparison between Celestun and Chuburna during the rainy season showed significant differences for energy balance ($p < 0.001$), sensible heat ($p < 0.001$), latent heat ($p < 0.001$), solar radiation ($p < 0.01$), wind speed ($p < 0.001$), leaf temperature ($p < 0.001$), air temperature ($p < 0.01$), and boundary layer ($p < 0.001$). No significant differences were detected for leaf length ($p > 0.05$) and angle ($p > 0.05$).

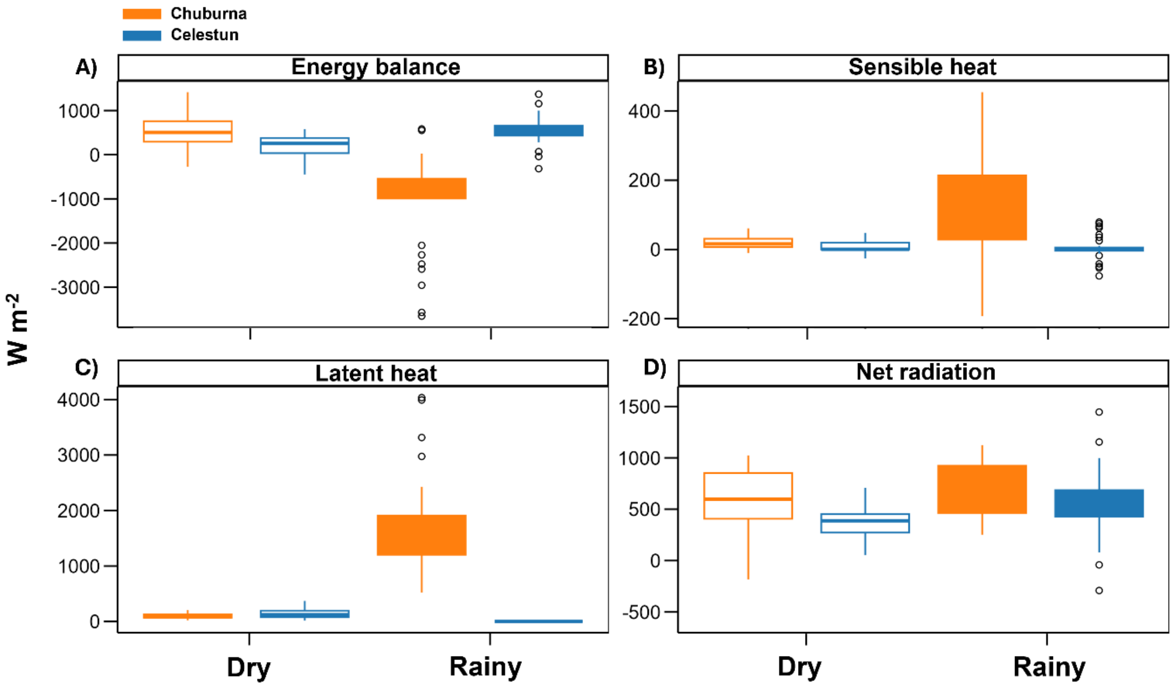

Figure 3.5 Energy balance components (W m⁻²) in scrub *Rhizophora mangle* leaves across sites and seasons. (A) Total energy balance, (B) Sensible heat (convection and conduction), (C) Latent heat (transpiration), and (D) Net radiation. Blue represents the conserved mangrove in Celestun, while orange indicates the disturbed mangrove in Chuburna. Hollow boxplots correspond to the dry season, and solid-filled boxplots represent the rainy season.

Table 3.3. Maximum energy balance components and microenvironmental variables of the energy balance (12:00 h) per site and season. Data are presented as means ± standard error. Significant differences between seasons are indicated by lower case and differences between sites are indicated by capital letter. Differences are revealed by Kruskal-Wallis tests.

Site	Season	Energy balance (W m^{-2})	Sensible heat (W m^{-2})	Latent heat (W m^{-2})	Net raditation (W m^{-2})	Solar radiation (W m-2)	Wind speed (m s^{-1})	Leaf temperature (°C)	Leaf lenght (cm)	Air temperature (°C)	Boundary layer (mm)	Angle (°)
Celestun	Dry	31.97 ± 65.4^{aA}	17.38 ± 5.58^{aA}	155.27 ± 13.89^{aA}	204.63 ± 57.88^{aA}	432.66 ± 45.95^{aA}	1.71 ± 0.23^{aA}	35.55 ± 0.69^{aA}	10.31 ± 0.12^{aA}	32.42 ± 0.89^{aA}	0.01 ± 0a^{A}	49.29 ± 3.53^{aA}
	Rainy	437.62 ± 112.19^{bA}	2.9 ± 3.64^{bA}	0 ± 0^{bA}	440.53 ± 112.71^{bA}	493.13 ± 45.72^{bA}	0.23 ± 0.03^{bA}	33.3 ± 0.43^{bA}	9.01 ± 0.17^{bA}	35.72 ± 2.09^{aA}	0.03 ± 0^{bA}	45.54 ± 3.14^{aA}
Chuburna	Dry	509.82 ± 44.78^{aB}	20.38 ± 3.82^{aB}	100.36 ± 7.08^{aB}	630.56 ± 43.13^{aB}	494 ±41.33^{aA}	1.11 ± 0.11^{aA}	36.57 ± 0.8^{aA}	9.14 ± 0.12^{aB}	35.34 ± 0.28^{aB}	0.01 ± 0^{aA}	29.86 ± 2.12^{aB}
	Rainy	-1053.55 ± 133.2^{bB}	160.54 ± 28.98^{bB}	1521.8 ± 118.10^{bB}	628.79 ± 34.8^{bB}	758.65 ± 61^{bB}	0.76 ± 0.11^{bB}	36.49 ± 0.8^{aB}	9.1 ± 0.11^{aA}	31.78 ± 0.65^{bB}	0 ± 0^{bB}	39.76 ± 2.86^{bA}

3.3.2.6 Aerodynamic resistance

The aerodynamic resistance at the leaf level was higher in Celestun during the rainy season, indicating lower transpiration efficiency compared to other conditions. In contrast, the lower values in Chuburna and in Celestun during the dry season suggest higher water loss, likely due to a greater vapor pressure deficit and lower boundary layer resistance. This highlights how environmental conditions and boundary layer structure influence leaf-level transpiration (Table 3.3).

During the dry season, aerodynamic resistance is low in both sites, facilitating heat and water vapor exchange with the atmosphere. Although Celestun has a higher latent heat (155.2 W m^{-2}) than Chuburna (100.36 W m^{-2}), the high VPD in both sites allows for efficient exchange. In contrast, during the rainy season, aerodynamic resistance in Celestún is considerable high, making atmospheric exchange more difficult, likely due to high humidity and low latent heat exchange (2 W m^{-2}). In Chuburna, aerodynamic resistance is nearly zero, enabling highly efficient exchange, consistent with the high latent heat value (1521.8 W m^{-2}). This suggests that in Chuburna, rainy season conditions promote greater transpiration and heat dissipation to the atmosphere (Table 3.3).

Table 3.3. Aerodynamic resistance (ar) of Celestun and Chuburna in two seasons considering the boundary layer and the diffusion coefficient of water vapor in the air*, latent heat (LE) and VPD**, and momentum***

Site	Season	ar (s m^{-1}) *	ar (s m^{-1}) **	ar (s m^{-1}) ***
Celestun	Dry	0.42	0.14	5.2
	Rainy	1.25	500.49	39.1
Chuburna	Dry	0.42	0.23	3.36
	Rainy	0.42	0.00	4.91

In both sites and seasons, the lowest aerodynamic resistance values, calculated using momentum theory, occur during the dry season, indicating higher latent heat exchange, these values are from the equations. During the rainy season, aerodynamic resistance increases, particularly in Celestun, where it reaches its highest value, suggesting a possible limitation in transpiration due to high relative humidity, which reduces the atmosphere's capacity to absorb water vapor. In Chuburna, aerodynamic resistance values are slightly lower than in Celestun during the rainy season, indicating potential microenvironmental differences.

3.4. DISCUSSION

3.4.1 Mangrove microenvironments: Conserved vs disturbed

During the dry season, VPD was higher in Celestun (conserved mangrove) compared to Chuburna (disturbed mangrove), despite that the latter showed higher air and substrate water temperatures, which contradicts our initial hypothesis. This can be explained by differences in canopy structure and vegetation cover between the two sites. In ecosystems with higher vegetation density, such as Celestun, the plant canopy acts as a physical barrier that reduces wind speed by generating friction and turbulence within the canopy layer (Álvarez *et al*., 2012; Nunez *et al*., 2002). This limits air mixing and the dissipation of heat and moisture, promoting more humid microclimatic conditions near the ground. In contrast, the disturbed site, characterized by more sparse vegetation, allows for greater wind penetration, which enhances the dissipation of both latent and sensible heat and facilitates the transport of moisture (Leclerc & Foken, 2014). This increased ventilation, combined with greater soil exposure and higher water temperatures, may enhance surface evaporation, increasing relative humidity, and thereby reducing local VPD (Beringer *et al*., 2003; Oke, 1987).

Moreover, the thermal behavior of water reflects these microenvironmental differences. In Celestun, the surface water temperature increased gradually, beginning around 9:00 h. In contrast, in Chuburna, the water temperature began rising as early as 6:30 h, displaying a steeper warming curve. This pattern suggests greater direct exposure to solar radiation and less canopy cover to buffer heat gains (Krauss *et al*., 2008). The contrast was most pronounced during the dry season, when average water temperatures in the disturbed mangrove (Chuburna) reached 36 °C, compared to approximately 30 °C in the conserved site (Celestun). This represents a 20% increase in water temperature in the disturbed mangrove of Chuburná relative to the conserved site in Celestún. Reduced vegetation cover and historical hydrological alteration in the disturbed site have likely diminished its capacity to buffer daily thermal fluctuations, resulting in an environment more prone to temperature extremes (McKee *et al*., 2007).

In the disturbed mangrove of Chuburna, elevated surface water temperatures and low vegetation density favor more intense evaporation, especially during the dry season. Coupled with higher wind speeds, this condition likely facilitates the dissipation of water vapor, preventing moisture from remaining within the local microenvironment. This process, known as moisture advection, has been documented as a mechanism by which vapor is transported by wind to other regions, thereby altering local humidity and temperature patterns (Stohl & James, 2005; Brubaker *et al.*, 1993). In contrast, in Celestun, the denser canopy structure restricts wind flow, reducing moisture loss through evaporation and supporting a more stable and humid microclimate (Baldocchi *et al.*, 2002; Monteith & Unsworth, 1990).

3.4.2 Thermoregulation in Stratum Gradient and the Influence of Microenvironmental Factors

Leaves exhibit diverse morphological and physiological traits that enable temperature regulation, including variations in leaf area, water content, thickness, angle, stomatal density and aperture, as well as spongy mesophyll and cuticle thickness (Li *et al.*, 2022; Naskar *et al.*, 2021; Ivanilson *et al.*, 2011). In this study, in the conserved mangrove of Celestun during the dry season, leaves in the upper stratum reached significantly higher temperatures and displayed an average leaf angle of 73.4°, while shaded leaves in the lower stratum were up to 6 °C cooler, with an average angle of 40.4°. These findings suggest a distinct thermal and functional stratification, despite the relatively short height of the trees—an unusual pattern, as vertical stratification is typically associated with taller canopy gradients (Lebrija-Trejos *et al.*, 2011).

This phenomenon has been documented in tropical forests, where canopy height correlates with thermal variation. For instance, upper-canopy leaves often exhibit midday temperatures ~2 °C higher than those in lower strata, promoting increased stomatal conductance and activation of photoprotective mechanisms such as the xanthophyll cycle (Miller *et al.*, 2021; Siddiq *et al.*, 2017; Slot *et al.*, 2016; Adams *et al.*, 2004).

In our study, VPD emerged as the primary driver of leaf temperature variation in the upper stratum during the dry season. Elevated VPD likely restricts thermoregulatory capacity by reducing stomatal conductance (Li *et al.*, 2018), supporting the hypothesis that transpiration declines significantly in scrub *Rhizophora mangle* mangroves under drought conditions (Ceron-Aguilera *et al*., 2025).

During the rainy season, the upper stratum showed reduced leaf angles (averaging 54.4°), and leaf temperatures in the lower stratum exceeded those in the upper foliar stratum by up to 3 °C. This reversal may reflect increased water temperature and ambient humidity, which enhance heat retention in lower layers (Vinod *et al*., 2023). Conversely, the upper stratum benefited from higher wind speeds and lower VPD, facilitating more efficient heat dissipation by sensible heat.

3.4.3 Anatomical Adaptations to Microenvironmental Conditions

The conserved scrub mangrove of *Rhizophora mangle* of Celestun exhibited anatomical differences primarily between canopy strata, with notable variations in cuticle thickness, mucilaginous idioblast area, total leaf thickness, and mesophyll thickness. Palisade parenchyma thickness is closely linked to total leaf thickness, a trait commonly associated with increased exposure to solar radiation (Coble & Cavaleri, 2017). Such thickening may also be related to the presence of hypodermal tissue, which in some species consists of multiple layers and serves as a water storage site. This reservoir can be critical for maintaining cell turgor and sustaining photosynthetic activity, particularly in upper stratum leaves exposed to more extreme conditions. These conditions were pronounced during the dry season, when higher values of porewater salinity (37.14 ± 0.39 ppt), VPD (2.71 ± 0.18 kPa), and PPF (1889.24 ± 20.52 µmol m^{-2} s^{-1}).

The hypodermis, in addition to functioning as a water storage site, may also act as an osmoregulatory tissue that helps maintain leaf turgor (Jiang *et al*., 2017), along with mucilaginous idioblasts (Pelozo *et al*., 2016; Reef & Lovelock, 2015). In *R. mangle*, Dos Santos et al. (2022) reported a hypodermis thickness of 190 µm, greater than the values found in our study for the upper canopy stratum (173 µm in the dry season and 178 µm in the rainy season), though still considerably thicker than that of other mangrove species such as *Avicennia germinans* (0.70 µm) or *Laguncularia racemosa* (0.10 µm). These anatomical differences may reflect both interspecific variation and phenotypic plasticity in response to microenvironmental conditions and forest conservation status.

Cuticle thickness is another key trait associated with protection against solar radiation and water loss due to its hydrophobic properties (Boanares *et al*., 2021; Guzmán-Delgado *et al*., 2021; Reef

& Lovelock, 2015; Naidoo *et al*., 2011). This is consistent with our results, where upper-canopy leaves exhibited significantly thicker cuticles. Specifically, in *R. mangle*, we observed cuticle thickness values of up to 12.74 µm, higher than the 9 µm reported by Ivanilson et al. (2011). Likewise, total leaf thickness in the upper canopy reached 718 µm, also surpassing the previously documented value of 581 µm. These findings support the idea that canopy stratification in mangrove forests—even in low-stature stands like those in Celestun—can generate distinct microclimatic zones that drive specific anatomical adaptations.

It is worth noting that foliar water uptake in mangroves is not limited to stomata but can also occur via structures such as cork warts, glands, trichomes, or even thin cuticles (especially on the abaxial surface). This capacity has been reported for various mangrove species, including *R. mangle*, *A. marina*, *A. germinans*, *A. schaueriana*, *Bruguiera gymnorhiza*, *Conocarpus erectus*, and *L. racemosa* (Dos Santos *et al*., 2022).

Mucilaginous idioblasts were located in the palisade mesophyll near the adaxial epidermis. The area of these idioblasts varied among species and tended to be negatively correlated with total leaf thickness (Tulyananda & Nilsen, 2017). Several types of idioblasts have been described in mangrove species, including mucilage-containing cells, tannin cells, crystal idioblasts, and laticifers, particularly in the genera *Rhizophora*, *Sonneratia*, *Osbornia*, and *Excoecaria*. In this study, we identified mucilaginous idioblasts in *R. mangle*, consistent with earlier reports by Victório *et al.* (2024).

With regard to substomatal cavity area, no significant differences were found between canopy strata or between seasons, despite clear variations in microclimatic conditions. This finding is relevant because larger substomatal cavities facilitate greater gas conductance, reduce internal pressure, and promote mass flow-driven gas exchange—primarily driven by transpiration (Kowalski, 2025). In this context, higher leaf temperatures in the upper canopy may increase reliance on non-diffusive gas exchange mechanisms, revealing potential physiological plasticity that is not necessarily accompanied by structural plasticity in these cavities. Further research is needed to evaluate this hypothesis.

Despite the height of the scrub *R. mangle*, we documented clear differences in leaf anatomical traits between strata. These differences may be more strongly associated with microenvironmental conditions such as VPD and solar radiation than with porewater salinity, which contrast with patterns reported for other species like *A. marina* (Naidoo *et al*., 2011). Overall, our results indicate that even in low-canopy mangrove forests, vertical stratification can produce microenvironmental gradients that significantly influence foliar structure. These findings underscore the importance of considering both microclimatic variation and forest conservation status when examining anatomical plasticity in key mangrove species such as *R. mangle*.

3.4.4 Contrasting Patterns in Hydrologically Disturbed Mangroves

In the hydrologically disturbed Churbuna mangrove, foliar thermal stratification was absent in both seasons, likely due to low tree density and greater penetration of net radiation. Sunflecks elevated lower-stratum leaf temperatures, while small leaf angles (15° dry season; 30° rainy season) increased radiation exposure. Such rapid thermal fluctuations—particularly when stomata are closed—can raise leaf temperatures by 1–2 °C per minute, heightening the risk of thermal damage (Schymanski *et al*., 2013; Way & Pearcy, 2012).

High relative humidity in the lower foliar stratum may also impede latent heat dissipation, exacerbating temperature increases (Vinod *et al*., 2023). Rainy season temperatures in this foliar stratum surpassed dry-season values, suggesting impaired heat dissipation that could compromise photosynthesis and stomatal regulation (Li *et al*., 2018). While temperatures below 30 °C may favor photosynthesis in some tropical forests, light limitation often offsets this benefit (Mau *et al*., 2018; Doughty & Goulden, 2008).

3.4.5 Implications for Leaf-Air Temperature Relationships

Although air temperature is frequently used as a proxy for leaf temperature, this relationship is inconsistent in tropical forests (Miller *et al.,* 2021; Dong *et al.,* 2017). Our results align with these studies: except during Celestun's rainy season, leaf temperatures consistently exceeded air temperatures at both sites. Evergreen species may be particularly vulnerable to VPD fluctuations, which can disrupt stomatal conductance and gas exchange (Siddiq *et al*., 2017).

Stomatal conductance is critical for thermoregulation via transpirational cooling (Schymanski *et al.,* 2013). Under high radiation and VPD, stomatal closure to conserve water may elevate leaf temperatures. While our stomatal conductance data were limited, the theoretical framework remains robust, especially for evergreen mangroves balancing gas exchange and thermal regulation (*Li et al*., 2018). In Celestún, dry-season transpiration likely moderated leaf temperatures to sustain photosynthesis.

Seasonal energy dynamics directly influence mangrove growth and reproduction. Quantifying these relationships is essential for modeling species distributions under climate change (Jones & Rotenberg, 2001) and understanding thermoregulatory impacts on photosynthesis, respiration, and root physiology (Salas-Rabaza *et al.*, 2024).

3.4.6 General Energy Balance

Given the height of scrub *Rhizophora mangle* individuals (1.8–2.0 m) in both studied mangrove populations, we assessed energy balance gradients at the individual level, including latent heat, sensible heat, net radiation, aerodynamic resistance, and microenvironmental variables. Our findings reveal fundamentally distinct thermoregulatory strategies between the conserved Celestun and the disturbed Chuburna mangroves, mediated by aerodynamic resistance and water diffusion via latent heat, reflecting their contrasting microenvironments.

In the conserved Celestun mangrove, we observed pronounced seasonal variations in key energy balance components, such as latent heat and net radiation. This suggests a robust capacity for physiological modulation—via transpiration and sensible heat transfer—in response to seasonal microclimate shifts. These patterns align with studies of mature mangroves, where efficient energy and carbon flux regulation has been documented (Freire *et al*., 2022).

Conversely, in the disturbed Chuburna mangrove, neither leaf temperature nor net radiation exhibited significant seasonal changes, indicating a diminished capacity for environmental response. This limitation likely lowers *R. mangle* density for the historical hydrological disruption. Studies in disturbed forests (e.g., post-hurricane systems) report similar energy balance alterations, including reduced heat dissipation efficiency and canopy structural impacts (Barr *et al*., 2013). Our results further suggest that Chuburna prioritizes physical heat dissipation over physiological regulation, whereas Celestun relies more on water-driven cooling mechanisms. Research in other ecosystems—such as West African Sudanian savannas—highlights how landscape heterogeneity and soil degradation can skew eddy covariance measurements and energy balance closure (Nadolski *et al*., 2024).

The Celestun - Chuburna comparison underscores how mangrove conservation status regulate energy balance resilience, with direct implications for climate adaptability and ecological functionality. These differences affect not only biodiversity (e.g., fauna, epiphytes) but also coastal ecosystem services (Bimrah *et al*., 2022).

Under climate change, understanding mangrove energy strategies is critical (Adame *et al.,* 2021), particularly in tropical regions facing rising temperatures. Mangroves interact with both hydrology and ambient temperatures, influencing carbon sequestration, evapotranspiration (water fluxes), and biodiversity maintenance. Their ecosystem services—especially climate regulation and biodiversity support—are pivotal. Emerging vulnerabilities reflect a dichotomy: conserved systems risk carbon starvation during droughts due to stomatal limitations, while disturbed systems face overheating during heatwaves (Sippo *et al*., 2018).

3.4. CONCLUSION

Our results demonstrate striking differences in microenvironmental conditions and thermoregulation strategies between the conserved mangrove of Celestun and the disturbed mangrove of Chuburna. In Celestun, the denser canopy created a stable microclimate with higher humidity, despite exhibiting higher VPD than Chuburna. This apparent contradiction is explained by vegetation structure: greater canopy coverage in Celestun reduces wind speed and limits air mixing, whereas in Chuburná, sparse vegetation density allows greater wind penetration that enhances heat and moisture dissipation. These structural differences were clearly reflected in water thermal dynamics, where Chuburna showed earlier warming and reached temperatures 20% higher, demonstrating reduced thermal buffering capacity due to loss of tree cover.

At the foliar level, the mangroves exhibited contrasting adaptations. In Celestun, clear thermal stratification between strata was observed, along with specialized anatomical traits such as thicker cuticles, leaf thickness, palisade parenchyma and mucilaginous idioblasts in the upper stratum - characteristics associated with exposure to higher VPD and radiation stress. These physiological mechanisms enable active leaf temperature regulation. Conversely, in Chuburna, the absence of thermal stratification and reduced leaf angles reflect greater dependence on physical heat dissipation processes, with diminished physiological control due to historical hydrological disturbance at the site.

The ecological implications of these differences are significant. Conserved mangroves like Celestun maintain more efficient energy balance through physiological regulation mechanisms, better supporting ecosystem functions including carbon storage and biodiversity maintenance. However, they face risks of physiological stress during prolonged droughts. In contrast, disturbed mangroves like Chuburna are more vulnerable to thermal extremes due to their reduced regulatory capacity, potentially compromising their recovery and persistence under climate change. This dichotomy underscores the importance of considering both microenvironmental factors and functional adaptations in mangrove conservation and restoration efforts, particularly under scenarios of rising temperatures and extreme climate events. Preservation of canopy structure emerges as a critical factor for maintaining the thermal resilience and ecological functions of these coastal ecosystems.

Monitoring environmental and physicochemical variables in conserved, restored, and disturbed mangrove forests is crucial. It helps us better understand plant species' physiological strategies and their responses to climate change. Our findings also suggest that temperature measurements could serve as a practical indicator of energy dissipation strategies in mangroves. This approach could streamline monitoring during forest assessments and restoration efforts.

CAPÍTULO IV

DISCUSIÓN, CONCLUSIÓN Y PERSPECTIVAS

4.1. DISCUSIÓN GENERAL

Este estudio evaluó los efectos de la variabilidad estacional del microambiente —incluyendo el déficit de presión de vapor (DPV), la radiación solar, el flujo de fotones fotosintéticos (PPF), la velocidad del viento y la formación de rocío— sobre las respuestas fisiológicas y anatómicas de los manglares enanos de *Rhizophora mangle* en Yucatán. La densidad de flujo de savia y las tasas de flujo de savia mostraron valores notablemente altos en comparación con otros ecosistemas de manglar (Leng & Cao, 2020; Krauss, 2007; Scholz *et al*., 2002), particularmente durante la temporada de lluvias, donde los manglares chaparros estudiados presentaron la mayor densidad de flujo de savia. Este hallazgo es ecológicamente significativo, ya que los manglares chaparros están ampliamente distribuidos en la Península de Yucatán y representan importantes sumideros de carbono en los suelos a pesar del estrés por salinidad intersticial (Herrera-Silveira *et al*., 2020).

Estudios recientes destacan que los manglares chaparros son reservorios excepcionales de carbono, aunque emiten flujos moderados de metano y CO_2 (Salas-Rabaza *et al*., 2024). Sin embargo, sus funciones ecológicas más amplias y los servicios ecosistémicos que prestan siguen siendo poco estudiados. Para abordar esta brecha, nuestro estudio cuantificó el transporte de agua de los manglares chaparros a distintas escalas; desde el flujo de savia y la transpiración a nivel individual hasta estimaciones por unidad de área. Enfoques multiescalares como este son fundamentales para ampliar la investigación hacia otros ecotipos, especialmente si se combinan con diferentes métodos para cuantificar la densidad del flujo de savia —que permiten capturar contribuciones específicas por especie— en lugar de depender exclusivamente de torres de covarianza de remolinos (Alvarado *et al*., 2021; Freire *et al*., 2020). Aunque la covarianza de remolinos proporciona datos de alta resolución temporal, no permite separar los flujos de calor latente entre la transpiración de la vegetación y la evaporación del suelo. Nuestra metodología permite generar conocimientos escalables, reduciendo las suposiciones de que los flujos de calor latente provienen predominantemente de la transpiración.

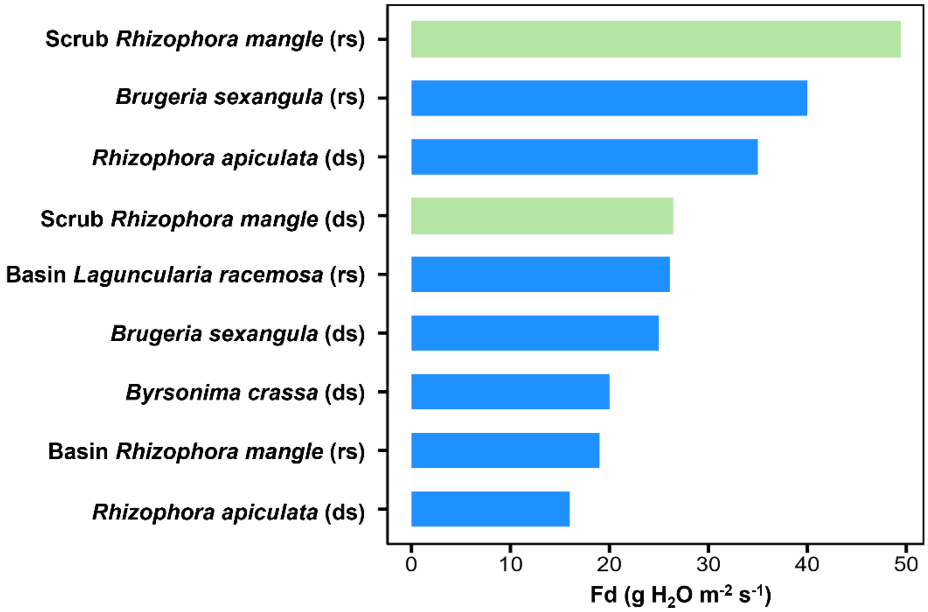

Figure 4.1 Análisis comparativo de la densidad media de flujo de savia (Fd; g H_2O m^{-2} s^{-1}) en especies de manglar a partir de múltiples estudios, considerando el ecotipo (cuando fue especificado) y la estacionalidad. Rs: temporada de lluvias; ds: temporada seca. Los datos del presente estudio están resaltados en verde.

Además, reportamos la primera evidencia documentada de flujo de savia nocturno en *Rhizophora mangle* para la Península de Yucatán. Este hallazgo es ecológicamente relevante, ya que demuestra que incluso cuando la transpiración está inactiva durante la noche, el movimiento de agua puede facilitar procesos de crecimiento, la fijación de carbono por la mañana y la reparación de embolismos (Wu *et al*., 2023; Dawson *et al*., 2007), especialmente en períodos de alta disponibilidad de agua como la temporada de lluvias. Asimismo, nuestros resultados corroboran que los manglares chaparros poseen un sistema vascular resistente a la cavitación (Cisneros-De la Cruz *et al*., 2022), y que las hojas no muestran variación estacional en el área de la cavidad subestomática sugiriendo que el intercambio de gases- asociado a la fotosíntesis y transpiración- no se encuentra comprometido, independientemente de la variabilidad estacional. Aunque habría que considerar el efecto de la temperatura foliar sobre el intercambio de gases entre la cavidad subestomática y la atmósfera.

En cuanto a la dinámica del balance energético, los análisis comparativos entre los manglares de Celestún (conservado) y Chuburná (perturbado) revelan cómo el estado estructural y ambiental del ecosistema influye en su eficiencia termodinámica. La estratificación térmica del dosel dependió del microclima: Celestún presentó gradientes de temperatura claros entre los estratos superior e inferior, mientras que en Chuburná no se observó estratificación vertical significativa. Durante la temporada seca, el balance energético cercano al equilibrio en Celestún ($Rn \approx H + LE$), con el 75.8% de la radiación neta destinada al calor latente (LE), refleja una alta eficiencia fisiológica en el uso del agua y una regulación estomática efectiva. Esto coincide con sistemas de manglar conservados, donde la densa cobertura del dosel maximiza la transpiración y minimiza el calentamiento superficial (Alongi, 2014; Barr *et al.,* 2010). En contraste, Chuburná mostró una inestabilidad pronunciada durante la temporada de lluvias, con un balance energético fuertemente negativo ($Rn \ll H + LE$) y una pérdida desproporcionada de calor latente ($LE > Rn$). Esta anomalía probablemente se debe a la alteración hidrológica histórica, que compromete la disponibilidad de agua en el suelo e interfiere con el control de la transpiración, exacerbando el estrés hidráulico y los flujos turbulentos de energía (Krauss et al., 2008).

Además, la dominancia de procesos físicos (por ejemplo, un alto flujo de calor sensible) en Chuburná sugiere una menor eficiencia fisiológica en comparación con Celestún, donde predomina la transpiración foliar regulada (proceso biológico). Esta observación concuerda con estudios previos que demuestran que los manglares degradados tienden a presentar mayor carga térmica superficial debido a la disminución de la cobertura del dosel y a una mayor exposición a la radiación solar (Alongi, 2014). El marcado desequilibrio del balance energético en Chuburná durante la temporada de lluvias refuerza la hipótesis de que las alteraciones hidrológicas no solo modifican la estructura del manglar, sino que también afectan su fisioecología. Esto provoca un desacoplamiento entre la energía disponible y su partición en flujos turbulentos, lo que termina comprometiendo la capacidad del ecosistema para autorregularse térmicamente.

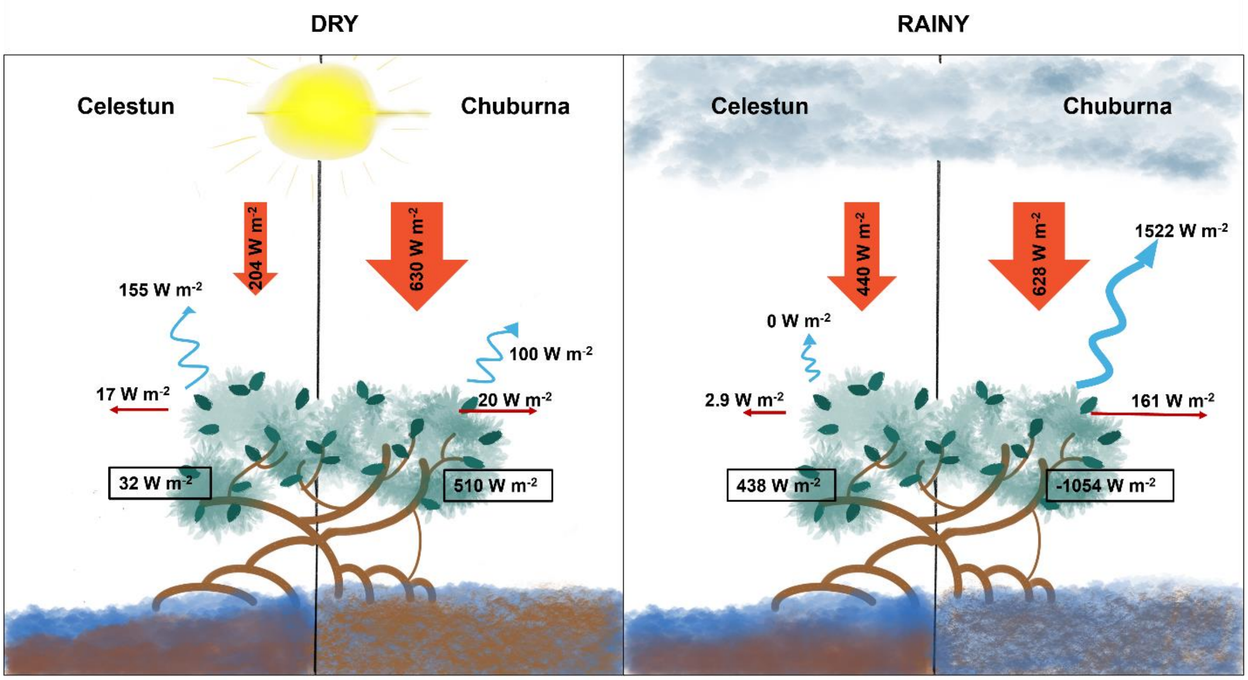

Figure 4.2 Comparación de los valores máximos promedio de calor latente (azul), calor sensible (rojo), radiación neta (naranja) y balance energético (caja negra) entre sitios de manglar chaparro de *Rhizophora mangle* conservado (Celestún) y perturbado (Chuburná) durante la temporada seca y de lluvias.

Estos hallazgos subrayan la importancia crítica de mantener la integridad hidrológica de los ecosistemas de manglar para conservar su capacidad de autorregulación térmica. El amortiguamiento microclimático que proporcionan estos ecosistemas sustenta una diversidad de flora y fauna —incluyendo crustáceos de importancia comercial, poblaciones de peces y comunidades epifíticas (Williams *et al*., 2003; Lee *et al*., 2019)—, al tiempo que mantiene la estabilidad climática regional. Nuestra metodología demuestra que instrumentos accesibles (termómetros infrarrojos, piranómetros, sensores de luz) pueden monitorear de manera eficaz los balances energéticos en manglares donde no es viable instalar torres de covarianza de remolinos. Ampliar estas evaluaciones a lo largo de gradientes de conservación —desde sitios prístinos hasta restaurados y degradados— es crucial para cuantificar: (1) su resiliencia climática frente a disturbios crecientes (Sasmito *et al*., 2020; Ward *et al.,* 2016), (2) su potencial de secuestro de carbono (Kelleway *et al*., 2020), y (3) su valor como soluciones costeras basadas en la naturaleza (Bimrah *et al*., 2022; Taillardat *et al*., 2020). Estos avances científicos son esenciales para valorar los servicios ecosistémicos de los manglares, que generan beneficios económicos estimados en ~1.6 millones de USD por km² al año (Costanza *et al*., 2014). La evidencia respalda el desarrollo urgente de políticas públicas basadas en ciencia que integren la conservación de manglares con la protección de las comunidades costeras (Friess *et al*., 2020; Aburto-Oropeza *et al*., 2008), particularmente en países en desarrollo donde el 90% de los manglares enfrenta amenazas antropogénicas (Goldberg *et al*., 2023).

4.2 CONCLUSIÓN

- El flujo de savia y la transpiración están impulsados principalmente por la variación temporal. La demanda evaporativa, la radiación solar y el flujo de fotones fotosintéticos controlan la dinámica del movimiento de agua en el manglar chaparro de *Rhizophora mangle*.

- Los manglares chaparros de *R. mangle* contribuyen significativamente al flujo de agua hacia la atmósfera a través de la transpiración. Esto se debe a su alta densidad arbórea y estrategia perennifolia, lo que favorece la regulación climática local.

- La temporada de lluvias promueve un mayor flujo de agua en los manglares chaparros. Durante este periodo, el agua se moviliza tanto de día como de noche, facilitando la reparación de embolismos, el aumento del índice de área foliar (LAI) y la reducción de la salinidad intersticial

- La alta densidad de árboles reduce la penetración del viento, limitando la pérdida de calor por convección. Esta disminución en la velocidad de viento retiene la humedad y favorece un alto déficit de presión de vapor (VPD). En contraste, el manglar perturbado mostró temperaturas más altas y mayor evaporación.

- La diferencia de 6°C entre el manglar conservado y el perturbado resalta su papel regulador térmico. Este efecto de “enfriamiento” se debe a la intercepción de hasta el 70% de la radiación entrante, lo que genera temperaturas y niveles de humedad óptimos para la biodiversidad del ecosistema.

- Se observó estratificación térmica en los manglares chaparros conservados. En Celestún, se encontró una clara estratificación foliar, a diferencia del manglar perturbado de Chuburná, donde no se observaron diferencias significativas en la temperatura foliar entre las estaciones se y lluviosa.

- Las hojas del estrato alto presentaron mayor grosor, una cutícula más gruesa y células de idioblastos de mayor tamaño, lo que favorece la retención de agua bajo condiciones de estrés. Estos rasgos superan los valores previamente reportados para *R. mangle*, lo que subraya su plasticidad en ambientes extremos.

- El manglar chaparro conservado en Celestún reguló activamente la temperatura mediante calor latente (transpiración) y la variación estacional de la radiación neta, lo cual indica salud fisiológica y un efecto positivo en el microambiente. En contraste, el manglar perturbado en Chuburná disipó la energía principalmente mediante calor sensible, reflejando una capacidad limitada para regular la temperatura y una dominancia de las condiciones microambientales.

4.3 PERSPECTIVAS

- Monitoreo a largo plazo del balance energético y los flujos de agua en amnglares con diferentes estados de conservación. Evaluar estos procesos en manglares conservados, restaurados y degradados permitirá comprender mejor su papel como reguladores climáticos y su resiliencia ante disturbios ambientales.

- Evaluación y modelado de estrategias de termorregulación frente al cambio climático. Esto ofrecerá información sobre el estado actual de las respuestas fisiológicas que influyen en los procesos ecológicos y las implicaciones del aumento de temperatura asociado al cambio climático.

- Estudio integrado de la fisiología y anatomía vegetal dese el nivel foliar hasta el ecosistémico. Un enfoque multiescalar permitirá una compresión más profunda del funcionamiento de las especies y su contribución a los flujos de agua y energía a nivel ecosistema.

- Incorporación de parámetros fisiológicos en las estrategias de restauración ecológica. Aunque los etidios se han centrado principalmente en árboles maduros por su importancia ecológica, comprender las estrategias fisiecológicas también es esencial en las etapas tempranas de la restauración activa y pasiva, para evaluar su éxito y mejorar las técnicas de restauración.

- Inclusión de variables microambientales en la evaluación de manglares conservados, degradados y restaurados. Eso permitirá diagnósticos más precisos sobre el funcionamiento del ecosistema y las estrategias adaptativas bajo diferentes condiciones ambientales.

- Los manglares chaparros como sistemas modelo para el estudio del intercambio de gases, los flujos de agua y el balance energético. Su alta plasticidad los convierte en sistemas ideales para explorar estrategias de regulación térmica. La identificación de genes y metabolitos asociados a la tolerancia térmica podría incluso permitir transferir este conocimiento a otras especies con menor tolerancia.

BIBLIOGRAFÍA

Adams, J. B., Colloty, B. M., & Bate, G. C. (2004). The distribution and state of mangroves along the coast of Transkei, eastern Cape Province, South Africa. Wetlands Ecology and Management, 12, 531–541.

Adame, M. F., Brown, C. J., Bejarano, M., et al. (2018). The undervalued contribution of mangrove protection in Mexico to carbon emission targets. Conservation Letters, 11(e12445). https://doi.org/10.1111/conl.12445

Agráz-Hernández; Noriega-Trejo, R.; López-Portillo, J.; Flores-Verdugo, F.J.; Jiménez-Zacarías, J.J., 2006.Guía de Campo. Identificación de los Manglares en México. Universidad Autónoma de Campeche. 45 p.

Alongi, D. M. (2014). Carbon cycling and storage in mangrove forests. Annals of Review of Marine Science, 6, 195–219. https://doi.org/10.1146/annurev-marine-010213-135020

Araújo, M. B., Ferri-Yáñez, F., Bozinovic, F., Marquet, P. A., Valladares, F., & Chown, S. L. (2013). Heat freezes niche evolution. Ecology Letters, 16, 1206–1219.

Arceo-Carranza, D., Gamboa, E., Teutli-Hernández, C., Badillo-Alemán, M., & Herrera-Silveira, J. A. (2016). Fish as an indicator of ecological restoration of mangroves on the north coast of Yucatán. *Revista Mexicana de Biodiversidad*, *87*(2), 489–496. https://doi.org/10.1016/j.rmb.2016.03.001

Asbjornsen, H., Goldsmith, G. R., Alvarado-Barrientos, M. S., Rebel, K., Van Osch, F. P., Rietkerk, M., Chen, J., Gotsch, S., Tobón, C., Geissert, D. R., Gómez-Tagle, A., Vache, K., & Dawson, T. E. (2011). Ecohydrological advances and applications in plant-water relations research: A review. *Journal of Plant Ecology*, *4*(1–2), 3–22. https://doi.org/10.1093/jpe/rtr005

Augusto da Silva, C. R., Dos Santos Silva, M., Dos Santos Lopes Ferreira, L. M., Batista Leite, K. R., & Benedito da Silva, L. (2016). Morphological and anatomical aspects of the leaves of Rhizophora mangle L. (Rhizophoraceae) under different lighting conditions. *Revista de Biologia Neotropical*, *12*(2), 74. https://doi.org/10.5216/rbn.v12i2.33405

Bachofen, C., Poyatos, R., Flo, V., Martínez-Vilalta, J., Mencuccini, M., Granda, V., & Grossiord, C. (2023). Stand structure of Central European forests matters more than climate for transpiration sensitivity to VPD. *Journal of Applied Ecology*, *60*(5), 886–897. https://doi.org/10.1111/1365-2664.14383

Baldocchi, D. D. (2003). Assessing the eddy covariance technique for evaluating carbon dioxide exchange rates of ecosystems: past, present and future. Global Change Biology, 9(4), 479–492. https://doi.org/10.1046/j.1365-2486.2003.00629.x

Ball, J. T., Woodrow, I. E., & Berry, J. A. (1987). A model predicting stomatal conductance and its contribution to the control of photosynthesis under different environmental conditions. *Progress in Photosynthesis Research*, *January 2015*. https://doi.org/10.1007/978-94-017-0519-6

Ball, M. C. (2002). Interactive effects of salinity and irradiance on growth: Implications for mangrove forest structure along salinity gradients. *Trees - Structure and Function*, *16*(2–3), 126–139. https://doi.org/10.1007/s00468-002-0169-3

Ball, M. C. (1998). Mangrove Species Richness in Relation to Salinity and Waterlogging: A Case Study Along the Adelaide River Floodplain, Northern Australia. *Global Ecology and Biogeography Letters*, *7*(1), 73–82. https://doi.org/10.2307/2997699

Barnuevo, A., & Asaeda, T. (2018). *Integrating the ecophysiology and biochemical stress indicators into the paradigm of mangrove ecology and a rehabilitation blueprint*. 1–17.

Barr, J. G., Delonge, M. S., & Fuentes, J. D. (2014). Seasonal evapotranspiration patterns in mangrove forests. *Journal of Geophysical Research*, *119*(7), 3886–3899. https://doi.org/10.1002/2013JD021083

Batllori-Sampedro, E., & Febles-Patrón, J. L. (2007). Límites máximos permisibles para el aprovechamiento del ecosistema de manglar. *Gaceta Ecológica*, *82*, 5–23.

Becker, P., Asmat, A., Mohamad, J., Moksin, M., & Tyree, M. T. (1997). Sap flow rates of mangrove trees are not unusually low. *Trees - Structure and Function*, *11*(7), 432–435. https://doi.org/10.1007/s004680050104

Benyon, R. G., Marcar, N. E., Theiveyanathan, S., Tunningley, W. M., & Nicholson, A. T. (2001). Species differences in transpiration on a saline discharge site. *AgriculturalWaterManagment*, *50*, 65–81. https://doi.org/Benyon, R. G., Marcar, N. E., Theiveyanathan, S., Tunningley, W. M., & Nicholson, A. T. (2001). Species differences in transpiration on a saline discharge site. Agricultural Water Management, 50(1), 65–81. doi:10.1016/s0378-3774(00)00121-9

Beringer, J., et al. (2016). An introduction to the Australian and New Zealand flux tower network - OzFlux. Biogeosciences, 13(21), 5895–5916.

Bimrah, K., Dasgupta, R., Hashimoto, S., Saizen, I., & Dhyani, S. (2022). Ecosystem Services of Mangroves: A Systematic Review and Synthesis of Contemporary Scientific Literature. In *Sustainability (Switzerland)* (Vol. 14, Issue 19). MDPI. https://doi.org/10.3390/su141912051

Blanken, P. D., Black, T. A., Yang, P. C., Neumann, H. H., Nesic, Z., Staebler, R., Den Hartog, G., Novak, M. D., & Lee, X. (1997). Energy balance and canopy conductance of a boreal aspen forest: Partitioning overstory and understory components. *Journal of Geophysical Research Atmospheres*, *102*(24), 28915–28927. https://doi.org/10.1029/97jd00193

Blonder, B., & Michaletz, S. T. (2018). A model for leaf temperature decoupling from air temperature. Agricultural and Forest Meteorology, 262, 354–360. https://doi.org/10.1016/j.agrformet.2018.07.012

Boanares, D., Bueno, A., de Souza, A. X., Kozovits, A. R., Sousa, H. C., Pimenta, L. P. S., Isaias, R. M. dos S., & França, M. G. C. (2021). Cuticular wax composition contributes to different strategies of foliar water uptake in six plant species from foggy rupestrian grassland in tropical mountains. Phytochemistry, 190, 112894. https://doi.org/10.1016/j.phytochem.2021.112894

Bonan, G. B. (2015). Ecological Climatology: Concepts and Applications (3rd ed.). Cambridge University Press.

Broughton, K. J., Payton, P., Tan, D. K. Y., Tissue, D. T., & Bange, M. P. (2021). Effect of vapour pressure deficit on gas exchange of field-grown cotton. *Journal of Cotton Research*, *4*(1). https://doi.org/10.1186/s42397-021-00105-4

Brubaker, K., & Entekhabi, D. (1996). Asymmetric recovery from wet versus dry soil moisture anomalies. Journal of Applied Meteorology, 35(1), 94–109.

Bucci, S. J., Goldstein, G., Meinzer, F. C., Scholz, F. G., Franco, A. C., & Bustamante, M. (2004). Functional convergence in hydraulic architecture and water relations of tropical savanna trees: from leaf to whole plant. *Tree Physiology*, *24*(8), 891–899. https://doi.org/10.1093/treephys/24.8.891

Cabañas-Mendoza, M. D. R., Santamaría, J. M., Sauri-Duch, E., Escobedo-Graciamedrano, R. M., & Andrade, J. L. (2020). Salinity affects ph and lead availability in two mangrove plant species. In *Environmental Research Communications* (Vol. 2, Issue 6). Institute of Physics. https://doi.org/10.1088/2515-7620/ab9992

Campbell, G. S., Norman, J. M., & Norman, J. M. (1998). *An Introduction to Environmental Biophysics* (Springer).

Cerón-Aguilera, G. (2020). Comparación morfo-fisiológica del desarrollo de los propágulos de manglar de franja y chaparro de Rhizophora mangle L. de Celestún, Yucatán [Tesis de Maestría, Centro de Investigación Científica de Yucatán].

Cerón-Aguilera, G., Yáñez-Espinosa, L., Echevarría-Machado, I., Méndez-Alonzo, R., Herrera-Silveira, J., Us-Santamaría, R., Salas-Rabaza, J. A., González-Muñoz, K. E., & Andrade, J. L. (2025). Dinámica estacional y factores microambientales de la transpiración en matorrales Rhizophora mangle L. Árboles de Yucatán. Bosques, 16(2), 351. https://doi.org/10.3390/f16020351

Chiew, F. H. S., & McMahon, T. A. (2002). Modelling the impacts of climate change on Australian streamflow. *Hydrological Processes*, *16*(6), 1235–1245. https://doi.org/10.1002/hyp.1059

Cinco-Castro, S., & Herrera-Silveira, J. (2020). Vulnerability of mangrove ecosystems to climate change effects: The case of the Yucatan Peninsula. *Ocean and Coastal Management*, *192*. https://doi.org/10.1016/j.ocecoaman.2020.105196

Cisneros-De La Cruz, D. J., Yáñez-Espinosa, L., Reyes-García, C., Us-Santamaria, R., & Andrade, J. L. (2022). Hydraulic architecture of seedlings and adults of Rhizophora mangle L. in fringe and scrub mangrove. *Botanical Sciences*, *100*(2), 370–382. https://doi.org/10.17129/botsci.2906

Cisneros-De la Cruz, D., Orozco-Fuentes, S., & López-Portillo, J. (2022). Hydraulic architecture of Rhizophora mangle in fringe and dwarf mangrove ecotypes. Hydrobiologia, 849, 2443–2457. https://doi.org/10.1007/s10750-021-04763-9

Coble, A. P., & Cavaleri, M. A. (2014). Light drives vertical gradients of leaf morphology in a sugar maple (Acer saccharum) forest. Tree Physiology, 34(2), 146–158. https://doi.org/10.1093/treephys/tpt126

Coble, A. P., & Cavaleri, M. A. (2017). Vertical leaf mass per area gradient of mature sugar maple reflects both height-driven increases in vascular tissue and light-driven increases in palisade layer thickness. Tree Physiology, 37(10), 1337–1351. https://doi.org/10.1093/treephys/tpx016

Collazo-ortega, M. (2013). *Relaciones Hídricas*. *January*.

Cooke, S. J., & Suski, C. D. (2008). *Ecological Restoration and Physiology : An Overdue Integration*. *58*(10), 957–968.

Coopman, R.E.; Nguyen, H.T.; Mencuccini, M.; Oliveira, R.S.; Sack, L.; Lovelock, C.E.; Ball, M.C. (2021). Harvesting water from unsaturated atmospheres: deliquescence of salt secreted onto leaf surfaces drives reverse sap flow in a dominant arid climate mangrove, *Avicennia marina*. *New Phytol. 231*, 1401–1414, https://doi.org/10.1111/nph.17461

Cruiziat, P., Cochard, H., & Améglio, T. (2002). Hydraulic architecture of trees: Main concepts and results. *Annals of Forest Science*, *59*(7), 723–752. https://doi.org/10.1051/forest:2002060

Dawson, T., Burgess, S., Kevin P. T, Louis, S., Oliveira, Fisher, J., Simonin, K., & Ambrose, A. (2007). Nighttime transpiration in woody plants from contrasting ecosystems. *Tree Physiology*, *27*, 561–575. https://doi.org/10.1093/treephys/27.4.561

De Boeck, H. J., Dreesen, F. E., Janssens, I. A., & Nijs, I. (2010). Climatic characteristics of heat waves and their simulation in plant experiments. *Global Change Biology*, *16*(7), 1992–2000. https://doi.org/10.1111/j.1365-2486.2009.02049.x de Oliveira, J. P. V., Duarte, V. P., de Castro, E. M., Magalhães, P. C., & Pereira, F. J. (2022). Stomatal cavity modulates the gas exchange of Sorghum bicolor (L.) Moench. grown under different water levels. *Protoplasma*, *259*(4), 1081–1097. https://doi.org/10.1007/s00709-021-01722-1

de Oliveira, J. P. V., Duarte, V. P., de Castro, E. M., Magalhães, P. C., & Pereira, F. J. (2023). Contrasting leaf intercellular space development in sorghum and maize modulates different tolerance capacity to water limitation. *Journal of Plant Research*, *136*(4), 535–548. https://doi.org/10.1007/s10265-023-01463-7

Deb Burman, P. K., Chakraborty, S., El-Madany, T. S., Ramasubramanian, R., Gogoi, N., Gnanamoorthy, P., Murkute, C., Nagarajan, R., & Karipot, A. (2022). A comparative study of ecohydrologies of a tropical mangrove and a broadleaf deciduous forest using eddy covariance measurement. *Meteorology and Atmospheric Physics*, *134*(1). https://doi.org/10.1007/s00703-021-00840-y

Degradation, L., Bateman, A., Lewandrowski, W., & Stevens, J. C. (2019). *Ecophysiological indicators to assess drought responses of arid zone native seedlings in reconstructed soils*. *April*. https://doi.org/10.1002/ldr.2660

Diamond, S. E. (2018). Contemporary climate-driven range shifts: Putting evolution back on the table. Functional Ecology, 32, 1652–1665. https://doi.org/10.1111/1365-2435.13095

Donato, D. C., Kauffman, J. B., Murdiyarso, D., Kanzaki, M., Kuhlman, I., Stidham, M., & Bredehoeft, J. (2011). Mangroves among the most carbon-rich forests in the tropics. Nature Geoscience, 4, 293–297. https://doi.org/10.1038/ngeo1123

Dong, N., Prentice, I. C., Harrison, S. P., Song, Q. H., & Zhang, Y. P. (2017). Biophysical homoeostasis of leaf temperature: A neglected process for vegetation and land-surface modelling. Global Ecology and Biogeography, 26, 998–1007. https://doi.org/10.1111/geb.12614

Erratum: Nature Plants, 2, 16147. https://doi.org/10.1038/nplants.2016.147

Escribano-Rocafort, A. G., Ventre-Lespiaucq, A. B., Granado-Yela, C., López-Pintor, A., Delgado, J. A., Muñoz, V., Dorado, G. A., & Balaguer, L. (2014). Simplifying data acquisition in plant canopies- Measurements of leaf angles with a cell phone. *Methods in Ecology and Evolution*, *5*(2), 132–140. https://doi.org/10.1111/2041-210X.12141

Esteban, J. H. P. Æ. J. M. A. (2008). *A review of mangrove rehabilitation in the Philippines: successes, failures and future prospects*. 345–358. https://doi.org/10.1007/s11273-008-9101-y

Evans, L. S., & Bromberg, A. (2010). Characterization of cork warts and aerenchyma in leaves of rhizophora mangle and rhizophora racemosa. *Journal of the Torrey Botanical Society*, *137*(1), 30–38. https://doi.org/10.3159/09-RA-024.1

Ewel, K. C., Twilley, R. R., & Ong, J. E. (1998). Different Kinds of Mangrove Forests Provide Different Goods and Services. *Global Ecology and Biogeography Letters*, *7*(1), 83. https://doi.org/10.2307/2997700

Fang, W., Liu, J., Lu, N., & Li, R. (2024). The dynamics of nocturnal sap flow components of a typical revegetation shrub species on the semiarid Loess Plateau, China. *Frontiers in Plant Science*, *15*. https://doi.org/10.3389/fpls.2024.1370362

Farella, M. M., Fisher, J. B., Jiao, W., Key, K. B., & Barnes, M. L. (2022). Thermal remote sensing for plant ecology from leaf to globe. Journal of Ecology, 110, 1996–2014. https://doi.org/10.1111/1365-2745.13957

Feller, I. C., Lovelock, C. E., & McKee, K. L. (2007). Nutrient addition differentially affects ecological processes of Avicennia germinans in nitrogen versus phosphorus limited mangrove ecosystems. *Ecosystems*, *10*(3), 347–359. https://doi.org/10.1007/s10021-007-9025-z

Fernandes de Oliveira, A., Piga, G. K., Najoui, S., Becca, G., Marceddu, S., Rigoldi, M. P., Satta, D., Bagella, S., & Nieddu, G. (2024). UV light and adaptive divergence of leaf physiology, anatomy, and ultrastructure drive heat stress tolerance in genetically distant grapevines. Frontiers in Plant Science, 15, 1399840. https://doi.org/10.3389/fpls.2024.1399840

Flo, V., Martínez-Vilalta, J., Granda, V., Mencuccini, M., & Poyatos, R. (2022). Vapour pressure deficit is the main driver of tree canopy conductance across biomes. *Agricultural and Forest Meteorology*, *322*. https://doi.org/10.1016/j.agrformet.2022.109029

Forster, M. A. (2014). How significant is nocturnal sap flow? *Tree Physiology*, *34*(7), 757–765. https://doi.org/10.1093/treephys/tpu051

Friess, D. A., Adame, M. F., Adams, J. B., & Lovelock, C. E. (2022). Mangrove forests under climate change in a 2°C world. WIREs Climate Change, 13(4), e792. https://doi.org/10.1002/wcc.792

G. Gilbert Mc Millen, & John H. Mc Clendon. (1979). Leaf Angle : An Adaptive Feature of Sun and Shade Leaves. *The University of Chicago Press*, *140*(4), 437–442. https://doi.org/.0006-8071/79/4004-0009$00.75

Garcia, J. dos S., Boanares, D., Costa França, M. G., Sershen, & López-Portillo, J. (2022). Foliar water uptake in eight mangrove species: Implications of morpho-anatomical traits. Flora, 293, 152100. https://doi.org/10.1016/j.flora.2022.152100

Gilman, E. L., Ellison, J., Duke, N. C., & Field, C. (2008). Threats to mangroves from climate change and adaptation options: A review. Aquatic Botany, 89(2), 237–250. https://doi.org/10.1016/j.aquabot.2007.12.009

Giri, C., Ochieng, E., Tieszen, L. L., Zhu, Z., Singh, A., Loveland, T., Masek, J., & Duke, N. (2011). *Status and distribution of mangrove forests of the world using earth*. 154–159. https://doi.org/10.1111/j.1466-8238.2010.00584.x

González Muños, K. E. (2022). Influencia de la sal secretada en el balance de energía de Avicennia germinans L. en un manglar chaparro de la Península de Yucatán [Tesis de Licenciatura, Universidad Autónoma Chapingo].

Görgen, K., Lynch, A. H., Marshall, A. G., & Beringer, J. (2006). Impact of abrupt land cover changes by savanna fire on northern Australian climate. Journal of Geophysical Research, 111, D19106. https://doi.org/10.1029/2005JD006860

Granier, A. (1987). Evaluation of transpiration in a Douglas-fir stand by means of sap flow measurements. *Tree Physiology*, *3*(4), 309–320. https://doi.org/10.1093/treephys/3.4.309

Grossiord, C., Buckley, T. N., Cernusak, L. A., Novick, K. A., Poulter, B., Siegwolf, R. T. W., Sperry, J. S., & McDowell, N. G. (2020). Plant responses to rising vapor pressure deficit. In *New Phytologist* (Vol. 226, Issue 6, pp. 1550–1566). Blackwell Publishing Ltd. https://doi.org/10.1111/nph.16485

Guo, Z., Zhang, K., Lin, H., Majcher, B. M., Lee, C. K. F., Still, C. J., & Wu, J. (2023). Plant canopies exhibit stronger thermoregulation capability at the seasonal than diurnal timescales. Agricultural and Forest Meteorology, 339, 109582. https://doi.org/10.1016/j.agrformet.2023.109582

Gutiérrez-Mendoza, J., & Herrera-silveira, J. A. (2015). Almacenes de Carbono en manglares de tipo chaparro en un escenario cárstico. *Estado Actual Del Conocimiento Del Ciclo Del Carbono y Sus Interacciones En México: Síntesis a 2014.*, *January 2015*, 460–469.

Guzmán-Delgado, P., Laca, E., & Zwieniecki, M. A. (2021). Unravelling foliar water uptake pathways: The contribution of stomata and the cuticle. Plant, Cell & Environment, 44(5), 1728–1740. https://doi.org/10.1111/pce.14041

Hayat, M.; Iqbal, S.; Zha, T.; Jia, X.; Qian, D.; Bourque, C.P.A.; Khan, A.; Tian, Y.; Bai, Y.; Liu, P.; et al. (2021). Biophysical control on nighttime sap flow in *Salix psammophila* in a semiarid shrubland ecosystem. *Agric. For. Meteorol*, 300, 108329. https://doi.org/10.1016/j.agrformet.2021.108329

Haworth, M., Marino, G., Loreto, F., & Centritto, M. (2021). Integrating stomatal physiology and morphology: evolution of stomatal control and development of future crops. *Oecologia*, *197*(4), 867–883. https://doi.org/10.1007/s00442-021-04857-3

Hallé, F.; Oldeman, R.A.A.; Tomlinson, P.B.; Hallé, F.; Oldeman, R.A.A.; Tomlinson, P.B. Forests and Vegetation. (1978) In *Tropical Trees and Forests*; Springer: Berlin/Heidelberg, Germany, 1978

Herrera-Silveira, J. (1994). Spatial heterogeneity and seasonal patterns in a tropical coastal lagoon. *Coastal Research*, *10*(3), 738–746. http://www.eoearth.org/view/article/51cbed4a7896bb431f69118c

Herrera-Silveira, J. A., Pech-Cardenas, M. A., Morales-Ojeda, S. M., Cinco-Castro, S., Camacho-Rico, A., Sosa, J. P. C., Mendoza-Martinez, J. E., Pech-Poot, E. Y., Montero, J., & Teutli-Hernandez, C. (2020). Blue carbon of Mexico, carbon stocks and fluxes: A systematic review. In *PeerJ* (Vol. 8). PeerJ Inc. https://doi.org/10.7717/peerj.8790

Hirano, T., Monji, N., Hamotani, K., Jintana, V., & Yabuki, K. (1996). Transpirational Characteristics of Mangrove Species in Southern Thailand. *Environment Control in Biology*, *34*(4), 285–293. https://doi.org/10.2525/ecb1963.34.285

Hogan, J. A., Medina, E., Mancera-Pineda, J. E., López-Hoffman, L., & Castañeda-Moya, E. (2021). Ecophysiological responses of mangroves to environmental change. Frontiers in Forests and Global Change, 4, 651056. https://doi.org/10.3389/ffgc.2021.651056

Hölttäa, T.; Linkosaloa, T.; Riikonena, A.; Sevantob, S.; Nikinmaa, E. (2015). An analysis of Granier sap flow method, its sensitivity to heat storage and a new approach to improve its time dynamics. *Agricul. And Forest. Meteorol.* 211, 2-12. http://dx.doi.org/10.1016/j.agrformet.2015.05.005

Hoppe-Speer, S. C. L., Adams, J. B., Rajkaran, A., & Bailey, D. (2011). The response of the red mangrove Rhizophora mucronata Lam. to salinity and inundation in South Africa. *Aquatic Botany*, *95*(2), 71–76. https://doi.org/10.1016/j.aquabot.2011.03.006

Horner, H. T. (2012). Peperomia leaf cell wall interface between the multiple hypodermis and crystal-containing photosynthetic layer displays unusual pit fields. Annals of Botany, 109(7), 1307–1316. https://doi.org/10.1093/aob/mcs074

Ivanilson Lucena, Vanessa E. de O. Maciel, Janaina B. da Silva, Josiclêda D. Galvíncio, Rejane M. de M. Pimentel Ivanilson Lucen, Vanessa E. de O. Maciel, Janaina B. da Silva, Josiclêda D. Galvíncio, R. M. de M. P. (2011). *Leaf structure of mangrove species to understand the spectral responses*. *02*, 019–031. https://doi.org/10.5935/2237-2202.20110002

Jackson, M., Andrade, J. L., Holbrook, N. M., Cavelier, J., & Jackson, P. (1997). Control of transpiration from the upper canopy of a tropical forest. the role of stomatal, boundary layer and hydraulic architecture components. *Plant, Cell and Environment*, *20*, 1242–1252. https://doi.org/10.1046/j.1365-3040.1997.d01-26.x

Jarvis, P. G., & Mcnaughton, K. G. (1986). *Stomatal Control of Transpiration: Scaling Up from Leaf' to Region*.

Jasechko, S., Sharp, Z. D., Gibson, J. J., Birks, S. J., Yi, Y., & Fawcett, P. J. (2013). Terrestrial water fluxes dominated by transpiration. *Nature*, *496*(7445), 347–350. https://doi.org/10.1038/nature11983

Jiang, G.-F., Goodale, U. M., Liu, Y.-Y., Hao, G.-Y., & Cao, K.-F. (2017). Salt management strategy defines the stem and leaf hydraulic characteristics of six mangrove tree species. Tree Physiology, 37(3), 389–401. https://doi.org/10.1093/treephys/tpw131

Jones, H. G. (2014). Plants and microclimate: A quantitative approach to environmental plant physiology. In *Plants and Microclimate: A Quantitative Approach to Environmental Plant Physiology*. https://doi.org/10.1017/CBO9780511845727

Jones, H. G., & Rotenberg, E. (2001). Energy, radiation and temperature regulation in plants. In eLS. John Wiley & Sons, Ltd. https://doi.org/10.1038/npg.els.0003199

Ken W. Krauss, Catherine E. Lovelock, Karen L. McKee, Laura López-Hoffman, Sharon M.L. Ewe, Wayne P. Sousa (2008). Environmental drivers in mangrove establishment and early development: A review. Aquatic Botany, 89(2), 105–127. https://doi.org/10.1016/j.aquabot.2007.12.014

Khan, M. A., Ungar, I. A., & Showalter, A. M. (2014). Salt tolerance in mangroves: Plant adaptations and their physiological mechanisms. Trees, 28(3), 891–902. https://doi.org/10.1007/s00468-014-1037-z

Kimball, S., Funk, J. L., Sandquist, D. R., & Ehleringer, J. R. (2016). Ecophysiological considerations for restoration. In M. A. Palmer, J. B. Zedler, & D. A. Falk (Eds.), Foundations of restoration ecology (2nd ed.). Island Press.

Ko Èstner, B. (2001). Evaporation and transpiration from forests in Central Europe ± relevance of patch-level studies for spatial scaling. *Meteorol. Atmos.*, *76*, 69–82.

Kool, D., Agam, N., Lazarovitch, N., Heitman, J. L., Sauer, T. J., & Ben-gal, A. (2014). *A review of approaches for evapotranspiration partitioning*. *184*, 56–70.

Kowalski, A. S. (2025). An elucidatory model of oxygen's partial pressure inside substomatal cavities. Biogeosciences, 22, 785–789. https://doi.org/10.5194/bg-22-785-2025

Krauss, K. W., Duberstein, J. A., & Conner, W. H. (Año no disponible). [Referencia incompleta, falta título y fuente]. https://doi.org/10.1002/hyp.10130

Krauss, K. W., Lovelock, C. E., Chen, L., Berger, U., Ball, M. C., Reef, R., Peters, R., Bowen, H., Vovides, A. G., Ward, E. J., Wimmler, M. C., Carr, J., Bunting, P., & Duberstein, J. A. (2022). Mangroves provide blue carbon ecological value at a low freshwater cost. *Scientific Reports*, *12*(1). https://doi.org/10.1038/s41598-022-21514-8

Krauss, K. W., Lovelock, C. E., McKee, K. L., López-Hoffman, L., Ewe, S. M. L., & Sousa, W. P. (2008). Environmental drivers in mangrove establishment and early development: A review. *Aquatic Botany*, *89*(2), 105–127. https://doi.org/10.1016/j.aquabot.2007.12.014

Krauss, K. W., Mckee, K. L., & Hester, M. W. (2014). Water use characteristics of black mangrove (Avicennia germinans) communities along an ecotone with marsh at a northern geographical limit. *Ecohydrology*, *7*(2), 354–365. https://doi.org/10.1002/eco.1353

Krauss, K. W., Young, P. J., Chambers, J. L., Doyle, T. W., & Twilley, R. R. (2007). Sap flow characteristics of neotropical mangroves in flooded and drained soils. *Tree Physiology*, *27*(5), 775–783. https://doi.org/10.1093/treephys/27.5.775

Kumagai, T., Saitoh, T. M., Sato, Y., Morooka, T., Manfroi, O. J., Kuraji, K., & Suzuki, M. (2004). Transpiration, canopy conductance and the decoupling coefficient of a lowland mixed dipterocarp forest in Sarawak, Borneo: Dry spell effects. Journal of Hydrology, 287(1–4), 237–251. https://doi.org/10.1016/j.jhydrol.2003.10.002

Lambers, H., Stuart Chapin III, F., & Pons, T. L. (2008). Plant Physiological Ecology. In *Springer*. https://doi.org/10.1017/CBO9781107415324.004

Lavinsky, A. O., Magalhães, P. C., Ávila, R. G., Diniz, M. M., & de Souza, T. C. (2015). Partitioning between primary and secondary metabolism of carbon allocated to roots in four maize genotypes under water deficit and its effects on productivity. *Crop Journal*, *3*(5), 379–386. https://doi.org/10.1016/j.cj.2015.04.008

Lebrija-Trejos E, Pérez-García EA, Meave JA, Poorter L, Bongers F. Environmental changes during secondary succession in a tropical dry forest in Mexico. *Journal of Tropical Ecology*. 2011;27(5):477-489. https://doi:10.1017/S0266467411000253

Leclerc, M. Y., & Foken, T. (2014). Micrometeorology. Springer Science & Business Media.

Leng, B., & Cao, K. F. (2020). The sap flow of six tree species and stand water use of a mangrove forest in Hainan, China. *Global Ecology and Conservation*, *24*. https://doi.org/10.1016/j.gecco.2020.e01233

Lewandrowski, W., Erickson, T. E., Dixon, K. W., & Stevens, J. C. (2017). *Increasing the germination envelope under water stress improves seedling emergence in two dominant grass species across different pulse rainfall events*. 997–1007. https://doi.org/10.1111/1365-2664.12816

Li, W., Zhang, Y., Wang, N., Liang, C., Xie, B., Qin, Z., Yuan, Y., & Cao, J. (2023). Nocturnal Water Use Partitioning and Its Environmental and Stomatal Control Mechanism in Caragana korshinskii Kom in a Semi-Arid Region of Northern China. *Forests*, *14*(11). https://doi.org/10.3390/f14112154

Liang, J., Wei, Z., Lee, X., Wright, J. S., Cui, X., Chen, H., & Lin, G. (2019). Evapotranspiration Characteristics Distinct to Mangrove Ecosystems Are Revealed by Multiple-Site Observations and a Modified Two-Source Model. *Water Resources Research*, *55*(12), 11250–11273. https://doi.org/10.1029/2019WR024729

Lima, C. S., Torres-boeger, M. R., Carvalho, L. L., & Soffiatti, P. (2013). *Sclerophylly in mangrove tree species from South Brazil Esclerofilia de las especies de manglares del sur de Brasil*. 1159–1166. https://doi.org/10.7550/rmb.32149

Lin, G., & Sternberg, L. da S. L. (1992). Comparative study of water uptake and photosynthetic gas exchange between scrub and fringe red mangroves, Rhizophora mangle L. *Oecologia*, *90*(3), 399–403. https://doi.org/10.1007/BF00317697

Lin, H., Tu, C., Fang, J., Gioli, B., Loubet, B., Gruening, C., Zhou, G., Beringer, J., Huang, J., Dušek, J., Liddell, M., Buysse, P., Shi, P., Song, Q., Han, S., Magliulo, V., Li, Y., & Grace, J. (2020). Forests buffer thermal fluctuation better than non-forests. Agricultural and Forest Meteorology, 288–289, 107994. https://doi.org/10.1016/j.agrformet.2020.107994

Lovelock, C. E., Cahoon, D. R., Friess, D. A., Guntenspergen, G. R., Krauss, K. W., Reef, R., … Woodroffe, C. D. (2016). The vulnerability of Indo-Pacific mangrove forests to sea-level rise. Nature, 526, 559–563. https://doi.org/10.1038/nature15538

Lovelock, C. E., & Clough, B. F. (1992). Influence of solar radiation and leaf angle on leaf xanthophyll concentrations in mangroves. *Oecologia*, *91*(4), 518–525. https://doi.org/10.1007/BF00650325

Lovelock, C. E., & Feller, I. C. (2003). Photosynthetic performance and resource utilization of two mangrove species coexisting in a hypersaline scrub forest. Oecologia, 134, 455–462. https://doi.org/10.1007/s00442-002-1146-2

Lu, P.; Urban, L.; Zhao, P. (2004). Granier's thermal dissipation probe (TDP) method for measuring sap flow in trees: Theory and practice. Acta Botanica Sinica, 46, 6, 631-646,

Lucena, I., Maciel, V. E. de O., Silva, J. B. da, Galvíncio, J. D., & Pimentel, R. M. de M. (2011). Leaf structure of mangrove species to understand the spectral responses. Journal of Hyperspectral Remote Sensing, 2, 19–31.

Lugo, A. E. (1980). Mangrove ecosystems: successional or steady state? Biotropica, 12 (Supplement), 65–72. https://doi.org/10.2307/2388153

Lugo, A. E. , & Snedaker, S. C. (1974). The ecology of mangroves. *Annual Rev. Ecol. Syst*, *in 7*, 39–64.

Madrid, E. N., Armitage, A. R., & Lopez-Portillo, J. (2014). Avicennia germinans (black mangrove) vessel architecture is linked to chilling and salinity tolerance in the Gulf of Mexico. *Frontiers in Plant Science*, *5*(SEP). https://doi.org/10.3389/fpls.2014.00503

Mahmood, R., Pielke, R. A. Sr., Hubbard, K. G., Niyogi, D., Dirmeyer, P. A., McAlpine, C., Carleton, A. M., Hale, R., Gameda, S., Beltrán-Przekurat, A., Baker, B., McNider, R., Legates, D. R., Shepherd, M., Du, J., Blanken, P. D., Frauenfeld, O. W., Nair, U. S., & Fall, S. (2014). Land cover changes and their biogeophysical effects on climate. International Journal of Climatology, 34(4), 929–953. https://doi.org/10.1002/joc.3736

Manzoni, S., Vico, G., Katul, G., Palmroth, S., & Porporato, A. (2014). Optimal plant water-use strategies under stochastic rainfall. *Water Resources Research*, *50*(7), 5379–5394. https://doi.org/10.1002/2014WR015375

Martínez Reyes, G. C. (2024). Influencia de la salinidad en la tolerancia al estrés hídrico de las plántulas de Rhizophora mangle L. [Tesis de Licenciatura, Universidad Autónoma Chapingo].

McJannet, D., Wallace, J., Fitch, P., Disher, M., & Reddell, P. (2007). Water balance of tropical rainforest canopies in north Queensland, Australia. *Hydrological Processes*, *21*(25), 3473–3484. https://doi.org/10.1002/hyp.6618

McKee, K. L., Cahoon, D. R., & Feller, I. C. (2007). Caribbean mangroves adjust to rising sea level through biotic controls on change in soil elevation. Global Ecology and Biogeography, 16, 545–556.

Mcleod, E., Chmura, G. L., Bouillon, S., Salm, R., Björk, M., Duarte, C. M., Lovelock, C. E., Schlesinger, W. H., Silliman, B. R., Mcleod, E., Chmura, G. L., Bouillon, S., Salm, R., Björk, M., Duarte, C. M., Lovelock, C. E., Schlesinger, W. H., & Silliman, B. R. (2011). *A blueprint for blue carbon: toward an improved understanding of the role of vegetated coastal habitats in sequestering CO2*. https://doi.org/10.1890/110004

Medlyn, B. E., Duursma, R. A., Eamus, D., Ellsworth, D. S., Prentice, I. C., Barton, C. V. M., Crous, K. Y., De Angelis, P., Freeman, M., & Wingate, L. (2011). Reconciling the optimal and empirical approaches to modelling stomatal conductance. Global Change Biology, 17, 2134–2144. https://doi.org/10.1111/j.1365-2486.2010.02375.x

Mencuccini, M., Manzoni, S., & Christoffersen, B. (2019). Modelling water fluxes in plants: from tissues to biosphere. In *New Phytologist* (Vol. 222, Issue 3, pp. 1207–1222). Blackwell Publishing Ltd. https://doi.org/10.1111/nph.15681

Méndez-Alonzo, R., López-Portillo, J., Moctezuma, C., Bartlett, M. K., & Sack, L. (2016). Osmotic and hydraulic adjustment of mangrove saplings to extreme salinity. *Tree Physiology*, *36*(12), 1562–1572. https://doi.org/10.1093/treephys/tpw073

Michaletz, S. T., Weiser, M. D., McDowell, N. G., Zhou, J., Kaspari, M., Helliker, B. R., & Enquist, B. J. (2016). The energetic and carbon economic origins of leaf thermoregulation. Nature Plants, 2, 16129. https://doi.org/10.1038/nplants.2016.129

Miller, B. D., et al. (2021). Only sun-lit leaves of the uppermost canopy exceed both air temperature and photosynthetic thermal optima in a wet tropical forest. Agricultural and Forest Meteorology, 301–302, 108347. https://doi.org/10.1016/j.agrformet.2021.108347

Monteith, J. L., & Unsworth, M. H. (1990). Principles of Environmental Physics (2nd ed.). Butterworth-Heinemann, Elsevier, Oxford.

Morales-Ojeda, S.M., Medina-Gómez, I., Ramírez-Ramírez, J., Osorio, M. I., Teutli-Hernández, C., Aguilar-Trujillo, A., Pech-Poot, E., Carrillo-Baeza, L. & Camacho -Rico, A. (2019). Almacenes y flujos en lagunas Costeras: Laguna Celestún. En: Estado del Ciclo del Carbono: Agenda Azul y Verde. (224-239 pp.) Programa Mexicano del Carbono. Texcoco, Estado de México, México.

Muñoz-villers, L. E., Holwerda, F., & Alvarado-barrientos, M. S. (2015). *Efectos hidrológicos de la conversión del bosque de niebla en el centro de Veracruz, México Hydrological effects of cloud forest conversion in central Veracruz, Mexico*. *36*(3), 395–407. https://doi.org/10.4067/S0717-92002015000300007

Muñoz-villers, L. E., Holwerda, F., Gómez-cárdenas, M., Equihua, M., & Asbjornsen, H. (2012). *Water balances of old-growth and regenerating montane cloud forests in central Veracruz, Mexico*. *463*, 53–66. https://doi.org/10.1016/j.jhydrol.2011.01.062

Mursyid, H., Daulay, M. H., Pratama, A. A., Laraswati, D., Novita, N., Malik, A., & Maryudi, A. (2021). Governance issues related to the management and conservation of mangrove ecosystems to support climate change mitigation actions in Indonesia. *Forest Policy and Economics*, *133*. https://doi.org/10.1016/j.forpol.2021.102622

Naidoo, G. (2016). The mangroves of South Africa: An ecophysiological review. South African Journal of Botany, 107, 101–113. https://doi.org/10.1016/j.sajb.2016.04.014

Naithani, K. J., Ewers, B. E., & Pendall, E. (2012). Sap flux-scaled transpiration and stomatal conductance response to soil and atmospheric drought in a semi-arid sagebrush ecosystem. *Journal of Hydrology*, *464–465*, 176–185. https://doi.org/10.1016/j.jhydrol.2012.07.008

Naskar, S., Mondal, S., & Ankure, S. (2021). Leaf Anatomical Adaptations of Mangroves. In M. N. Grigore (Ed.), Handbook of Halophytes. Springer, Cham. https://doi.org/10.1007/978-3-030-57635-6_36

Nelson, J. A., Sha, O. P., Poyatos, R., Zhang, Y., Blanken, P. D., Gimeno, T. E., Wohlfahrt, G., Black, T. A., Knohl, A., Hörtnagl, L., Magliulo, V., Besnard, S., Weber, U., Carvalhais, N., Migliavacca, M., Reichstein, M., & Jung, M. (2020). *Ecosystem transpiration and evaporation : Insights from three water flux partitioning methods across FLUXNET sites*. *January*, 6916–6930. https://doi.org/10.1111/gcb.15314

Ni, X. L., Meng, Y., Zheng, S. S., & Liu, W. Z. (2014). Programmed cell death during aerenchyma formation in Typha angustifolia leaves. *Aquatic Botany*, *113*, 8–18. https://doi.org/10.1016/j.aquabot.2013.10.004

Niinemets, Ü. (2007). Photosynthesis and resource distribution through plant canopies. Plant, Cell & Environment, 30(8), 1052–1071. https://doi.org/10.1111/j.1365-3040.2007.01683.x

Nobel, P. S. (2020). *Physicochemical and Environmental Plant Physiology*.

Nolan, R. H., Tarin, T., Santini, N. S., McAdam, S. A. M., Ruman, R., & Eamus, D. (2017). Differences in osmotic adjustment, foliar abscisic acid dynamics, and stomatal regulation between an isohydric and anisohydric woody angiosperm during drought. *Plant Cell and Environment*, *40*(12), 3122–3134. https://doi.org/10.1111/pce.13077

Novick, K. A., Konings, A. G., & Gentine, P. (2019). Beyond soil water potential: An expanded view on isohydricity including land–atmosphere interactions and phenology. *Plant Cell and Environment*, *42*(6), 1802–1815. https://doi.org/10.1111/pce.13517

Ogle, K., Barber, J. J., Barron-Gafford, G. A., Bentley, L. P., Young, J. M., Huxman, T. E., Loik, M. E., & Tissue, D. T. (2015). Quantifying ecological memory in plant and ecosystem processes. *Ecology Letters*, *18*(3), 221–235. https://doi.org/10.1111/ele.12399

Oke, T. R. (1987). Boundary Layer Climates (2nd ed.). Routledge/John Wiley & Sons: London/New York.

Oki, T., & Kanae, S. (2006). Global hydrological cycles and world water resources. *Science*, *313*(5790), 1068–1072. https://doi.org/10.1126/science.1128845

Olson, M. E.; Soriano, D.; Rosell, J. A.; Anfodillo, T.; Donoghue, M. J.; Edwards, E. J.; Méndez-Alonzo, R. Plant height and hydraulic vulnerability to drought and cold. **2018**. *Proceedings of the National Academy of Sciences*, *115*(29), 7551-7556. https://doi.org/10.1073/pnas.1721728115

Orozco Medina, I., Susana Alvarado Barrientos, M., López-de la Cruz, J., & Iván Ramírez Orozco, A. (2019). Evaluation of the effect of different radiation approaches on the estimation of evapotranspiration using the FAO Penman-Monteith. *Acta Universitaria*, *29*. https://doi.org/10.15174.au.2019.2481

Osmond, C. B., Austin, M. P., Berry, J. A., Billings, W. D., Boyer, J. S., Dacey, J. W. H., Nobel, P. S., Smith, S. D., & Winner, W. E. (1987). Stress Physiology and the Distribution of Plants. *BioScience*, *37*(1), 38–48. https://doi.org/10.2307/1310176

Parida, A. K., & Jha, B. (2010). Salt tolerance mechanisms in mangroves: a review. Trees, 24, 199–217. https://doi.org/10.1007/s00468-010-0394-7

Pelozo, A., Boeger, M. R., Sereneski-de-Lima, C., & Soffiatti, P. (2016). Leaf morphological strategies of seedlings and saplings of Rhizophora mangle (Rhizophoraceae), Laguncularia racemosa (Combretaceae) and Avicennia schaueriana (Acanthaceae) from Southern Brazil. Revista de Biología Tropical, 64(1), 305–317. http://dx.doi.org/10.15517/rbt.v64i1.17923

Posit Team. RStudio: Integrated Development Environment for R. Posit Software, PBC, Boston. http://www.posit.co/ (2023).

Pounds, J. A., Bustamante, M. R., Coloma, L. A., Consuegra, J. A., Fogden, M. P. L., Foster, P. N., La Marca, E., Masters, K. L., Merino-Viteri, A., Puschendorf, R., Ron, S. R., Sánchez-Azofeifa, G. A., Still, C. J., & Young, B. E. (2006). Widespread amphibian extinctions from epidemic disease driven by global warming. In *Nature* (Vol. 439, Issue 7073, pp. 161–167). Nature Publishing Group. https://doi.org/10.1038/nature04246

Poyatos, R., Granda, V., Flo, V., Adams, M. A., Adorján, B., Aguadé, D., Aidar, M. P. M., Allen, S., Alvarado-barrientos, M. S., Anderson-teixeira, K. J., Mcdowell, N., Mcmahon, S., Meir, P., Mészáros, I., Migliavacca, M., Mölder, M., Montagnani, L., Moore, G. W., Nakada, R., … Martínez-vilalta, J. (2020). *Global transpiration data from sap flow measurements : the SAPFLUXNET database*. *October*, 1–57.

Read, J., Sanson, G., & Garine-wichatitsky, M. De. (2006). *Sclerophylly in two contrasting tropical environments : Low nutrients vs . low rainfall*. *July 2014*. https://doi.org/10.3732/ajb.93.11.1601

Reef, R., & Lovelock, C. E. (2015). Regulation of water balance in Mangroves. *Annals of Botany*, *115*(3), 385–395. https://doi.org/10.1093/aob/mcu174

Rindyastuti, R., Rachmawati, D., & Sancayaningsih, R. P. (2018). *Ecophysiological and growth characters of ten woody plant species in determining their carbon sequestration*. *19*(2), 660–669. https://doi.org/10.13057/biodiv/d190238

Robert, E. M. R., Schmitz, N., Okello, J. A., Boeren, I., Beeckman, H., & Koedam, N. (2011). Mangrove growth rings: Fact or fiction? *Trees – Structure and Function*, *25*(1), 49–58. https://doi.org/10.1007/s00468-010-0487-9

Rodda, S. R., Thumaty, K. C., Jha, C. S., & Dadhwal, V. K. (2016). *Seasonal Variations of Carbon Dioxide , Water Vapor and Energy Fluxes in Tropical Indian Mangroves*. 1–18. https://doi.org/10.3390/f7020035

Rodríguez-pérez, L. (2006). Implicaciones fisiológicas de la osmorregulación en plantas Physiological implications of osmoregulation in plants. *Agronomía Colombiana*, *24*(1), 28–37.

Salas-Acosta, E. R., Luis Andrade, J., Adrián Perera-Burgos, J., Us-Santamaría, R., Figueroa-Espinoza, B., Uuh-Sonda, J. M., & Cejudo, E. (2022). Transpiration of a Tropical Dry Deciduous Forest in Yucatan, Mexico. *Atmosphere*, *13*(271). https://doi.org/10.3390/atmos13020271

Salas-Rabaza, J. A., Reyes-García, C., Méndez-Alonzo, R., Us-Santamaría, R., Flores-Mena, S., & Andrade, J. L. (2024). Hydroperiod modulates early growth and biomass partitioning in Rhizophora mangle L. *Aquatic Botany*, *191*. https://doi.org/10.1016/j.aquabot.2023.103747

Sánchez, A. R., Pineda, J. E. M., Casas, X. M., & Calderón, J. H. M. (2021). Influence of edaphic salinity on leaf morphoanatomical functional traits on juvenile and adult trees of red mangrove (Rhizophora mangle): Implications with relation to climate change. *Forests*, *12*(11). https://doi.org/10.3390/f12111586

Santini, N. S., & Lovelock, C. (2015). *The response of the mangrove Avicennia marina to heterogeneous salinity measured using a split-root approach The use of fresh and saline water sources by the mangrove Avicennia marina*. *May*. https://doi.org/10.1007/s11104-015-2489-2

SEMARNAT. (2021). Programa de manejo reserva de la biosfera ría Celestún. México: Comisión Nacional de Áreas Naturales Protegidas, CDMX.

Servicio Meteorológico Nacional. https://smn.conagua.gob.mx/es/climatologia/informacion-climatologica/normales-climatologicas-por-estado?estado=yuc (22 Enero 2025).

Scholz, F. G., Bucci, S. J., Goldstein, G., Meinzer, F. C., & Franco, A. C. (2002). Hydraulic redistribution of soil water by neotropical savanna trees. *Tree Physiology*, *22*(9), 603–612. https://doi.org/10.1093/treephys/22.9.603

Sievers, M., Brown, C. J., Tulloch, V. J. D., Pearson, R. M., Haig, J. A., Turschwell, M. P., & Connolly, R. M. (2019). The role of vegetated coastal wetlands for marine megafauna conservation. Trends in Ecology & Evolution, 34(9), 807–817. https://doi.org/10.1016/j.tree.2019.04.004

Silveira, J. H., Morales-Ojeda, S. M., & Ramirez-ramirez, J. (2019). *Capítulo 12 Almacenes y flujos en lagunas costeras : laguna celestún*. *Septiembre*

Sippo, J. Z., Lovelock, C. E., Santos, I. R., Sanders, C. J., & Maher, D. T. (2018). Mangrove mortality in a changing climate: An overview. *Estuarine, Coastal and Shelf Science*, *215*, 241–249. https://doi.org/10.1016/j.ecss.2018.10.011

Sirvydas, A., Kučinskas, V., Kerpauskas, P., Nadzeikiene, J., & Kusta, A. (2010). Solar radiation energy pulsations in a plant leaf. *Journal of Environmental Engineering* *and Landscape Management*, *18*(3), 188–195. https://doi.org/10.3846/jeelm.2010.22

Slot, M., Garcia, M. N., & Winter, K. (2016). Temperature response of CO2 exchange in three tropical tree species. Functional Plant Biology, 43(5), 468–478.

Snyder, K. A., James, J. J., Richards, J. H., & Donovan, L. A. (2008). Does hydraulic lift or nighttime transpiration facilitate nitrogen acquisition? *Plant and Soil*, *306*(1–2), 159–166. https://doi.org/10.1007/s11104-008-9567-7

Spalding, M. D., Worthington, T., & Spalding, M. (2018). *Mangrove Restoration Potential A global map highlighting a critical opportunity*. *October*. https://doi.org/10.17863/CAM.39153

Steppe, K., Vandegehuchte, M. W., Tognetti, R., & Mencuccini, M. (2015). Sap flow as a key trait in the understanding of plant hydraulic functioning. *Tree Physiology*, *35*(4), 341–345. https://doi.org/10.1093/treephys/tpv033

Stout, D. G., & Simpson, G. M. (1978). Drought resistance of sorghum bicolor. 1. Drought avoidance mechanisms related to lbaf water status. *Can. J. Plant.Sci*, *58*, 213–224. https://doi.org/10.4141/cjps78-031

Suárez, J. C., Casanoves, F., Bieng, M. A. N., Melgarejo, L. M., Di Rienzo, J. A., & Armas, C. (2021). Prediction model for sap flow in cacao trees under different radiation intensities in the western Colombian Amazon. *Scientific Reports*, *11*(1), 1–13. https://doi.org/10.1038/s41598-021-89876-z

Suárez, N., & Medina, E. (2005). Salinity effects on the rate of leaf gas exchange and growth of the mangrove, Avicennia germinans L. Photosynthetica, 43, 217–221. https://doi.org/10.1007/s11099-005-0040-2

Taillardat, P., Friess, D. A., & Lupascu, M. (2018). Mangrove blue carbon strategies for climate change mitigation are most effective at the national scale. Biology Letters, 14(10), 20180251. https://doi.org/10.1098/rsbl.2018.0251

Tang, J., Bolstad, P. V., Ewers, B. E., Desai, A. R., Davis, K. J., & Carey, E. V. (2006). Sap flux-upscaled canopy transpiration, stomatal conductance, and water use efficiency in an old growth forest in the Great Lakes region of the United States. *Journal of Geophysical Research: Biogeosciences*, *111*(2), 1–12. https://doi.org/10.1029/2005JG000083

Tarin, T., Yepez, E., Garatuza-payan, J., & Rodriguez, J. C. (2020). *Evapotranspiration flux partitioning at a multi-species shrubland with stable isotopes of soil, plant, and atmosphere water pools Evapotranspiration flux partitioning at a multi-species shrubland with stable isotopes of soil, plant, and atmosphere wat*. *Septiembre*. https://doi.org/10.20937/ATM.52710

Terashima, I., Hanba, Y. T., Tazoe, Y., Vyas, P., & Yano, S. (2006). Irradiance and phenotype: Comparative eco-development of sun and shade leaves in relation to photosynthetic CO2 diffusion. *Journal of Experimental Botany*, *57*(2 SPEC. ISS.), 343–354. https://doi.org/10.1093/jxb/erj014

Teutli, C., & Silveira, J. H. (2020). *Restauración ecológica de manglares de México*. *April*.

Tomlinson, P. B. (2016). The Botany of mangroves. In *Nature* (Second Edition, Issue 2551). Cambridge University Press, Cambridge. https://doi.org/10.1017/CBO9781139946575

Tulyananda, T., & Nilsen, E. T. (2017). The role of idioblasts in leaf water relations of tropical Rhododendron. American Journal of Botany, 104(6), 828–839. https://doi.org/10.3732/ajb.1600425

Twilley, R. R., Castañeda-Moya, E., Rivera-Monroy, V. H., & Rovai, A. (2017). Productivity and carbon dynamics in mangrove wetlands. In V. H. Rivera-Monroy, S. Y. Lee, E. Kristensen, & R. R. Twilley (Eds.), *Mangrove ecosystems: A global biogeographic perspective. Structure, function, and services* (pp. 113–162). Springer. https://doi.org/10.1007/978-3-319-62206-4

Tyree, M. T. (2003). The ascent of water. *Nature*, *423*(1999), 923. https://doi.org/10.1126/science.20.503.246

Tyree, M. T., & Zimmermann, M. H. (2002). *Hydraulic Architecture of Whole Plants and Plant Performance*. https://doi.org/10.1007/978-3-662-04931-0_6

UNEP. (2016). *Options for Ecosystem-based Adaptation in Coastal Environments*. *February*, 110. https://doi.org/10.13140/RG.2.2.22812.49288

Uuh-Sonda, J. M., Figueroa-Espinoza, B., Gutiérrez-Jurado, H. A., & Méndez-Barroso, L. A. (2022). Ecosystem Productivity and Evapotranspiration Dynamics of a Seasonally Dry Tropical Forest of the Yucatan Peninsula. *Journal of Geophysical Research: Biogeosciences*, *127*(1). https://doi.org/10.1029/2019JG005629

Valderrama, L., Troche, C., Rodriguez, M. T., Marquez, D., Vázquez, B., Velázquez, S., Vázquez, A., Cruz, M. I., & Ressl, R. (2014). Evaluation of mangrove cover changes in Mexico during the 1970-2005 Period. *Wetlands*, *34*(4), 747–758. https://doi.org/10.1007/s13157-014-0539-9

Velázquez-Salazar, S., Rodríguez-Zúñiga, M. T., Alcántara-Maya, J. A., Villeda-Chávez, E., Valderrama-Landeros, L., Tro-che-Souza, C., & Vázquez-Balderas, B. (2020). *Manglares de México. Actualización y análisis de los datos 2020*. www.biodiversidad.gob.mx/

Vinod, N., Slot, M., McGregor, I. R., Ordway, E. M., Smith, M. N., Taylor, T. C., Sack, L., Buckley, T. N., & Anderson-Teixeira, K. J. (2023). Thermal sensitivity across forest vertical profiles: patterns, mechanisms, and ecological implications. New Phytologist, 237(1), 22–47. https://doi.org/10.1111/nph.18539

Wang, G., Shen, Y., Yang, X., Chen, Z., & Mo, B. (2019). Scaling up sap flow measurements from the stem scale to the individual scale for multibranched Caragana korshinskii on the Chinese Loess Plateau. *Forests*, *10*(9). https://doi.org/10.3390/f10090785

Wang, K., & Dickinson, R. E. (2012). *A review of global terrestrial evapotranspiraiton: observation, modeling, climatology, and climatic variability*. *2011*. https://doi.org/10.1029/2011RG000373

Ward, J. D., Sutton, P. C., Werner, A. D., Costanza, R., Mohr, S. H., et al. (2016). Is decoupling GDP growth from environmental impact possible? PLOS ONE, 11(10), e0164733. https://doi.org/10.1371/journal.pone.0164733

Werner, A., & Stelzer, R. (1990). Physiological responses of the mangrove Rhizophora mangle grown in the absence and presence of NaCl. Plant, Cell & Environment, 13(3), 243–255. https://doi.org/10.1111/j.1365-3040.1990.tb01306.x

Williams, S. E., Bolitho, E. E., & Fox, S. (2003). Climate change in Australian tropical rainforests: An impending environmental catastrophe. *Proceedings of the Royal Society B: Biological Sciences*, *270*(1527), 1887–1892. https://doi.org/10.1098/rspb.2003.2464

Wilson, K. B., Hanson, P. J., Mulholland, P. J., Baldocchi, D. D., & Wullschleger, S. D. (2008). *A comparison of methods for determining forest evapotranspiration and its components : sap-flow, soil water budget , eddy covariance and catchment water balance*. *106*(2001), 153–168.

Wu, J., Liu, H., Zhu, J., Gong, L., Xu, L., Jin, G., Li, J., Hauer, R., & Xu, C. (2020). Nocturnal sap flow is mainly caused by stem refilling rather than nocturnal transpiration for Acer truncatum in urban environment. *Urban Forestry and Urban Greening*, *56*. https://doi.org/10.1016/j.ufug.2020.126800

Wu, S., Gu, X., Zheng, Y., & Chen, L. (2023). Nocturnal sap flow as compensation for water deficits: an implicit water-saving strategy used by mangroves in stressful environments. *Frontiers in Plant Science*, *14*. https://doi.org/10.3389/fpls.2023.1118970

Zaldivar-Jimenez, M. a., Herrera-Silveira, J. a., Teutli-Hernandez, C., Comin, F. a., Andrade, J. L., Molina, C. C., & Ceballos, R. P. (2010). Conceptual Framework for Mangrove Restoration in the Yucatan Peninsula. *Ecological Restoration*, *28*(3), 333–342. https://doi.org/10.3368/er.28.3.333

Zeppel, M. J. B., Anderegg, W. R. L., Adams, H. D., Hudson, P., Cook, A., Rumman, R., Eamus, D., Tissue, D. T., & Pacala, S. W. (2019). Embolism recovery strategies and nocturnal water loss across species influenced by biogeographic origin. *Ecology and Evolution*, *9*(9), 5348–5361. https://doi.org/10.1002/ece3.5126